Interaction Forces in Coupled Magnetic Pendulums

by

Mariam Lahlou

A thesis
presented to the University of Waterloo
in fulfillment of the
thesis requirement for the degree of
Master of Applied Science
in
Systems Design Engineering

Waterloo, Ontario, Canada, 2022

Author's Declaration

I hereby declare that I am the sole author of this thesis. This is a true copy of the thesis, including any required final revisions, as accepted by my examiners.

I understand that my thesis may be made electronically available to the public.

Abstract

In this research, we investigated the non-linear motion and magnetic forces in a chain of magnetic pendulums with cylindrical magnets to eventually better understand the behaviour of Josephson junction-effect devices. We studied the nonlinear motions of our system through the interaction forces between the magnets and analytically derived the equations of motion with the aim of simulating the dynamics of the system. To obtain the natural frequencies of our analytical system, we used the Fast Fourier transform. Finally, we validated the accuracy of our simulated system's response by comparing its behaviour to that of an experimental setup consisting of two coupled magnetic pendulums.

Ultimately, we solved for the equations of motions of our magnets and integrated the magnetic forces from the magnetic field function. We also experimentally validated the nonlinear response of the system as well as its equilibrium points and natural frequency. The results we obtained through comparing the simulated system response and the designed experiment response indicated that our analytical model can accurately predict the behaviour of such a system.

Acknowledgements

I would like to first thank my supervisors, Dr. Glenn Heppler and Dr. Eihab Abdel-Rahman, for her invaluable patience and feedback. I also could not have undertaken this journey without them generously providing knowledge and expertise.

Additionally, my appreciation goes out to my family and friends for their encouragement and support all through my studies. Their belief in me has kept my spirits and motivation high during this process.

Dedication

This is dedicated to the ones I love.

Table of Contents

List of Figures

[1]Reproduced from [3], with permission of American Association of Physics Teachers.
[2]Reproduced from [4], with the permission of AIP Publishing.
[3]Reproduced from [5], with the permission of AIP Publishing.
[4]Reproduced from [6], with permission of American Association of Physics Teachers.

List of Tables

Chapter 1

Introduction

Coupled magnetic oscillator systems are very interesting not only for energy harvesting but also for helping researchers have a better understanding of the vibration of atoms in a lattice. Magnetic pendulums are a type of coupled magnetic oscillator system and consist of oscillating pendulums with magnets attached at their ends hence coupled magnetically. Studies have suggested using coupled magnetic pendulums to better understand the Josephson junction which is used for coupling energy between two superconductors. Josephson junction weak links are interesting because of their wide variety of existing and potential applications such as in quantum computing. With memory cell circuit design in quantum computing being based on coupled arrays of Josephson junctions, studying coupled magnetic pendulums can ultimately help better understand this fairly new and more efficient computing technology. Therefore, our goal is to create a mechanical analogue of Josephson junction that can be used to better understand quantum computing.

1.1 Overview

Quantum computing is a fairly new technology that has gained a lot of interest because it make information processing faster and more efficient partly due to its dissipation-less nature. It can make a big positive difference in various fields such as finance, military and intelligence applications, drug design and discovery, aerospace design, utilities (nuclear fusion), polymer design, machine learning and artificial intelligence (AI) [8]. In this thesis, we study the motion of a system of magnetic oscillators to provide a mechanical analog of memory cells used in quantum computing.

Coupled oscillators can be categorized into two types: linearly coupled and nonlinearly coupled. Nonlinear oscillators have more interesting dynamics than the linear ones which is why they will be our focus here. Coupled magnetic oscillators belong to the latter class [9].

The goal of this research is to devise a model of magnetic pendulums in a chain and investigate the nonlinear dynamics of the model and the interaction forces among the pendulums. The pendulums are used in the model to better understand coupled Josephson junctions which form the basis of memory cell circuit design in quantum computing. Our analytical model was created using Mathematica and will be compared to the behaviour of the system examined experimentally to ensure its accuracy.

In order to write the equations of motion for our system, we evaluated the interaction forces between the magnets while taking their geometry into account. To evaluate the validity of the model, we designed and constructed a system of coupled magnetic pendulum constituted of a suspension system holding two pendulums with cylindrical magnets at their ends. The equations of motion of the magnetic pendulums were used to simulate the system response and compared to the results of experimental testing in order to tune the model parameters. Ultimately, we were able to numerically solve the equations of motion and validate the nonlinear response of the system including its equilibrium points and natural frequency.

1.2 Literature Review

This section provides background on quantum computing and how the motion of coupled magnetic oscillators could be used to improve this fairly new technology. The first subsection 1.2.1 describes the history of quantum computing and its advantage for information processing. Subsection 1.2.2 covers quantum computing component memory cells, Josephson Junctions and the mechanics of their motion. Finally, subsection 1.2.3 highlights how the motion of coupled magnetic oscillators relates to that of Josephson Junctions, and thus memory cells.

1.2.1 Quantum Computing

Quantum computing is the use of quantum-mechanical systems for information processing. With the emergence of nanotechnology, quantum computing is becoming increasingly predominant in the development of more compact and efficient computers [2]. In general, energy dissipation is common in computing with every irreversible operation causing bit losses and consequently energy loss. However, in quantum computing, the quantum logic circuits are reversible which helps avoid energy loss when processing a bit.

History of Quantum Computing

Quantum computing is not a new concept. In fact, so far, many people have suggested the ideas of quantum computers and formalized their models. The idea of using quantum mechanics for computational purposes has been explored as early as 1980 where Benioff [10] noted that constructing a computer based on quantum mechanics is possible and proposed building it. He started out by making smaller logic circuits thus showing that atomic-scale circuit as one of the components of quantum computers can be built. Benioff suggested representing every two binary digits using spins of elementary particles making computation fully quantum-mechanically performed without consuming energy [11].

That same year, Manin [12] also proposed the idea of quantum computers in his book "Computable and Non-Computable". In 1981, Feynman [13] in his lecture "Simulating Physics with Computers", described a quantum computer that can simulate physics. He argued that regular computers cannot adequately simulate complex quantum mechanical phenomena:

> ...nature isn't classical, dammit, and if you want to make a simulation of nature, you'd better make it quantum mechanical, and by golly it's a wonderful problem, because it doesn't look so easy...

He pointed out the key features for quantum computers which generally should be useful and obey laws of quantum mechanics.

After Benioff, Manin, and Feynman introduced the concept of quantum computers, researchers started proposing models for such computers and the nature of the algorithms that could be run on them [14]. Deutsch [15] proposed a model called the *quantum computer* which is considered the first computational model for quantum computing. In this work, he describes what a quantum algorithm would look like and predicts that "one day it will become technologically possible to build quantum computers." To further his point, Deutsch also developed a sample algorithm that would run faster on a quantum computer.

In 1993, Vazirani and Bernstein [16] elaborated on Deutsch's work by proposing the *universal quantum Turing Machine* which generalizes Deutsch's model. This algorithm showed clear quantum-classical separation even when small errors are allowed. They also described a quantum version of the Fourier transform, which was used [16] to develop an algorithm to factor large numbers. This algorithm, also known as *Shor's algorithm*, factors numbers with a quantum computer that would involve six qubits and thus further proving the possibilities of quantum computers.

In 1996, Grover [17] proposed a quantum search algorithm that would speed search functions on quantum computers. This algorithm can search data in unstructured database in the order of $\sqrt{n}$.

The first model of a quantum computer was only implemented in 1998 by Chuang and Gershenfeld [18]. The 2-qubit quantum computer is based on chemical applications of Nuclear Magnetic Resonance (NMR). In 2000, Knill, Laflamme, and Martinez [19] were able to develop a seven-qubit NMR quantum computer while implementing Shor's Algorrithm.

Currently, it is possible to develop quantum computers with more than 10-qubits. Many fundamental theories for applications of quantum computing have also been established [11].

Characteristics of Quantum Computing

As we can see, research on quantum computing has been gaining interest. The speed of classical computing being still insufficient to satisfy the constantly increasing needs of technology, quantum computation could make information processing much faster and more practical.

Quantum computers process information by using atoms at the micro level and the properties quantum-mechanical systems. The basic unit of information used in quantum computers is the quantum bit also called a *qubit*. It is based on a the principle of *Quantum Superposition*, that the 0 and 1 states can overlap [11]. While in regular computers, information is represented by means of a bit which can have only one value of 0 or 1, quantum computers use qubits which can represent more information than in bits as illustrated in Figure 1.1.

Some scientist have already constructed quantum computers that can carry out basic operations [2]. Many of these quantum computers adopt quantum mechanics by using quantum logic gates to avoid redundant theories and algorithms.

A quantum gate is a basic quantum circuit operating on a small number of qubits [2]. There are various quantum gates with different functionalities most notably the NOT, CNOT, controlled-V, and controlled-V+ gates as seen in Figure 1.2(V gate is the square

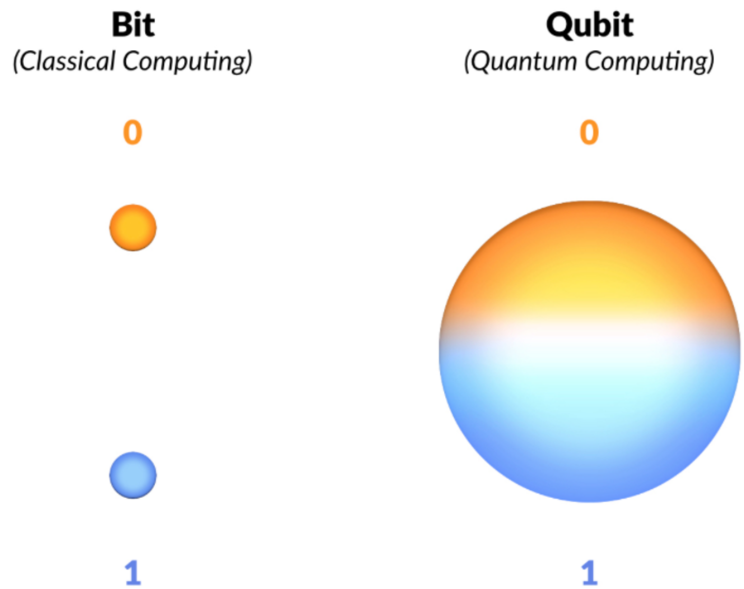

Figure 1.1: Classical qubits are zero or one. Qubits are a superposition of zero and one [1].

root of NOT gate). In this figure, the colored dot represents the control, while the circle represents the target, and the contact qubits are illustrated by the vertical lines.

As opposed to classical computing, neither AND, OR, XOR, NAND or FANOUT can be used in quantum computing. The AND, OR, XOR and NAND gates are not reversible while the FANOUT involves duplication or cloning of states. Additionally, in quantum computing, the number of outputs must equal the number of inputs. For reference, Figure 1.3 represent an example of a circuit in classical computing and quantum computing respectively that performs addition/subtraction also know as a full-adder.

Although the two-level qubit systems is the most generally used to build quantum computers, there are other types of quantum computing architectures. For example, it is possible to build a quantum computer with qutrits which are three-level systems with states of 0, 1 or 2 or a superposition of those states.

1.2.2 Memory Cells

Just like for any computing device, depending on the computing task at hand, there are two main components in quantum computing needed for the device to operate properly:

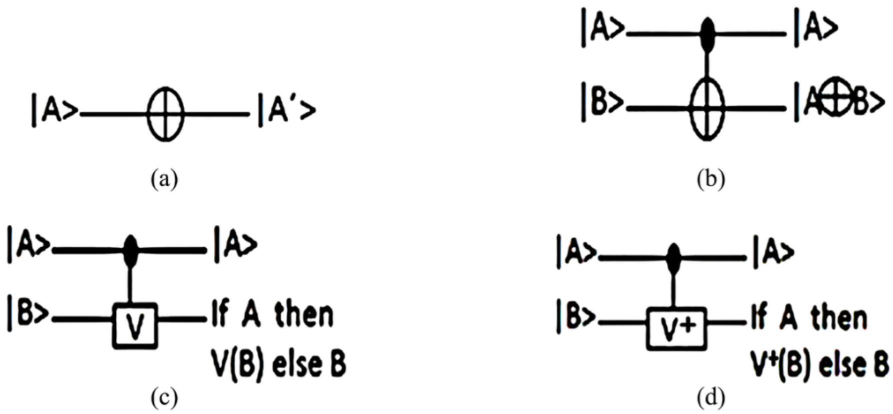

Figure 1.2: Basic Quantum gates [2].

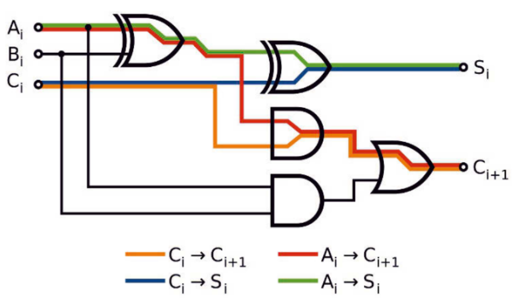

(a) Classical computing [14].

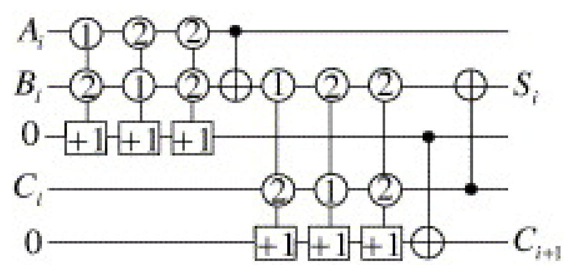

(b) Quantum computing [20].

Figure 1.3: Full-adder circuit in different computing.

a long-lived memory and a fast data-bus for communication between different registers or processors [21]. The cells of the memory unit have to be well isolated from the rest of the system. Several types of memory cells have been developed by tunnelling Josephson junctions. The main advantages of using a Josephson junction as a qubit (classical bit) is that it is not only easily controllable by an applied magnetic field [22], but also helps create a system with states that can be manipulated and well protected against decoherence.

Another advantage of using a Josephson junction as a memory cell is the resemblance of its dynamics to that of a pendulum under an applied torque. This allowed many researches to use the motion of pendulum systems under constant torque to better understand Josephson junction-effect devices.

Figure 1.4 shows the circuit diagram of a Josephson Junction (JJ). The Josephson

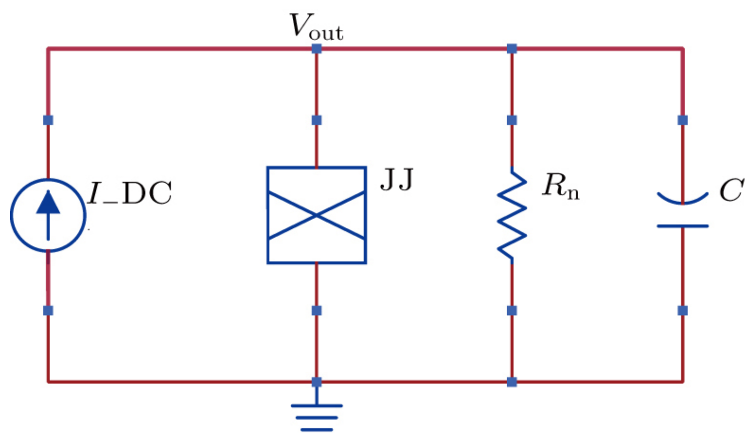

Figure 1.4: Schematic diagram of a circuit with a Josephson junction.

voltage-phase relationship defines the instantaneous voltage across the junction V in terms of the rate of ϕ which is the phase difference that the two superconductors of the junction will be driven apart at [23]:

$$V = \frac{h}{2e}\dot{\phi} \tag{1.1}$$

where h is Planck's constant and e is the electron charge. In cases where the maximum current realizable by the JJ I is larger than the bias current I_{DC}, the current through the JJ is limited to:

$$I_j = I_c \sin\phi$$

Noting that the voltage drop across all branches of the circuit is equal to V_{out}, we apply Kirchhoff's current law to the circuit and set the sum of the currents through the capacitor C, the resistor R_n and the junction equal to the bias current I_{DC} [23]:

$$C\dot{V}_{out} + \frac{V_{out}}{R_n} + I\sin\phi = I_{DC} \tag{1.2}$$

Using the relationship between the junction voltage and phase in Equation (1.2), it reduces to:

$$\frac{hC}{2e}\ddot{\phi} + \frac{h}{2eR_N}\dot{\phi} + I\sin\phi = I_{DC} \tag{1.3}$$

Equation (1.3) is analogous to the equation of motion of a damped pendulum under a constant torque T, namely:

$$mL^2\ddot{\theta} + b\dot{\theta} + mgL\sin\theta = T \tag{1.4}$$

where m is the pendulum effective mass, L is its distance from the suspension point, b is the viscous damping coefficient, and g is the acceleration of gravity. This mechanical analog has been use by many in visualizing the dynamics of Josephson junctions; the earliest being Anderson and Rowell [24] in 1963.

1.2.3 Josephson Junctions and Coupled magnetic systems

Different magnetic pendulum models have been used to better understand the Josephson coupling energy between two superconductors. Sullivan and Zimmerman [3] model seen in Figure 1.5 is an example of a mechanical analog of a single (point) Junction. In this model, an electric motor produces a constant torque source that rotates magnet-studded disk which in turn moves the pendulum at the right end. The constant torque represents the constant current source of a Josephson Junction.

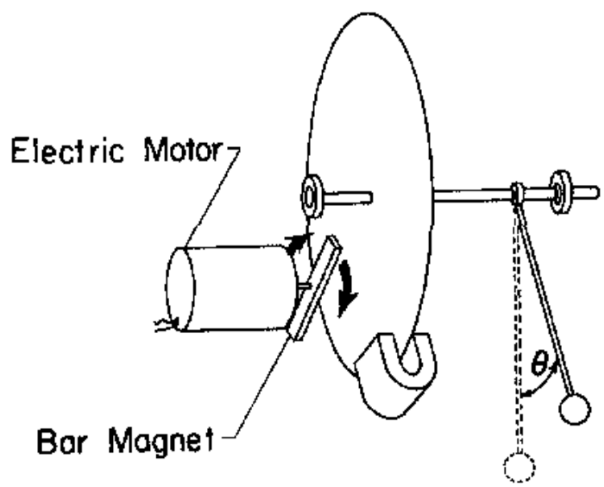

Figure 1.5: Sullivan's mechanical analog of a point JJ[1].

A year later, Hansma and Rochlin [4] based their mechanical analog, illustrated in Figure 1.6, on that of Sullivan and Zimmerman. Their system contains a pair of masses fixed to the disc at the right end which are used as pendulum bobs. These two masses can be changed and used to vary the effective pendulum mass without altering the moment of inertia [4].

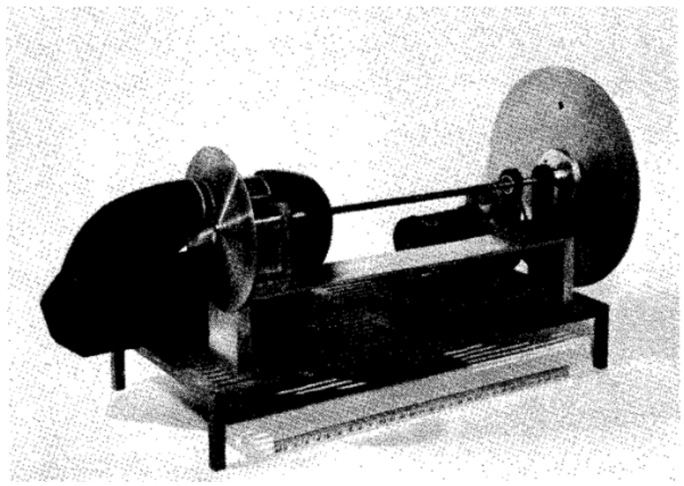

Figure 1.6: Hansma and Rochlin's mechanical analog of a point JJ[2].

Another interesting model [5] illustrated in Figure 1.7 presents a mechanical analogue of the Josephson transmission line. The constant torque that moves the disks seen in the figure is produced by the air that passes through the nozzles at the top which is blown against the edges of each aluminum disks. Similarly to Hansma and Rochlin's model, the two masses symmetrically fastened on each disk are used as pendulum bobs to the same end. Again, the constant torque is analogous to a constant current source.

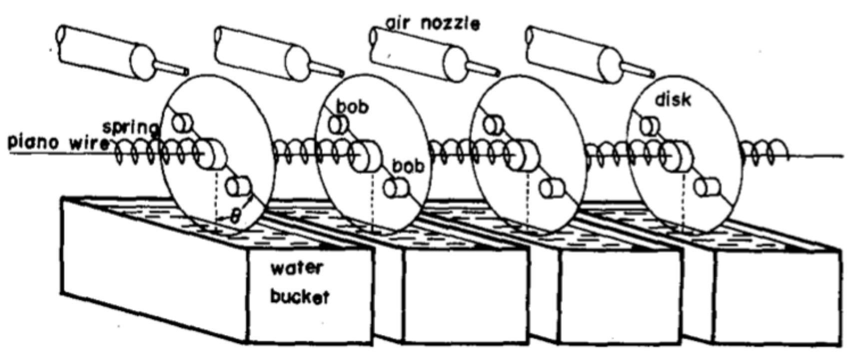

Figure 1.7: Mechanical analogue of a JJ transmission line[3].

Blackburn et al. [25] experimentally investigated the motion of a damped pendulum driven by linear motor that serves as a mechanical analogue of a current biased JJ. The results confirmed the existence of separate regions of periodic and chaotic pendulum motions. The system also served as an experimental probe of biased Josephson devices whose characteristic time scales were approximately 10^{12} shorter than those of the pendulums. This research represents one of the first direct and accurate measurement of chaos in a real physical system rather than simulations.

More recently, Luca et al. [26] demonstrated the analogy between an over-damped pendulum and an over-damped JJ and analyzed their corresponding properties. They noted that the current-voltage characteristics of the JJ device can be found by deriving an analytical expression for the normalized driving moment of the pendulum as a function of the time average of the angular frequency.

Altshuler and Garcıa used a system of pendulums and pulleys [6] to investigate the magnetic field dependence on the maximum JJ current I. The picture in the left panel of Figure 1.8 shows a three-pendulum experiment that corresponds to the applied field associated with the maximum critical current. The three pictures on the right represent the analogs for the cases of: (a) $I_j = 0$, (b) $0 \leq I_j \leq I$ and (c) $I_j \approx I$.

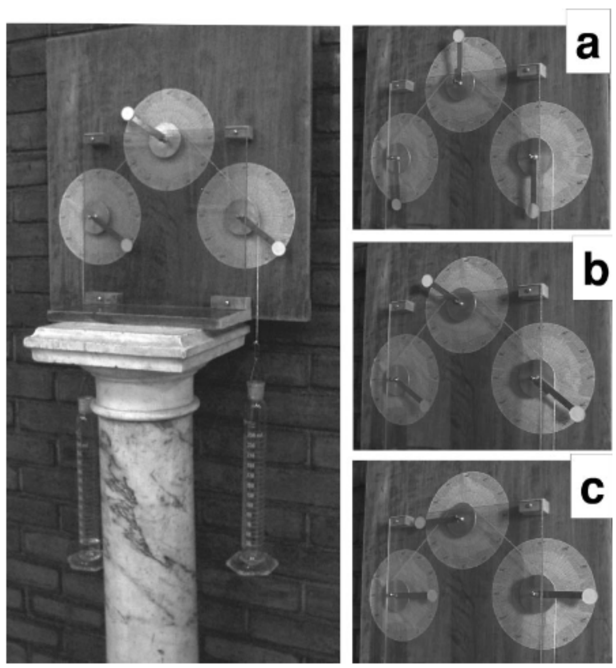

Figure 1.8: Altshuler and Garcia's model[4].

Many researchers adopted under-damped pendulums as a mechanical analogue for arrays of discrete JJs. Watanabe et al. [27] analyzed a system of periodic sine-Gordon equations representing an array of coupled under-damped pendulums hanging from a common support rod under constant torque as well as an array of discrete JJs. They found travelling waves in the system dynamics comparable to experimental measurements of the current-voltage characteristics of a ring of eight under-damped JJs. The waves were classified in to two categories: low-velocity kinks and high-velocity whirling modes. In each case, they found that the measured voltage locations of the resonant steps were in good agreement with model predictions.

1.3 Thesis Layout

The thesis is organized in five chapters. In Chapter 2, the system of magnetic pendulums is introduced in details presenting each the design of each component. Chapter 3 covers the derivation the equations of motion governing a system of two magnetic pendulums. Chapter 4 discusses the interaction forces related to the response of the system and compares the results of the analytical model to the experimental results. Finally, conclusions and future work are discussed in Chapter 5.

1.4 Contribution

An initial model by Saeidi Hosseini [9] used an ideal point source model to represent the magnets and derive the pendulums' equations of motion. The current work builds on that by replacing the point source magnet model with a three dimensional magnet model and taking its geometry into account. Mr. Carl Azzi [28] redesigned the pendulum system to increase its resistance to out-of-plane bending. The prototyping and manufacturing of the coupled magnetic oscillator system was revised by Mr. Del Rosso [29] under the supervision of Professors Glenn Heppler and Eihab Abdel-Rahman.

Chapter 2

Pendulum Array

In this chapter, we describe the experimental set up of the pendulum array under study. It is composed of a set of identical magnetic pendulums. Section 2.1 describes the overall system, the materials used, and the process of making the custom parts. Section 2.2 looks into the pendulum arm component of our system, while section 2.3 discusses the suspension system. Finally, section 2.4 describes the testing and data collection process.

2.1 Materials and Design

The physical system consists of an array of eight identical magnetic pendulums suspended at equidistant points along a rod. The pendulums can be arranged such that the magnets are in repulsive or attractive interaction. For the context of this work, we only used two pendulums in our system mounted such that there is repulsive interaction between them. In a typical experiment, a pendulum would be released from a 90° degrees angle with respect to the vertical line while the second pendulum is stationary and aligned with the vertical line and the two pendulums would be allowed to oscillate freely until they settle down. We record the motions of the pair of pendulums using a video camera and we measure the angles of the two pendulums make with the vertical line by dividing the video recording into individual frames.

The first prototype of the system, developed by Saeidi Hosseini [9] is shown in the left panel of Figure 2.1. The second prototype with improved suspension system, pendulum design, and materials is shown in the right panel of the figure. The magnets were kept unchanged, as DA2-N52 magnets [7], in the prototype # 2 due to their strength compared to their size.

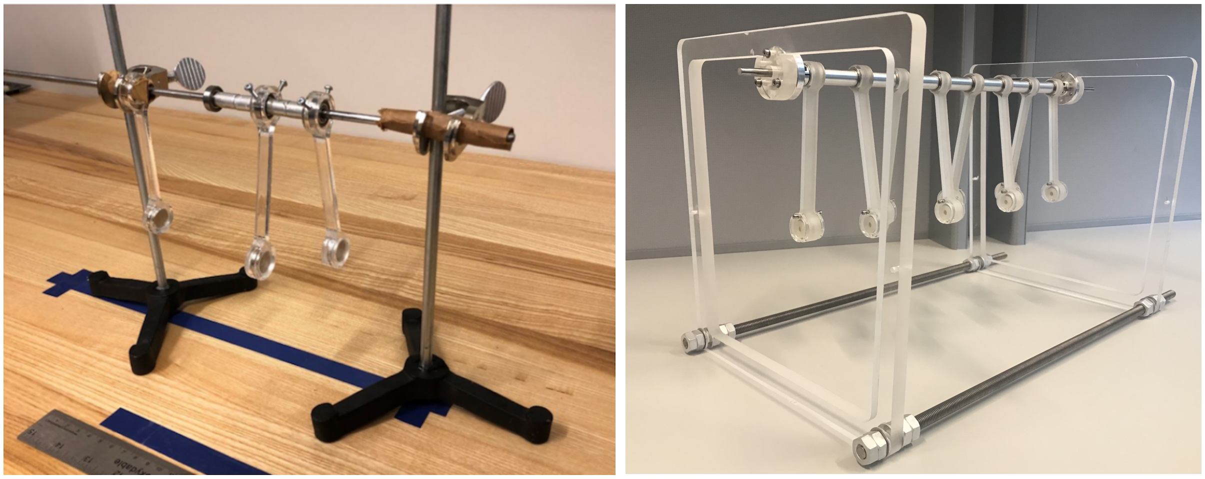

Figure 2.1: Prototypes # 1 and #2 of the pendulum array

The final magnet dimensions and properties are listed in Table 2.1. We compute the magnetization of our magnet by dividing the residual flux density by the permeability of free space. The permeability of free space μ_0 being a physical constant equal to $4\pi \times 10^{-7}$ H/m.

Table 2.1: The dimensions and properties of DA2-N52 magnets [7]

Description	Symbol	Value
Diameter	D	15.875 mm
Thickness	h	3.175 mm
Volume	$V = \frac{\pi}{4} D^2 h$	628 mm^3
Mass	m_m	4.71×10^{-3} kg
Residual flux density	B_r	1.275 Tesla
Magnetization	$M_\circ = \frac{B_r}{\mu_\circ}$	1.01342×10^6 A/m

There are three main components of the overall new prototype supporting the pendulum array: the suspension system, the crossarms, and the pendulums. The suspension system is our new prototype consists of two trapezoidal shaped legs made from acrylic holding a 500 mm long suspension rod. The trapezoidal legs provide a full view of the moving pendulums from the front of the system and the suspension rod was chosen such that no bending will occur due to the pendulums' weight or magnetic force.

The pendulums that go into the rod and are help by it consist of an acrylic arm with a cylindrical magnet at the end. In our new prototype, the length of the pendulum was changed to be 121 mm. This length allows a clear visibility of the motion of the magnets while still avoiding bending due to the magnetic force. To keep the distance between the magnets uniform, we used spacer of either 35 or 40 mm length and placed them in the suspension rod between the pendulums.

Wherever possible parts were made from aluminum and acrylic to avoid disturbing the magnetic field and reduce cost. The custom acrylic parts can be fabricated using laser and waterjet cutting. Although laser cutting is cheaper and faster turnout, we chose waterjet cutting to obtain higher dimensional accuracy for the thickness of the parts (thickness being 1/2").

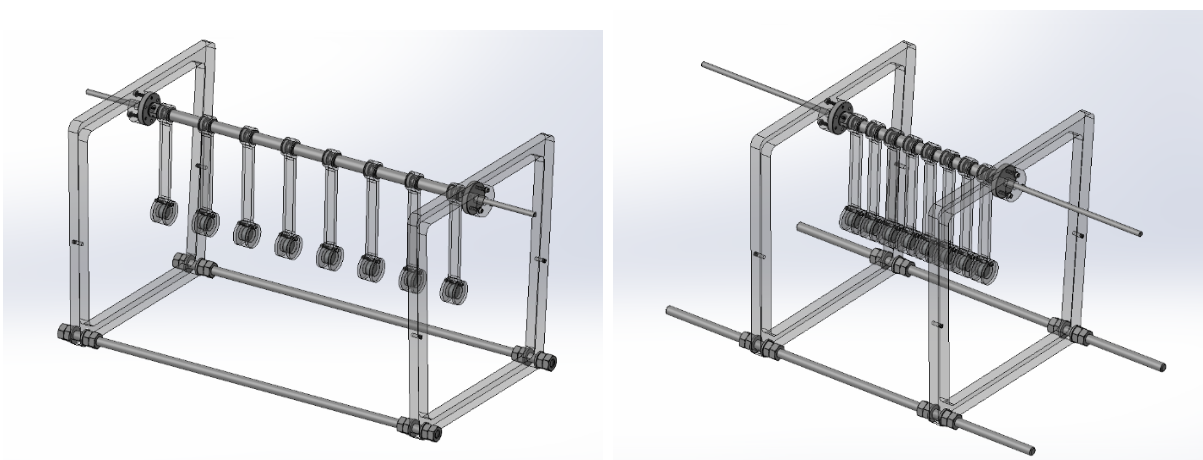

Figure 2.2: System at maximum alongside minimum extension

Another new feature of prototype #2 is that the distance between the pendulums can be altered by either changing the spacers set between the pendulum arms along the suspension rod or removing them altogether to obtain the minimum distance. Since the suspension rods as well as the ones connecting the trapezoidal legs from the bottom are fixed to the legs with nuts, the location of the nuts can be accordingly shifted so that the distance between the legs is closer or further apart as shown in the Figure 2.2. We use this attribute in our experiments to see how changing the distance between the magnets affects the equilibrium angles.

2.2 Pendulum Design

The next components of the system are the pendulums. One of the main features of the new pendulum design is that magnets can be added or removed without complete disassembly of the system through the removable magnet covers. Since the magnet covers are only fixed at one spot, they can be spun upwards such that the spacers and magnet can be pushed out from the side as shown in Figure 2.3. This provides a quick way to alter the system without completely removing the pendulum from the suspension rod.

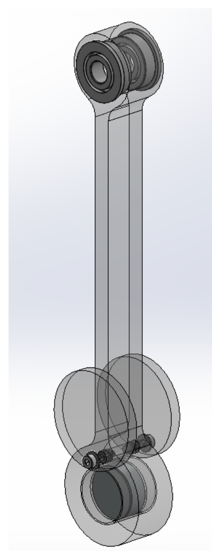

Figure 2.3: Pendulum arm with removable magnet covers.

As seen in the figure, the upper loop holds a bearing that will connect the pendulum to a beam to a circular rod. Meanwhile, the loop at the bottom side holds our magnet that will be responsible for the interaction forces between our pendulums. Table 2.2 presents the dimensions of the pendulum arms. We consider the acceleration due to gravity g to be 9.80665 m/s^2 and use it in the next section to compute the weight of the magnet and later on as one of our parameters in the equation of motion.

Table 2.2: Dimensions and parameter values for the pendulum arm.

Description	Symbol	Value
Pendulum separation distance	a	35 or 40 mm
Distance from center of gravity to origin	d	83.78 mm
Pendulum length	ℓ	121 mm
Pendulum thickness	t	12.5 mm
Pendulum mass	m	24.51×10^{-3} kg

2.3 Suspension System

As seen in Figure 2.2, the design we ended up going with for our suspension system were the trapezoidal legs as they gave a full view of the pendulums' motion from a front-side angle. This suspension system is designed for lab use where videos need to be taken of the pendulums full travel in order to collect motion data and later compare it to the simulations.

The choice of the shaft was based on the bearing which has an inner diameter of 5mm, so the shaft should have the same diameter. We also chose two different spacers that will separate the pendulums on the shaft: a 35mm and a 40mm spacer. After that, we calculated the deflection to see if the shaft can support eight pendulums each separated by a 35 mm or 40 mm distance. To make sure the suspension rod can hold all our pendulums, we compute the maximum deflection using the following equation

$$\delta_{max} = -\frac{5qL^4}{384EI} \tag{2.1}$$

where q is the distributed load on the rod, L the length, E Young's modulus of elasticity of the rod as seen on Table 2.3, and I the area moment of inertia of the cross section. The distributed load q can be found by dividing the total weight applied on the rod by all eight pendulums, W_{total}, by the rod's total length, L_{total}:

$$q = \frac{W_{total}}{L_{total}} = \frac{M_{total}g}{L_{total}} \tag{2.2}$$

As seen in Figure 2.4, the distance between the magnetic pendulums, a, and the distance between the first and last magnetic pendulums to the supports are either 35 mm and 40mm. We will compute the total distributed load for both cases.

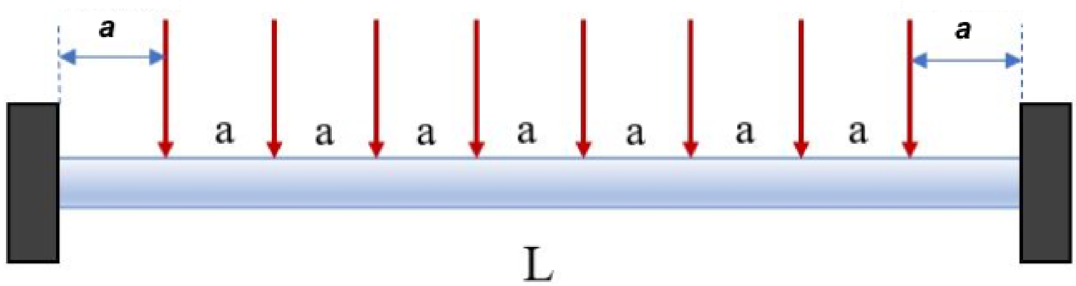

Figure 2.4: Side view of the rod loaded by eight equally spaced magnetic pendulums.

- **Case 1:** $a = 35mm$
  According to the figure, the total length of the rod when the separation distance between the magnets is 35 mm is

$$L_{total} = 9 \times 35 = 315mm = 0.315m$$

The chosen magnet's mass is 4.71 g and the identified pendulum's total mass is 31.96 g. Therefore, the total distributed load is

$$q = \frac{M_{total}g}{L_{total}} = 0.9953N/m \tag{2.3}$$

With the area moment of inertia of the rod cross section derived using:

$$I = \frac{\pi D_{dr}^4}{64} = 63.62mm^4 \tag{2.4}$$

where D_{dr} is the 5 mm drill rod diameter with a Young's modulus elasticity of $E = 193Gpa$. Using all these parameters, the maximum deflection is found

$$\delta_{max} = -\frac{5qL^4}{384EI} = -1.039 \times 10^{-5}m = -0.0104mm \tag{2.5}$$

- **Case 2:** $a = 40mm$
  According to the figure, the total length of the rod when the separation distance between the magnets is 40 mm is

  $$L_{total} = 9 \times 40 = 360mm = 0.360m$$

  The chosen magnet's mass is 4.71 g and the identified pendulum's total mass is 31.96 g. Therefore, the total distributed load is

  $$q = \frac{M_{total}g}{L_{total}} = 0.87091N/m \tag{2.6}$$

  Using the same area moment of inertia of the rod cross section and Young's modulus elasticity as the previous case. Using all these parameters, the maximum deflection is found

  $$\delta_{max} = -\frac{5qL^4}{384EI} = -1.187 \times 10^{-5}m = -0.012mm \tag{2.7}$$

At the end, the deflection for both cases was smaller than 1 mm making the rod selected proper for the design. The table 2.3 shows all the characteristics of the shaft.

Table 2.3: Dimensions and parameter values for the Suspension Rod.

Description	Symbol	Value [SI]
Drill Rod Diameter	D_{dr}	6 mm
Drill Rod Length	L	500 mm
Drill Rod Moment of Inertia	$I = \frac{\pi D_{dr}^4}{64}$	63.62 mm^4
Drill Rod Young's Modulus	E	193 GPa

2.4 Testing and Data Collection

To test the balance of our system, we did a visual check to ensure that with 35mm and 40mm spacers the pendulum arms did not bend due to magnetic forces. The trapezoidal design was carried around the lab from various locations on the system over the course of a week and no signs of stress or failure appeared. Test parts were cut from $\frac{1}{2}$" acrylic using a laser cutter. The oscillation of each pendulum was timed to ensure they ran for the same amount of time ± 5 seconds.

Once the testing was complete, we gathered our experimental data by taking a video of the system's full oscillation from the front. In this research, we focused on a system consisting of two pendulums. Once the video was taken and slowed down for each of our separation distance cases, we divided the videos into multiple frames per seconds and measured the angles of both pendulum using an online protractor.

Chapter 3

System of Equations

In this chapter, we investigate the nonlinear equations of motion of a system of two magnetically interacting pendulums. To that end, we compute the magnetic field between the magnets and ultimately evaluate the magnetic force.

Firstly, section 3.1 describes the frames of reference used to write the equations, two body fixed frames $\boldsymbol{\mathcal{F}}_i$ and $\boldsymbol{\mathcal{F}}_j$ and an inertial frame $\boldsymbol{\mathcal{F}}_o$. In this section, we find the transformation matrices from the body frames to the inertial frame. We also describe the transformation matrices from cylindrical frames where the magnetic force is evaluated to Cartesian frames where the equations of motion are written. Section 3.2 describes the magnetic field then use it to find the magnetic force between the magnets. Finally, section 3.3 presents our equations of motion for a system made of two magnetically interacting pendulums.

3.1 Geometry

3.1.1 Frames of Reference

We describe three frames of reference are presented in Figure 3.1:

- An inertial Cartesian frame $\boldsymbol{\mathcal{F}}_o$ with basis vectors $\hat{\mathrm{i}}$, $\hat{\mathrm{j}}$ and $\hat{\mathrm{k}}$ fixed at point O along the pendulum suspension axis
- A body fixed Cartesian frame $\boldsymbol{\mathcal{F}}_i$ attached to pendulum i at the center of its magnet with basis vectors $\hat{\mathrm{i}}_{\boldsymbol{i}}$, $\hat{\mathrm{j}}_{\boldsymbol{i}}$ and $\hat{\mathrm{k}}_{\boldsymbol{i}}$

- A body fixed Cartesian frame $\boldsymbol{\mathcal{F}}_j$ attached to pendulum j at the center of its magnet with basis vectors $\hat{\mathrm{i}}_{\boldsymbol{j}}$, $\hat{\mathrm{j}}_{\boldsymbol{j}}$ and $\hat{\mathrm{k}}_{\boldsymbol{j}}$

where the z-axes of all three frames will remained aligned at all times, such that

$$\hat{\mathrm{k}} = \hat{\mathrm{k}}_{\boldsymbol{i}} = \hat{\mathrm{k}}_{\boldsymbol{j}}$$

The locations of pendulums i and j are described in terms of:

- θ_i and θ_j the angles they make, respectively, with respect to the vertical x-axis. Or in other words θ_i and θ_j are the angles between the global $\hat{\mathrm{i}}$ basis vector and the $\hat{\mathrm{i}}_{\boldsymbol{i}}$ and $\hat{\mathrm{i}}_{\boldsymbol{j}}$ basis vectors.
- θ_{ij} the angle of pendulum j makes with respect to pendulum i such that $\theta_{ji} = \theta_j - \theta_i$

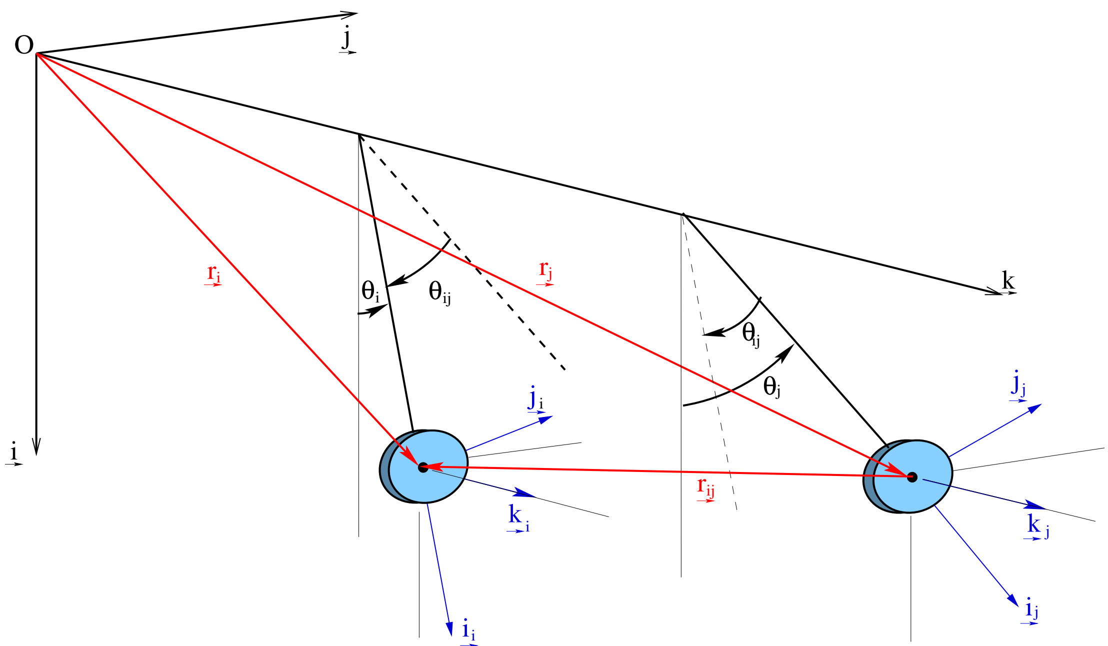

Figure 3.1: Perspective view of pendulums i and j.

Let $\boldsymbol{\mathcal{F}}_{c_n}$ be a companion cylindrical frame attached to the centre of the magnet of pendulum n with basis vectors $\hat{\rho}_{c_n}$, $\hat{\phi}_{c_n}$ and $\hat{\mathrm{k}}_{\boldsymbol{c_n}}$. It is assumed that the origin of the inertial frame is situated so that pendulum n is positioned at a distance of $z_n = nd$ from the origin of the inertial frame where d is the distance between two successive pendulums. This guarantees that $z_n - \frac{h_m}{2} > 0$ for $n = 1, 2, ..., N$.

3.1.2 Transformation Matrices

To be able to write the equations of motion in a common frame, we will establish transformation matrices among those frames. Since the z-axes are always aligned, all transformation matrices will reduce to rotations around $\hat{\mathrm{k}}$. The transformation matrix from the inertial frame $\vec{\boldsymbol{\mathcal{F}}}_o$ to pendulum i's body fixed frame $\vec{\boldsymbol{\mathcal{F}}}_i$ is

$$\boldsymbol{C}_{io} = \begin{bmatrix} \cos\theta_i & \sin\theta_i & 0 \\ -\sin\theta_i & \cos\theta_i & 0 \\ 0 & 0 & 1 \end{bmatrix} \tag{3.1}$$

its inverse gives the transformation matrix from $\vec{\boldsymbol{\mathcal{F}}}_i$ to $\vec{\boldsymbol{\mathcal{F}}}_o$ is

$$\boldsymbol{C}_{oi} = \begin{bmatrix} \cos\theta_i & -\sin\theta_i & 0 \\ \sin\theta_i & \cos\theta_i & 0 \\ 0 & 0 & 1 \end{bmatrix} \tag{3.2}$$

Similarly, the transformation matrix from $\vec{\boldsymbol{\mathcal{F}}}_o$ to $\vec{\boldsymbol{\mathcal{F}}}_j$ is

$$\boldsymbol{C}_{jo} = \begin{bmatrix} \cos\theta_j & \sin\theta_j & 0 \\ -\sin\theta_j & \cos\theta_j & 0 \\ 0 & 0 & 1 \end{bmatrix} \tag{3.3}$$

and its inverse giving the transformation matrix from $\vec{\boldsymbol{\mathcal{F}}}_j$ to $\vec{\boldsymbol{\mathcal{F}}}_o$ is

$$\boldsymbol{C}_{oj} = \begin{bmatrix} \cos\theta_j & -\sin\theta_j & 0 \\ \sin\theta_j & \cos\theta_j & 0 \\ 0 & 0 & 1 \end{bmatrix} \tag{3.4}$$

Since $\theta_{ji} = \theta_j - \theta_i$, the transformation matrix from $\vec{\boldsymbol{\mathcal{F}}}_j$ to $\vec{\boldsymbol{\mathcal{F}}}_i$ is

$$\begin{aligned} \boldsymbol{C}_{ij} &= \begin{bmatrix} \cos(\theta_j - \theta_i) & \sin(\theta_j - \theta_i) & 0 \\ -\sin(\theta_j - \theta_i) & \cos(\theta_j - \theta_i) & 0 \\ 0 & 0 & 1 \end{bmatrix} \\ &= \begin{bmatrix} \cos\theta_{ji} & \sin\theta_{ji} & 0 \\ -\sin\theta_{ji} & \cos\theta_{ji} & 0 \\ 0 & 0 & 1 \end{bmatrix} \end{aligned} \tag{3.5}$$

and its inverse, the transformation from $\vec{\boldsymbol{\mathcal{F}}}_i$ to $\vec{\boldsymbol{\mathcal{F}}}_j$, is

$$\begin{aligned}
\boldsymbol{C}_{ji} &= \begin{bmatrix} \cos(\theta_i - \theta_j) & \sin(\theta_i - \theta_j) & 0 \\ -\sin(\theta_i - \theta_j) & \cos(\theta_i - \theta_j) & 0 \\ 0 & 0 & 1 \end{bmatrix} \\
&= \begin{bmatrix} \cos\theta_{ij} & \sin\theta_{ij} & 0 \\ -\sin\theta_{ij} & \cos\theta_{ij} & 0 \\ 0 & 0 & 1 \end{bmatrix} \\
&= \begin{bmatrix} \cos\theta_{ji} & -\sin\theta_{ji} & 0 \\ \sin\theta_{ji} & \cos\theta_{ji} & 0 \\ 0 & 0 & 1 \end{bmatrix} \\
&= \boldsymbol{C}_{ij}^T
\end{aligned} \tag{3.6}$$

where

$$\theta_{ij} = \theta_i - \theta_j$$

Let $\boldsymbol{C}_{ic_i}$ be the transformation matrix from the cylindrical $\vec{\boldsymbol{\mathcal{F}}}_{c_i}$ to the Cartesian $\vec{\boldsymbol{\mathcal{F}}}_i$ frames attached to pendulum i such that

$$\boldsymbol{C}_{ic_i} = \begin{bmatrix} \cos\phi_i & -\sin\phi_i & 0 \\ \sin\phi & \cos\phi_i & 0 \\ 0 & 0 & 1 \end{bmatrix} \tag{3.7}$$

so that the inverse transformation from $\vec{\boldsymbol{\mathcal{F}}}_i$ to $\vec{\boldsymbol{\mathcal{F}}}_{c_i}$ is

$$\boldsymbol{C}_{c_ii} = \begin{bmatrix} \cos\phi_i & \sin\phi_i & 0 \\ -\sin\phi_i & \cos\phi_i & 0 \\ 0 & 0 & 1 \end{bmatrix} \tag{3.8}$$

Similarly $\boldsymbol{C}_{jc_j}$ is given by

$$\boldsymbol{C}_{jc_j} = \begin{bmatrix} \cos\phi_j & -\sin\phi_j & 0 \\ \sin\phi_j & \cos\phi_j & 0 \\ 0 & 0 & 1 \end{bmatrix} \tag{3.9}$$

so that the inverse transformation from $\vec{\boldsymbol{\mathcal{F}}}_j$ to $\vec{\boldsymbol{\mathcal{F}}}_{c_j}$ is

$$\boldsymbol{C}_{c_jj} = \begin{bmatrix} \cos\phi_j & \sin\phi_j & 0 \\ -\sin\phi_j & \cos\phi_j & 0 \\ 0 & 0 & 1 \end{bmatrix} \tag{3.10}$$

3.1.3 Magnets Position Vectors

With reference to Figure 3.1, $\vec{r_i}$ is the position vector of the center of magnet of pendulum i with respect to the inertial origin. Going from the fixed initial frame to frame F_i

$$\begin{aligned}
\vec{r_i} &= \vec{\boldsymbol{\mathcal{F}}}_o^T \boldsymbol{r}_{io} \\
&= \vec{\boldsymbol{\mathcal{F}}}_o^T \begin{bmatrix} x_i \\ y_i \\ z_i \end{bmatrix} \\
&= \vec{\boldsymbol{\mathcal{F}}}_i^T \boldsymbol{C}_{io} \begin{bmatrix} x_i \\ y_i \\ z_i \end{bmatrix} \\
&= \vec{\boldsymbol{\mathcal{F}}}_i^T \begin{bmatrix} x_i \cos\theta_i + y_i \sin\theta_i \\ -x_i \sin\theta_i + y_i \cos\theta_i \\ z_i \end{bmatrix} \\
&= \vec{\boldsymbol{\mathcal{F}}}_i^T \begin{bmatrix} \ell_i \\ 0 \\ z_i \end{bmatrix}
\end{aligned} \tag{3.11}$$

where l_i is the length of pendulum i from the pivot point to the center of its magnet such that

$$x_i = \ell_i \cos\theta_i \qquad \text{and} \qquad y_i = \ell_i \sin\theta_i$$

Also note that $\vec{\boldsymbol{\mathcal{F}}}_o$ and $\vec{\boldsymbol{\mathcal{F}}}_i$ are the vectrices for frames F_o and F_i given by

$$\vec{\boldsymbol{\mathcal{F}}}_o = \begin{bmatrix} \hat{\mathrm{i}}_{\boldsymbol{o}} \\ \hat{\mathrm{j}}_{\boldsymbol{o}} \\ \hat{\mathrm{k}}_{\boldsymbol{o}} \end{bmatrix} \quad \text{and} \quad \vec{\boldsymbol{\mathcal{F}}}_i = \begin{bmatrix} \hat{\mathrm{i}}_{\boldsymbol{i}} \\ \hat{\mathrm{j}}_{\boldsymbol{i}} \\ \hat{\mathrm{k}}_{\boldsymbol{i}} \end{bmatrix}$$

Similarly to $\vec{r_i}$, $\vec{r_j}$ represents the position of magnet of pendulum j with respect to the origin O such that

$$\begin{aligned}
\vec{r_j} &= \vec{\boldsymbol{\mathcal{F}}}_o^T \boldsymbol{r}_{jo} \\
&= \vec{\boldsymbol{\mathcal{F}}}_o^T \begin{bmatrix} x_j \\ y_j \\ z_j \end{bmatrix} \\
&= \vec{\boldsymbol{\mathcal{F}}}_j^T \boldsymbol{C}_{jo} \begin{bmatrix} x_j \\ y_j \\ z_j \end{bmatrix} \\
&= \vec{\boldsymbol{\mathcal{F}}}_j^T \begin{bmatrix} x_j \cos\theta_i + y_j \sin\theta_i \\ -x_j \sin\theta_i + y_j \cos\theta_i \\ z_j \end{bmatrix} \\
&= \vec{\boldsymbol{\mathcal{F}}}_j^T \begin{bmatrix} \ell_j \\ 0 \\ z_j \end{bmatrix}
\end{aligned} \tag{3.12}$$

with ℓ_j being the length of pendulum j such that

$$x_j = \ell_j \cos\theta_i \qquad \text{and} \qquad y_j = \ell_j \sin\theta_i$$

Since the position of the center of each circular magnet with respect to the inertial origin O is given by $\vec{r_i}$ and $\vec{r_j}$, the relative position of centre of magnet i with respect to center of magnet j is given by

$$\begin{aligned}
\vec{r_{ij}} &= \vec{r_i} - \vec{r_j} \\
&= \vec{\boldsymbol{\mathcal{F}}}_o^T \boldsymbol{r}_{ijo} \\
&= \vec{\boldsymbol{\mathcal{F}}}_o^T \begin{bmatrix} x_i - x_j \\ y_i - y_j \\ z_i - z_j \end{bmatrix} \\
&= \vec{\boldsymbol{\mathcal{F}}}_o^T \begin{bmatrix} x_{ij} \\ y_{ij} \\ z_{ij} \end{bmatrix} \\
&= -\vec{r_{ji}}
\end{aligned} \tag{3.13}$$

Figure 3.2 is a top down view of a two pendulum system, where the black rectangles represent the magnets and the small blue and green rectangles represent their center of mass. As seen in the figure, $\vec{r_{ij}}$ can be split into two components; $\vec{s_{ij}}$ and $\vec{z_{ij}}$ in the $\vec{i_0} - \vec{j_0}$

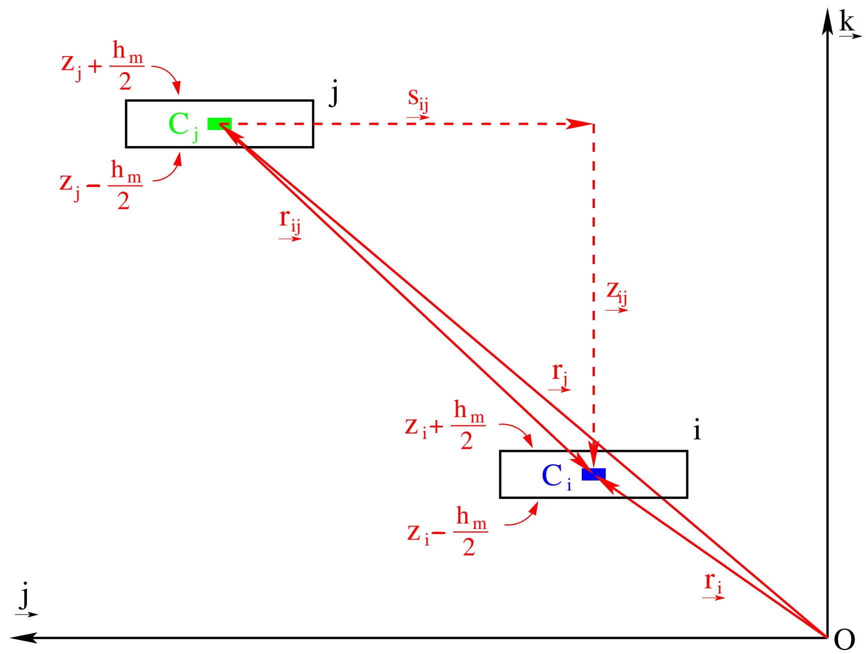

Figure 3.2: Top Down view of pendulums i and j.

plane and $\hat{\mathrm{k}}_{\mathbf{0}}$ direction respectively

$$\vec{r_{ij}} = \vec{s_{ij}} + \vec{z_{ij}} \tag{3.14}$$

With

$$\vec{s_{ij}} = \vec{\boldsymbol{\mathcal{F}}}_o^T \begin{bmatrix} x_{ij} \\ y_{ij} \\ 0 \end{bmatrix} \quad \text{and} \quad \vec{z_{ij}} = \vec{\boldsymbol{\mathcal{F}}}_o^T \begin{bmatrix} 0 \\ 0 \\ z_{ij} \end{bmatrix} = \vec{\boldsymbol{\mathcal{F}}}_o^T \begin{bmatrix} 0 \\ 0 \\ (i-j)\,d \end{bmatrix}$$

where d is the distance between each pendulum and we assume is the same throughout the system. We also assume that all pendulums have the same length ℓ so that the magnitude of $\vec{r_{ij}}$ is

$$|\vec{r_{ij}}| = \sqrt{\left(2\ell \sin\frac{\theta_{ij}}{2}\right)^2 + d^2} \tag{3.15}$$

and the magnitude of $\vec{s_{ij}}$ is

$$|\vec{s_{ij}}| = 2\ell \sin\frac{\theta_{ij}}{2} \tag{3.16}$$

Finally, with our magnet being cylindrical and homogeneously magnetized along the axial direction, we care about the flat surfaces of the magnets. As a result , we consider $\vec{h_i^-}$ and $\vec{h_i^+}$ as the positions of the center of the back and front faces respectively of magnet i with respect to the center of magnet j. With h_m being the the thickness of the magnets, $\vec{h_i^-}$ and $\vec{h_i^+}$ can be expressed as

$$\vec{h_i^-} = \vec{\boldsymbol{\mathcal{F}}}_i^T h_i^- = \vec{\boldsymbol{\mathcal{F}}}_i^T \begin{bmatrix} 0 \\ 0 \\ -\frac{h_m}{2} \end{bmatrix} \tag{3.17}$$

and

$$\vec{h_i^+} = \vec{\boldsymbol{\mathcal{F}}}_i^T h_i^+ = \vec{\boldsymbol{\mathcal{F}}}_i^T \begin{bmatrix} 0 \\ 0 \\ \frac{h_m}{2} \end{bmatrix} \tag{3.18}$$

3.2 Magnetic Forces

3.2.1 Magnetic Fields

The magnetic forces happen when one of the pendulums is present in the magnetic field of the other. Let's use Pendulum j as our reference. Both pendulums are identical with magnetization:

$$\vec{M} = \vec{\mathcal{F}}_j^T \begin{bmatrix} 0 \\ 0 \\ M_i \end{bmatrix} = \vec{\mathcal{F}}_j^T \begin{bmatrix} 0 \\ 0 \\ M_0 \end{bmatrix} \tag{3.19}$$

where the fixed frame for pendulum j is

$$\vec{\mathcal{F}}_j^T = \begin{bmatrix} i_j \\ j_j \\ k_j \end{bmatrix}, j = 1, 2, ...N \tag{3.20}$$

and N represents the number of identical pendulums.

According to the work of Bernal and Linares García [30], the magnetic field due to pendulum j is:

$$\vec{B}_j = \vec{\mathcal{F}}_{c_j}^T \begin{bmatrix} B_{\rho_j} \\ 0 \\ B_{z_j} \end{bmatrix} \tag{3.21}$$

where ρ_j is the radial coordinate in $\vec{F}_{c_j}^T$ the fixed frame cylindrical coordinate system at the center of magnet j where $\hat{\mathrm{k}}_{\boldsymbol{j}}$ and $\hat{\mathrm{k}}_{\boldsymbol{c_j}}$ align such that

$$\vec{\mathcal{F}}_{c_j}^T = \begin{bmatrix} \rho_j \\ \phi_j \\ K_j \end{bmatrix} \tag{3.22}$$

With B_ϕ being 0 due to the nature of our cylindrical magnets, we'll compute B_ρ and B_z using Equations (3.23) and (3.24) of [30]:

$$B_\rho\left(\rho_j, z\right) = \frac{\mu_0 M_0 R_m}{2} \int_0^\infty \left(e^{-k\|z^+\|} - e^{-k\|z^-\|}\right) J_1\left(kR_m\right) J_1\left(k\rho_j\right)\, dk \tag{3.23}$$

and

$$\begin{aligned} B_z\left(\rho_j, z\right) = &\quad \mu_0 M_0 \left(\rho, z^-\right) \\ &+ \frac{\mu_0 M_0 R_m}{2} \int_0^\infty \left(e^{-k\|z^+\|} - \operatorname{sgn}\left(z^-\right) \operatorname{sgn}\left(z^+\right) e^{-k\|z^-\|}\right) J_1\left(kR_m\right) J_0\left(k\rho_j\right)\, dk \end{aligned} \tag{3.24}$$

where z^-, being the smaller z-value, represents the location of an influence point with respect to the back face of magnet j such that

$$\begin{aligned} z^- &= z - \left(z_j - \frac{h_m}{2}\right) \\ &= z - z_j + \frac{h_m}{2} \end{aligned} \tag{3.25}$$

while z^+ is the larger z-value and the location of an influence point with respect to the front face of the magnet

$$
\begin{aligned}
z^{+} &= z - \left(z_j - \frac{h_m}{2}\right) - h_m \\
&= z - \left(z_j + \frac{h_m}{2}\right) \\
&= z - z_j - \frac{h_m}{2}
\end{aligned} \tag{3.26}
$$

As can be seen, both B_ρ and B_z are independent of ϕ and the variable ρ represents the radial coordinate of the magnet j in its fixed cylindrical frame, also identified as ρ_j.

B_ρ Magnetic Field

Starting with the magnetic field in the radial direction as it is the only one that affects the equation of motion of the system of interest. The integral in (3.23) is evaluated using (3.28) from Luke [31] which states that, for $a > 0$ and $b > 0$, integrals of the form

$$
I\left(\mu, \nu; \lambda\right) = \int_0^\infty e^{-pk} t^\lambda J_\mu\left(ak\right) J_\nu\left(bk\right)\, dk \tag{3.27}
$$

with inputs of $\mu = 1$, $\nu = 1$ and $\lambda = 0$, evaluate to

$$
I\left(1, 1; 0\right) = \frac{2}{\pi\kappa\sqrt{ab}} \left(\left(1 - \frac{1}{2}\kappa^2\right) K\left(\kappa\right) - E\left(\kappa\right)\right) \text{ for } \kappa^2 = \frac{4ab}{p^2 + \left(a + b\right)^2} \tag{3.28}
$$

with $K(\kappa)$ being the complete elliptic integral of the first kind, and $E(\kappa)$ the complete elliptic integral of the second kind defined by

$$
K(\kappa) = \int_0^{\frac{\pi}{2}} \frac{d\phi}{\sqrt{1 - \kappa^2 \sin\phi}}
$$

$$
E(\kappa) = \int_0^{\frac{\pi}{2}} \sqrt{1 - \kappa^2 \sin\phi}\, d\phi
$$

Assuming that all pendulums are equally spaced with a distance d and that pendulum i is located at $z_i = id$. To get the forces on magnet i due to magnet j of the $B_{\rho j}$ magnetic field will be evaluated both at the front and back face. Evaluating over the front face of the magnet in pendulum i with $z = z_i + \frac{h_m}{2}$ the magnetic field yields

$$\begin{aligned}
B_{\rho_j}\left(\rho_j, z\right)\Big|_{z_i+\frac{h_m}{2}} &= \frac{\mu_0 M_0 R_m}{2} \int_0^\infty \left(e^{-k||z^+||} - e^{-k||z^-||}\right) J_1\left(kR_m\right) J_1\left(k\rho_j\right)\, dk\Bigg|_{z_i+\frac{h_m}{2}} \\
&= \frac{\mu_0 M_0 R_m}{2} \int_0^\infty \left(e^{-k||(i-j)d||} - e^{-k||(i-j)d+h_m||}\right) J_1\left(kR_m\right) J_1\left(k\rho_j\right)\, dk \\
&= \frac{\mu_0 M_0 R_m}{2} \int_0^\infty e^{-k||(i-j)d||} J_1\left(kR_m\right) J_1\left(k\rho_j\right)\, dk \\
&\quad - \frac{\mu_0 M_0 R_m}{2} \int_0^\infty e^{-k||(i-j)d+h_m||} J_1\left(kR_m\right) J_1\left(k\rho_j\right)\, dk
\end{aligned} \tag{3.29}$$

now evaluating over the back face of the magnet in pendulum i at $z = z_i - \frac{h_m}{2}$ yields

$$\begin{aligned}
B_{\rho_j}\left(\rho_j, z\right)\Big|_{z_i-\frac{h_m}{2}} &= \frac{\mu_0 M_0 R_m}{2} \int_0^\infty \left(e^{-k||z^+||} - e^{-k||z^-||}\right) J_1\left(kR_m\right) J_1\left(k\rho_j\right)\, dk\Bigg|_{z_i-\frac{h_m}{2}} \\
&= \frac{\mu_0 M_0 R_m}{2} \int_0^\infty \left(e^{-k||(i-j)d-h_m||} - e^{-k||(i-j)d||}\right) J_1\left(kR_m\right) J_1\left(k\rho_j\right)\, dk \\
&= \frac{\mu_0 M_0 R_m}{2} \int_0^\infty e^{-k||(i-j)d-h_m||} J_1\left(kR_m\right) J_1\left(k\rho_j\right)\, dk \\
&\quad - \frac{\mu_0 M_0 R_m}{2} \int_0^\infty e^{-k||(i-j)d||} J_1\left(kR_m\right) J_1\left(k\rho_j\right)\, dk
\end{aligned} \tag{3.30}$$

Ignoring the case where $i = j$ because that corresponds to self influence, we integrate the B_ρ using equation (3.28) with inputs:

$$a = R_m, \qquad b = \rho_j,$$

$$p_1 = ||\left(i-j\right)d||, \qquad p_2 = ||\left(i-j\right)d - h_m||, \qquad p_3 = ||\left(i-j\right)d + h_m||$$

which gives for p_1, p_2 and p_3 respectively

$$
\begin{aligned}
\kappa_1^2 &= \frac{4ab}{p_1^2 + (a+b)^2} \\
&= \frac{4R_m\rho_j}{(i-j)^2 d^2 + (R_m+\rho_j)^2} \\
\kappa_2^2 &= \frac{4ab}{p_2^2 + (a+b)^2} \\
&= \frac{4R_m\rho_j}{||(i-j)\,d - h_m||^2 + (R_m+\rho_j)^2} \\
\kappa_3^2 &= \frac{4ab}{p_3^2 + (a+b)^2} \\
&= \frac{4R_m\rho_j}{||(i-j)\,d + h_m||^2 + (R_m+\rho_j)^2}
\end{aligned}
$$

Thus equations (3.29) and (3.30) respectively become

$$
\begin{aligned}
B_{\rho_j}(\rho_j, z)\big|_{z_i+\frac{h_m}{2}} = &\quad \frac{\mu_0 M_0 R_m}{2}\int_0^\infty e^{-k||(i-j)d||} J_1(kR_m)\, J_1(k\rho_j)\, dk \\
&- \frac{\mu_0 M_0 R_m}{2}\int_0^\infty e^{-k||(i-j)d+h_m||} J_1(kR_m)\, J_1(k\rho_j)\, dk \\
= &\quad \frac{\mu_0 M_0 R_m}{\pi\sqrt{R_m\rho_j}}\left(\frac{1}{\kappa_1}\left(\left(1-\frac{1}{2}\kappa_1^2\right)K(\kappa_1) - E(\kappa_1)\right)\right) - \\
&\quad \left(\frac{1}{\kappa_3}\left(\left(1-\frac{1}{2}\kappa_3^2\right)K(\kappa_3) - E(\kappa_3)\right)\right)
\end{aligned}
\tag{3.31}
$$

$$
\begin{aligned}
B_{\rho_j}(\rho_j, z)\big|_{z_i-\frac{h_m}{2}} = &\quad \frac{\mu_0 M_0 R_m}{2}\int_0^\infty e^{-k||(i-j)d||} J_1(kR_m)\, J_1(k\rho_j)\; dk \\
& - \frac{\mu_0 M_0 R_m}{2}\int_0^\infty e^{-k||(i-j)d+h_m||} J_1(kR_m)\, J_1(k\rho_j)\; dk \\
= &\quad \frac{\mu_0 M_0 R_m}{\pi\sqrt{R_m\rho_j}}\left(\frac{1}{\kappa_2}\left(\left(1-\frac{1}{2}\kappa_2^2\right)K(\kappa_2)-E(\kappa_2)\right)\right)- \\
&\quad \left(\frac{1}{\kappa_1}\left(\left(1-\frac{1}{2}\kappa_1^2\right)K(\kappa_1)-E(\kappa_1)\right)\right)
\end{aligned} \tag{3.32}
$$

and by subtracting (3.31) and (3.32)

$$
\begin{aligned}
B_{\rho j}\big|_{z_i+\frac{h_m}{2}} - B_{\rho j}\big|_{z_i-\frac{h_m}{2}} = & \frac{\mu_0 M_0 R_m}{\pi\sqrt{R_m\rho_j}}\Bigg[\frac{1}{\kappa_1}\left(\left(1-\frac{1}{2}\kappa_1^2\right)K(\kappa_1)-E(\kappa_1)\right)- \\
& \frac{1}{\kappa_3}\left(\left(1-\frac{1}{2}\kappa_3^2\right)K(\kappa_3)-E(\kappa_3)\right)- \\
& \frac{1}{\kappa_2}\left(\left(1-\frac{1}{2}\kappa_2^2\right)K(\kappa_2)-E(\kappa_2)\right)- \\
& \frac{1}{\kappa_1}\left(\left(1-\frac{1}{2}\kappa_1^2\right)K(\kappa_1)-E(\kappa_1)\right)\Bigg] \qquad (3.33) \\
= & \frac{\mu_0 M_0 R_m}{\pi\sqrt{R_m\rho_j}}\Bigg[\frac{2}{\kappa_1}\left(\left(1-\frac{1}{2}\kappa_1^2\right)K(\kappa_1)-E(\kappa_1)\right)- \\
& \frac{1}{\kappa_2}\left(\left(1-\frac{1}{2}\kappa_2^2\right)K(\kappa_2)-E(\kappa_2)\right)- \\
& \frac{1}{\kappa_3}\left(\left(1-\frac{1}{2}\kappa_3^2\right)K(\kappa_3)-E(\kappa_3)\right)\Bigg]
\end{aligned}
$$

B_z Magnetic Field

Now for completeness let's compute the magnetic field B_z. Evaluating the integral in (3.24) using the equation the same equation (3.27) from Luke [31] with inputs $\mu = 1$, $\nu = 0$ and

$\lambda = 0,$

$$\begin{cases} I\left(1,0;0\right) = -\frac{p\kappa K(\kappa)}{2\pi a\sqrt{ab}} + \frac{\Lambda_0(\alpha,\beta)}{2a} & \text{if} \quad a < b \\ I\left(1,0;0\right) = -\frac{p\kappa K(\kappa)}{2\pi a^2} + \frac{1}{2a} & \text{if} \quad a = b \\ I\left(1,0;0\right) = -\frac{p\kappa K(\kappa)}{2\pi a\sqrt{ab}} - \frac{\Lambda_0(\alpha,\beta)}{2a} + \frac{1}{a} & \text{if} \quad a > b \end{cases} \tag{3.34}$$

with

$$\sin(\alpha) = \kappa, \qquad \kappa^2 = \frac{4ab}{p^2+(a+b)^2}, \qquad \sin(\beta) = \frac{p}{\sqrt{(a-b)^2+p^2}}$$

where K is the complete elliptic integral of the first kind, defined by

$$K(\kappa^2) = \int_0^{\frac{\pi}{2}} \frac{d\phi}{\sqrt{1-\kappa^2\,\sin^2\phi}}$$

E the complete elliptic integral of the second kind, defined by

$$E(\kappa^2) = \int_0^{\frac{\pi}{2}} \sqrt{1-\kappa^2\sin^2\phi}\,d\phi$$

and $\Lambda_0(\alpha,\beta)$ is Heuman's [32] complete elliptic integral of the third kind, defined as follows:

$$\Lambda_0(\alpha,\beta) = \frac{2}{\pi}\,\Lambda(\alpha,\beta)$$

and that Laplace's form of the complete elliptic integral of the third kind is

$$\Pi(\alpha,q) = \int_0^{\frac{\pi}{2}} \frac{1}{(1-q\,\sin^2\psi)\sqrt{1-\kappa^2\,\sin^2\psi}}\,d\psi$$

where $\kappa = \sin\alpha$ and q is determined from the relation

$$\sin^2\beta = \frac{q-\kappa^2}{\kappa'^2\,q} \quad \text{where recall} \quad \kappa'^2 = 1-\kappa^2$$

provided that $\kappa^2 \leq q \leq 1$. Solving for q yields

$$q = \frac{\kappa^2}{1-(1-\kappa^2)\,\sin^2(\beta)}$$

With reference to Heuman [32], $\Pi(\alpha, q)$ has different forms depending on the value of q and that of

$$\tau(q) = q\,(q-\kappa^2)\,(q-1)$$

If $\tau(q) = 0$, by $q = 0$, κ^2 or 1, then the integral $\Pi(\alpha, q)$ can be expressed by integrals of the first and the second kind, together with elementary functions.
If $\tau(q) < 0$, it means we have a circular form so that either $\kappa^2 < q < 1$ or $q < 0$, Heuman only deals with the circular case.
The hyperbolic form arises when $\tau(q) > 0$ so that either $0 < q < \kappa^2$ or $q > 1$.
For $\kappa^2 < q < 1$, Heuman next defines Q as

$$Q = \frac{\kappa'^2\,\cos\beta\,\sin\beta}{\sqrt{1-\kappa'^2\,\sin^2\beta}}$$

where

$$\sin^2\beta = \frac{q-\kappa^2}{\kappa'^2\,q} \quad \text{and} \quad \cos^2\beta = \frac{(1-q)\,\kappa^2}{\kappa'^2\,q} \tag{3.35}$$

where, for the complementary modulus $\kappa' = \sqrt{1-\kappa^2}$, Finally, using the relations above, we can express Heuman's complete elliptic integral of the third kind as follow

$$\Lambda(\alpha, \beta) = Q\,\Pi(\alpha, q)$$

so that

$$\Lambda_0(\alpha, \beta) = \frac{2}{\pi}\,Q\,\Pi(\alpha, q)$$

which is what appears in the integral tables provided by Yudell [31]. This means that (3.34) can be written as

$$I(1,0;0) = \begin{cases} -\frac{p\,\kappa\,K(\kappa)}{2\pi\,R\sqrt{\rho_j\,R}} - \frac{\frac{2}{\pi}\,Q\,\Pi(\alpha,q)}{2\,R} + \frac{1}{R} & \text{for } \rho_j < R \\ -\frac{p\,\kappa\,K(\kappa)}{2\pi\,R^2} + \frac{1}{2\,R} & \text{for } \rho_j = R, \\ -\frac{p\,\kappa\,K(\kappa)}{2\pi\,R\sqrt{\rho_j\,R}} + \frac{\frac{2}{\pi}\,Q\,\Pi(\alpha,q)}{2\,R} & \text{for } \rho_j > R \end{cases} \tag{3.36}$$

where here

$$\kappa'^2 = 1-\kappa^2$$

$$Q = \frac{\kappa'^2\,\cos\beta\,\sin\beta}{\sqrt{1-\kappa'^2\,\sin^2\beta}}$$

Keeping the same assumptions as for B_ρ with regards to the uniform spacing and pendulum i located at $z_i = id$. To get the forces on magnet i due to magnet j of the B_z, magnetic field will be evaluated both at the front and back face. Evaluating over the front face of the magnet in pendulum i with $z = z_i + \frac{h_m}{2}$ the magnetic field yields

$$
\begin{aligned}
B_{z_j}\left(\rho_j, z\right)\Big|_{z_i+\frac{h_m}{2}} = & \, \mu_0 M_0\left(\rho_j, z^-\right) + \\
& \frac{\mu_0 M_0 R_m}{2}\int_0^\infty \left(e^{-k||z^+||} - \operatorname{sgn}\left(z^-\right)\operatorname{sgn}\left(z^+\right)e^{-k||z^-||}\right)\times \\
& \qquad J_1\left(kR_m\right)J_0\left(k\rho_j\right)\,dk\Big|_{z_i+\frac{h_m}{2}} \\
= & \, \mu_0 M_0\left(\rho_j, (i-j)\,d + h_m\right) + \\
& \frac{\mu_0 M_0 R_m}{2}\int_0^\infty \left(e^{-k||(i-j)d||} - \operatorname{sgn}\left((i-j)\,d + h_m\right)\right. \\
& \qquad \left.\operatorname{sgn}\left((i-j)\,d\right)e^{-k||(i-j)d+h_m||}\right)J_1\left(kR_m\right)J_0\left(k\rho_j\right)\,dk \\
= & \, \mu_0 M_0\left(\rho_j, (i-j)\,d + h_m\right) + \\
& \frac{\mu_0 M_0 R_m}{2}\int_0^\infty e^{-k||(i-j)d||}J_1\left(kR_m\right)J_0\left(k\rho_j\right)\,dk - \\
& \frac{\mu_0 M_0 R_m}{2}\int_0^\infty e^{-k||(i-j)d-h_m||}J_1\left(kR_m\right)J_0\left(k\rho_j\right)\,dk
\end{aligned}
\tag{3.37}
$$

Evaluating over the back face of the magnet in pendulum i with $z = z_i - \frac{h_m}{2}$ the magnetic field yields

$$\begin{aligned}
B_{z_j}\left(\rho_j, z\right)\Big|_{z_i-\frac{h_m}{2}} =&\, \mu_0 M_0\left(\rho_j, z^-\right) + \\
&\frac{\mu_0 M_0 R_m}{2}\int_0^\infty \left(e^{-k||z^+||} - \operatorname{sgn}\left(z^-\right)\operatorname{sgn}\left(z^+\right)e^{-k||z^-||}\right)\times \\
&\qquad J_1\left(kR_m\right)J_0\left(k\rho_j\right)\,dk\Big|_{z_i-\frac{h_m}{2}} \\
=&\, \mu_0 M_0\left(\rho_j, \left(i-j\right)d\right) + \\
&\frac{\mu_0 M_0 R_m}{2}\int_0^\infty \left(e^{-k||(i-j)d-h_m||} - \operatorname{sgn}\left(\left(i-j\right)d + h_m\right)\right. \\
&\qquad \left.\operatorname{sgn}\left(\left(i-j\right)d\right)e^{-k||(i-j)d||}\right)J_1\left(kR_m\right)J_0\left(k\rho_j\right)\,dk \\
=&\, \mu_0 M_0\left(\rho_j, \left(i-j\right)d\right) + \\
&\frac{\mu_0 M_0 R_m}{2}\int_0^\infty e^{-k||(i-j)d-h_m||}J_1\left(kR_m\right)J_0\left(k\rho_j\right)\,dk - \\
&\frac{\mu_0 M_0 R_m}{2}\int_0^\infty e^{-k||(i-j)d||}J_1\left(kR_m\right)J_0\left(k\rho_j\right)\,dk
\end{aligned} \tag{3.38}$$

Ignoring the case where $i - j = 0$ because that's when $\rho_j = 0$, we integrate the B_z using equation (3.34) with inputs:

$$\begin{aligned}
&a = R_m, \qquad b = \rho_j, \\
&p_1 = ||\left(i-j\right)d||, \qquad p_2 = ||\left(i-j\right)d - h_m||, \qquad p_3 = ||\left(i-j\right)d + h_m||
\end{aligned}$$

which gives for p_1, p_2 and p_3 respectively

$$\begin{aligned}
\alpha_1 &= \arcsin\left(\kappa_1\right)\\
\alpha_2 &= \arcsin\left(\kappa_2\right)\\
\alpha_3 &= \arcsin\left(\kappa_3\right)\\
\beta_1 &= \arcsin\left(\frac{p_1}{\sqrt{\left(a-b\right)^2+p_1^2}}\right)\\
\beta_2 &= \arcsin\left(\frac{p_2}{\sqrt{\left(a-b\right)^2+p_2^2}}\right)\\
\beta_3 &= \arcsin\left(\frac{p_3}{\sqrt{\left(a-b\right)^2+p_3^2}}\right)
\end{aligned}$$

Thus the B_z integrations in (3.37) and (3.38) become

- **When** $\rho > R_m$:

$$\begin{aligned}
B_{z_j}\left(\rho_j, z\right)\Big|_{z_i+\frac{h_m}{2}} =& \mu_0 M_0\left(\rho_j, \left(i-j\right)d + h_m\right) + \\
& \frac{\mu_0 M_0 R_m}{2}\int_0^\infty e^{-k||(i-j)d||} J_1\left(kR_m\right) J_0\left(k\rho_j\right)\, dk - \\
& \frac{\mu_0 M_0 R_m}{2}\int_0^\infty e^{-k||(i-j)d+h_m||} J_1\left(kR_m\right) J_0\left(k\rho_j\right)\, dk \\
=& \mu_0 M_0\left(\rho_j, p_3\right) - \\
& \frac{\mu_0 M_0 R_m}{4a}\left(\frac{p_1\kappa_1 K\left(\kappa_1\right)}{\pi\sqrt{ab}} - \Lambda_0\left(\alpha_1, q_1\right) - \right.\\
& \left.\frac{p_3\kappa_3 K\left(\kappa_3\right)}{\pi\sqrt{ab}} + \Lambda_0\left(\alpha_3, \beta_3\right)\right)
\end{aligned} \tag{3.39}$$

$$
\begin{aligned}
B_{z_j}\left(\rho_j, z\right)\Big|_{z_i-\frac{h_m}{2}} =& \mu_0 M_0\left(\rho_j, (i-j)\, d\right) + \\
& \frac{\mu_0 M_0 R_m}{2} \int_0^\infty e^{-k||(i-j)d-h_m||} J_1\left(kR_m\right) J_0\left(k\rho_j\right)\, dk - \\
& \frac{\mu_0 M_0 R_m}{2} \int_0^\infty e^{-k||(i-j)d||} J_1\left(kR_m\right) J_0\left(k\rho_j\right)\, dk \\
=& \mu_0 M_0\left(\rho_j, p_1\right) - \\
& \frac{\mu_0 M_0 R_m}{4a} \left(\frac{p_2 \kappa_2 K\left(\kappa_2\right)}{\pi\sqrt{ab}} - \Lambda_0\left(\alpha_2, \beta_2\right) - \right. \\
& \left. \frac{p_1 \kappa_1 K\left(\kappa_1\right)}{\pi\sqrt{ab}} + \Lambda_0\left(\alpha_1, q_1\right) \right)
\end{aligned}
\tag{3.40}
$$

Subtracting (3.39) from (3.40)

$$\begin{aligned}
B_{z_j}\Big|_{z_i+\frac{h_m}{2}} - B_{z_j}\Big|_{z_i-\frac{h_m}{2}} &= \frac{\mu_0 M_0 R_m}{4a}\left(\frac{p_1\kappa_1 K\left(\kappa_1\right)}{\pi\sqrt{ab}} - \Lambda_0\left(\alpha_1,\beta_1\right)\right. \\
&\quad \left. - \frac{p_3\kappa_3 K\left(\kappa_3\right)}{\pi\sqrt{ab}} + \Lambda_0\left(\alpha_3,\beta_3\right)\right) - \\
&\quad \frac{\mu_0 M_0 R_m}{4a}\left(\frac{p_2\kappa_2 K\left(\kappa_2\right)}{\pi\sqrt{ab}} - \Lambda_0\left(\alpha_2,\beta_2\right) - \right. \\
&\quad \left. \frac{p_1\kappa_1 K\left(\kappa_1\right)}{\pi\sqrt{ab}} + \Lambda_0\left(\alpha_1,\beta_1\right)\right) \\
&= \frac{\mu_0 M_0 R_m}{4a}\left(\frac{p_1\kappa_1 K\left(\kappa_1\right)}{\pi\sqrt{ab}} - \Lambda_0\left(\alpha_1,\beta_1\right) - \right. \\
\frac{p_3\kappa_3 K\left(\kappa_3\right)}{\pi\sqrt{ab}} + \Lambda_0\left(\alpha_3,\beta_3\right) - \\
&\quad \left. \frac{p_2\kappa_2 K\left(\kappa_2\right)}{\pi\sqrt{ab}} + \Lambda_0\left(\alpha_2,\beta_2\right) + \frac{p_1\kappa_1 K\left(\kappa_1\right)}{\pi\sqrt{ab}} - \Lambda_0\left(\alpha_1,\beta_1\right)\right) \\
&= \frac{\mu_0 M_0 R_m}{4a}\left(2\frac{p_1\kappa_1 K\left(\kappa_1\right)}{\pi\sqrt{ab}} - 2\Lambda_0\left(\alpha_1,\beta_1\right) - \right. \\
&\quad \frac{p_2\kappa_2 K\left(\kappa_2\right)}{\pi\sqrt{ab}} + \Lambda_0\left(\alpha_2,\beta_2\right) - \\
&\quad \left. \frac{p_3\kappa_3 K\left(\kappa_3\right)}{\pi\sqrt{ab}} + \Lambda_0\left(\alpha_3,\beta_3\right)\right)
\end{aligned} \tag{3.41}$$

- **When $\rho < R_m$:**

$$
\begin{aligned}
B_{z_j}\left(\rho_j, z\right)\Big|_{z_i+\frac{h_m}{2}} &= \mu_0 M_0\left(\rho_j, (i-j)\,d + h_m\right) + \\
&\qquad \frac{\mu_0 M_0 R_m}{2} \int_0^{\infty} e^{-k||(i-j)d||} J_1\left(K R_m\right) J_0\left(K \rho_j\right)\, dk \\
&\quad - \frac{\mu_0 M_0 R_m}{2} \int_0^{\infty} e^{-k||(i-j)d+h_m||} J_1\left(K R_m\right) J_0\left(K \rho_j\right)\, dk \\
&= \mu_0 M_0\left(\rho_j, p_3\right) \\
&\quad - \frac{\mu_0 M_0 R_m}{4a}\left(\frac{p_1 \kappa_1 K\left(\kappa_1\right)}{\pi\sqrt{ab}} + \Lambda_0\left(\alpha_1, \beta_1\right) - 2 - \right. \\
&\quad \left. \frac{p_3 \kappa_3 K\left(\kappa_3\right)}{\pi\sqrt{ab}} - \Lambda_0\left(\alpha_3, \beta_3\right) + 2\right)
\end{aligned}
\tag{3.42}
$$

$$
\begin{aligned}
B_{z_j}\left(\rho_j, z\right)\Big|_{z_i-\frac{h_m}{2}} &= \mu_0 M_0\left(\rho_j, (i-j)\,d\right) + \\
&\quad \frac{\mu_0 M_0 R_m}{2} \int_0^{\infty} e^{-k||(i-j)d-h_m||} J_1\left(K R_m\right) J_0\left(K \rho_j\right)\, dk - \\
&\quad \frac{\mu_0 M_0 R_m}{2} \int_0^{\infty} e^{-k||(i-j)d||} J_1\left(K R_m\right) J_0\left(K \rho_j\right)\, dk \\
&= \mu_0 M_0\left(\rho_j, p_1\right) - \\
&\quad \frac{\mu_0 M_0 R_m}{4a}\left(\frac{p_2 \kappa_2 K\left(\kappa_2\right)}{\pi\sqrt{ab}} + \Lambda_0\left(\alpha_2, \beta_2\right) - 2 - \right. \\
&\quad \left. \frac{p_1 \kappa_1 K\left(\kappa_1\right)}{\pi\sqrt{ab}} - \Lambda_0\left(\alpha_1, \beta_1\right) + 2\right)
\end{aligned}
\tag{3.43}
$$

Subtracting (3.42) from (3.43)

$$\begin{aligned}
B_{z_j}\Big|_{z_i+\frac{h_m}{2}} - B_{z_j}\Big|_{z_i-\frac{h_m}{2}} &= \frac{\mu_0 M_0 R_m}{4a}\left(\frac{p_1\kappa_1 K\left(\kappa_1\right)}{\pi\sqrt{ab}} + \Lambda_0\left(\alpha_1,\beta_1\right)\right. \\
&\quad \left. - \frac{p_3\kappa_3 K\left(\kappa_3\right)}{\pi\sqrt{ab}} - \Lambda_0\left(\alpha_3,\beta_3\right)\right) - \\
&\quad \frac{\mu_0 M_0 R_m}{4a}\left(\frac{p_2\kappa_2 K\left(\kappa_2\right)}{\pi\sqrt{ab}} + \Lambda_0\left(\alpha_2,\beta_2\right)\right. \\
&\quad \left. - \frac{p_1\kappa_1 K\left(\kappa_1\right)}{\pi\sqrt{ab}} - \Lambda_0\left(\alpha_1,\beta_1\right)\right) \\
&= \frac{\mu_0 M_0 R_m}{4a}\left(\frac{p_1\kappa_1 K\left(\kappa_1\right)}{\pi\sqrt{ab}} + \Lambda_0\left(\alpha_1,\beta_1\right) - \right. \\
&\quad \frac{p_3\kappa_3 K\left(\kappa_3\right)}{\pi\sqrt{ab}} - \Lambda_0\left(\alpha_3,\beta_3\right) - \\
&\quad \frac{p_2\kappa_2 K\left(\kappa_2\right)}{\pi\sqrt{ab}} - \Lambda_0\left(\alpha_2,\beta_2\right) + \\
&\quad \left. \frac{p_1\kappa_1 K\left(\kappa_1\right)}{\pi\sqrt{ab}} + \Lambda_0\left(\alpha_1,\beta_1\right)\right) \\
&= \frac{\mu_0 M_0 R_m}{4a}\left(2\frac{p_1\kappa_1 K\left(\kappa_1\right)}{\pi\sqrt{ab}} + 2\Lambda_0\left(\alpha_1,\beta_1\right) - \right. \\
&\quad \frac{p_2\kappa_2 K\left(\kappa_2\right)}{\pi\sqrt{ab}} - \Lambda_0\left(\alpha_2,\beta_2\right) - \\
&\quad \left. \frac{p_3\kappa_3 K\left(\kappa_3\right)}{\pi\sqrt{ab}} - \Lambda_0\left(\alpha_3,\beta_3\right)\right)
\end{aligned} \tag{3.44}$$

- **When $\rho = R_m$:**

$$
\begin{aligned}
B_{z_j}\left(\rho_j, z\right)\Big|_{z_i+\frac{h_m}{2}} = & \mu_0 M_0\left(\rho_j, (i-j)\, d + h_m\right) + \\
& \frac{\mu_0 M_0 R_m}{2} \int_0^\infty e^{-k||(i-j)d||} J_1\left(K R_m\right) J_0\left(K \rho_j\right)\, dk - \\
& \frac{\mu_0 M_0 R_m}{2} \int_0^\infty e^{-k||(i-j)d-h_m||} J_1\left(K R_m\right) J_0\left(K \rho_j\right)\, dk \\
= & \mu_0 M_0\left(\rho_j, p_3\right) - \\
& \frac{\mu_0 M_0 R_m}{4}\left(\frac{p_1 \kappa_1 K\left(\kappa_1\right)}{\pi a^2} - \frac{1}{a} - \frac{p_3 \kappa_3 K\left(\kappa_3\right)}{\pi a^2} + \frac{1}{a}\right)
\end{aligned}
\tag{3.45}
$$

$$
\begin{aligned}
B_{z_j}\left(\rho_j, z\right)\Big|_{z_i-\frac{h_m}{2}} = & \mu_0 M_0\left(\rho_j, (i-j)\, d\right) + \\
& \frac{\mu_0 M_0 R_m}{2} \int_0^\infty e^{-k||(i-j)d-h_m||} J_1\left(k R_m\right) J_0\left(k \rho_j\right)\, dk - \\
& \frac{\mu_0 M_0 R_m}{2} \int_0^\infty e^{-k||(i-j)d||} J_1\left(k R_m\right) J_0\left(k \rho_j\right)\, dk \\
= & \mu_0 M_0\left(\rho_j, p_1\right) - \\
& \frac{\mu_0 M_0 R_m}{4}\left(\frac{p_2 \kappa_2 K\left(\kappa_2\right)}{\pi a^2} - \frac{1}{a} - \right. \\
& \left. \frac{p_1 \kappa_1 K\left(\kappa_1\right)}{\pi a^2} + \frac{1}{a}\right)
\end{aligned}
\tag{3.46}
$$

Subtracting (3.45) from (3.46)

$$
\begin{aligned}
B_{z_j}\Big|_{z_i+\frac{h_m}{2}} - B_{z_j}\Big|_{z_i-\frac{h_m}{2}} &= \frac{\mu_0 M_0 R_m}{2a^2\pi}\left(p_1\kappa_1 K\left(\kappa_1\right) - p_3\kappa_3 K\left(\kappa_3\right)\right) - \\
&\quad \frac{\mu_0 M_0}{2a\pi}\left(p_2\kappa_2 K\left(\kappa_2\right) - p_1\kappa_1 K\left(\kappa_1\right)\right) \\
&= \frac{\mu_0 M_0}{2a\pi}\left(p_1\kappa_1 K\left(\kappa_1\right) - p_3\kappa_3 K\left(\kappa_3\right) - \right. \\
&\quad \left. p_2\kappa_2 K\left(\kappa_2\right) + p_1\kappa_1 K\left(\kappa_1\right)\right) \\
&= \frac{\mu_0 M_0}{2a\pi}\left(2p_1\kappa_1 K\left(\kappa_1\right) - p_2\kappa_2 K\left(\kappa_2\right) - p_3\kappa_3 K\left(\kappa_3\right)\right)
\end{aligned}
\tag{3.47}
$$

3.2.2 Integration of Forces

According to Eq 3.9 from Avila Bernal and Linares Garcia [30], we consider the force on magnet i due to magnet j to be

$$\vec{F}_{ij} = \oint \left(\vec{M}_i.\vec{n}_i\right)\vec{B}_j ds_i \tag{3.48}$$

where s_i is the surface of magnet i. In our system, all the magnets are arranged with the $\hat{k_i}$ vectors all parallel to $\hat{k_0}$ thus getting $M_i = M_0$ so

$$\vec{F}_{ij} = \oint \pm M_0 \vec{B}_j ds_i \tag{3.49}$$

The plus and negative signs in the equation above refer to the normal vector pointing to the negative direction at $z_i - h_m/2$ and the normal vector points to the positive direction at $z_i + h_m/2$. Therefore, the full force equation becomes

$$\begin{aligned}
\vec{F}_{ij} &= \iint M_0 \vec{B}_j \rho \, d\rho \, d\phi \Big|_{z_i+\frac{h_m}{2}} - \iint M_0 \vec{B}_j \rho \, d\rho \, d\phi \Big|_{z_i-\frac{h_m}{2}} \\
&= \vec{\boldsymbol{\mathcal{F}}}_i^T \iint M_0 \begin{bmatrix} B_{xj} \\ B_{yj} \\ B_{zj} \end{bmatrix} \rho \, d\rho \, d\phi \Bigg|_{z_i+\frac{h_m}{2}} - \vec{\boldsymbol{\mathcal{F}}}_i^T \iint M_0 \begin{bmatrix} B_{xj} \\ B_{yj} \\ B_{zj} \end{bmatrix} \rho \, d\rho \, d\phi \Bigg|_{z_i-\frac{h_m}{2}} \\
&= \vec{\boldsymbol{\mathcal{F}}}_i^T \begin{bmatrix} F_{ij_x} \\ F_{ij_y} \\ F_{ij_z} \end{bmatrix}
\end{aligned} \tag{3.50}$$

Magnetic Field Transformation Matrices

Using transformation matrices from (3.5) and (3.9), we can write $\vec{B}_j$ in Frame $\vec{F}_i$ as

$$
\begin{aligned}
\vec{B}_j &= \vec{\boldsymbol{\mathcal{F}}}_i^T \boldsymbol{C}_{ij} \boldsymbol{C}_{jc_j} \begin{bmatrix} B_{\rho_j} \\ 0 \\ B_{z_j} \end{bmatrix} \\
&= \vec{\boldsymbol{\mathcal{F}}}_i^T \begin{bmatrix} \cos\theta_{ji} & \sin\theta_{ji} & 0 \\ -\sin\theta_{ji} & \cos\theta_{ji} & 0 \\ 0 & 0 & 1 \end{bmatrix} \begin{bmatrix} \cos\phi_j & \sin\phi_j & 0 \\ -\sin\phi_j & \cos\phi_j & 0 \\ 0 & 0 & 1 \end{bmatrix} \begin{bmatrix} B_{\rho_j} \\ 0 \\ B_{z_j} \end{bmatrix} \\
&= \vec{\boldsymbol{\mathcal{F}}}_i^T \begin{bmatrix} \cos\theta_{ji} & \sin\theta_{ji} & 0 \\ -\sin\theta_{ji} & \cos\theta_{ji} & 0 \\ 0 & 0 & 1 \end{bmatrix} \begin{bmatrix} \cos\phi_j B_{\rho_j} \\ \sin\phi_j B_{\rho_j} \\ B_{z_j} \end{bmatrix} \\
&= \vec{\boldsymbol{\mathcal{F}}}_i^T \begin{bmatrix} \cos\theta_{ji}\cos\phi_j B_{\rho_j} + \sin\theta_{ji}\sin\phi_j B_{\rho_j} \\ -\sin\theta_{ji}\cos\phi_j B_{\rho_j} + \cos\theta_{ji}\sin\phi_j B_{\rho_j} \\ B_{z_j} \end{bmatrix} \\
&= \vec{\boldsymbol{\mathcal{F}}}_i^T \begin{bmatrix} (\cos\theta_{ji}\cos\phi_j + \sin\theta_{ji}\sin\phi_j)\, B_{\rho_j} \\ (\cos\theta_{ji}\sin\phi_j - \sin\theta_{ji}\cos\phi_j)\, B_{\rho_j} \\ B_{z_j} \end{bmatrix} \\
&= \vec{\boldsymbol{\mathcal{F}}}_i^T \begin{bmatrix} B_{x_j} \\ B_{y_j} \\ B_{z_j} \end{bmatrix}
\end{aligned}
\tag{3.51}
$$

We need this transformation matrix to calculate the force acting on magnet i due to magnet j when investigating $\vec{B}_j$. The integration is in the sense of a Riemann integral so it can be thought of as the sum of infinitesimal vectors and to do that everything must be expressed in the same frame.

Integration of F_{ij_x}

Using equations (3.50) and (3.33), we can find F_{ij_x}. The integration for both ρ and ϕ will depend on the sign of θ_{ij}. From the cases mentioned in Appendix A, the limit of integration over ρ can be simplified to be from $R + |s_{ij}|$ to $|R - |s_{ij}||$ for all cases.

As for the limits of integration over ϕ, or in other words over ψ, they can be

$$\begin{cases} \int_{\psi_j(\rho_j)}^{\pi} d\psi & \text{if} \quad s_{ij} < 0 \\ \\ \int_{0}^{\psi_j(\rho_j)} d\psi & \text{if} \quad s_{ij} > 0 \end{cases} \tag{3.52}$$

where $\psi_j\left(\rho_j\right)$ is given by equation (A.2), with

$$s_{ij} = 2\ell \sin\left(\frac{\theta_{ij}}{2}\right)$$

Using the transformation matrices, and integrating over ψ instead of ϕ yields

$$\begin{aligned} F_{ij_x} &= \iint M_0 B_{xj} \rho \, d\rho \, d\psi \bigg|_{z_i + \frac{h_m}{2}} - \iint M_0 B_{xj} \rho \, d\rho \, d\psi \bigg|_{z_i - \frac{h_m}{2}} \\ &= \quad \int_{R+|s_{ij}|}^{|R-|s_{ij}||} \int M_0 \left(\cos\theta_{ij}\cos\phi_j + \sin\theta_{ij}\sin\phi_j\right) B_{\rho_j} \bigg|_{z_i + \frac{h_m}{2}} \rho_j \, d\rho_j \, d\psi \\ &\quad - \int_{R+|s_{ij}|}^{|R-|s_{ij}||} \int M_0 \left(\cos\theta_{ij}\cos\phi_j + \sin\theta_{ij}\sin\phi_j\right) B_{\rho_j} \bigg|_{z_i - \frac{h_m}{2}} \rho_j \, d\rho_j \, d\psi \\ &= \int_{R+|s_{ij}|}^{|R-|s_{ij}||} \int M_0 \left(\cos\theta_{ij}\cos\phi_j + \sin\theta_{ij}\sin\phi_j\right) \left(B_{\rho_j}\big|_{z_i + \frac{h_m}{2}} - B_{\rho_j}\big|_{z_i - \frac{h_m}{2}} \right) \rho_j \, d\rho_j \, d\psi \end{aligned} \tag{3.53}$$

Now using equation (A.4) through (A.8) we get

$$F_{ij_x} = \begin{cases} 2\displaystyle\int_{R+|s_{ij}|}^{|R-|s_{ij}||} M_0 \Bigg[\Bigg(\cos\theta_{ij}\left(-\cos\left(\frac{\theta_{ij}}{2}+\psi_j\left(\rho_j\right)\right)-\cos\frac{\theta_{ij}}{2}\right) & \text{if} \quad s_{ij}<0 \\ \qquad +\sin\theta_{ij}\left(-\sin\left(\frac{\theta_{ij}}{2}+\psi_j\left(\rho_j\right)\right)-\sin\frac{\theta_{ij}}{2}\right)\Bigg]\times & \\ \qquad \left(B_{\rho_j}\Big|_{z_i+\frac{h_m}{2}} - B_{\rho_j}\Big|_{z_i-\frac{h_m}{2}}\right)\rho_j\,d\rho_j & \\ 2\displaystyle\int_{R+|s_{ij}|}^{|R-|s_{ij}||} M_0 \Bigg[\cos\theta_{ij}\left(\cos\left(\frac{\theta_{ij}}{2}+\psi_j\left(\rho_j\right)\right)-\cos\left(\frac{\theta_{ij}}{2}\right)\right) & \text{if} \quad s_{ij}>0 \\ \qquad +\sin\theta_{ij}\left(\sin\left(\frac{\theta_{ij}}{2}+\psi_j\left(\rho_j\right)\right)-\sin\left(\frac{\theta_{ij}}{2}\right)\right)\Bigg]\times & \\ \qquad \left(B_{\rho_j}\Big|_{z_i+\frac{h_m}{2}} - B_{\rho_j}\Big|_{z_i-\frac{h_m}{2}}\right)\rho_j\,d\rho_j & \\ 0 \qquad \text{if} \quad s_{ij}=0 & \end{cases} \tag{3.54}$$

Integration of F_{ij_y}

Similarly to F_{ij_x}, we use the transformation matrices in (3.51) and integrating over ψ instead of ϕ yields

$$
\begin{aligned}
F_{ij_y} &= \iint M_0 B_{yj} \rho \, d\rho \, d\psi \Big|_{z_i + \frac{h_m}{2}} - \iint M_0 B_{yj} \rho \, d\rho \, d\psi \Big|_{z_i - \frac{h_m}{2}} \\
&= \int_{R+|s_{ij}|}^{|R-|s_{ij}||} \int M_0 \left(\cos\theta_{ij} \sin\phi_j - \sin\theta_{ij} \cos\phi_j \right) B_{\rho_j} \Big|_{z_i + \frac{h_m}{2}} \rho_j \, d\rho_j \, d\psi \\
&\quad - \int_{R+|s_{ij}|}^{|R-|s_{ij}||} \int M_0 \left(\cos\theta_{ij} \sin\phi_j - \sin\theta_{ij} \cos\phi_j \right) B_{\rho_j} \Big|_{z_i - \frac{h_m}{2}} \rho_j \, d\rho_j \, d\psi \\
&= \int_{R+|s_{ij}|}^{|R-|s_{ij}||} \int M_0 \left(\cos\theta_{ij} \sin\phi_j - \sin\theta_{ij} \cos\phi_j \right) \left(B_{\rho_j}\big|_{z_i + \frac{h_m}{2}} - B_{\rho_j}\big|_{z_i - \frac{h_m}{2}} \right) \rho_j \, d\rho_j \, d\psi
\end{aligned}
\tag{3.55}
$$

Now again with equations (A.4) through (A.8), we get

$$
F_{ij_y} = \begin{cases}
\displaystyle\int_{R+|s_{ij}|}^{|R-|s_{ij}||} M_0 \Bigg[\left(\cos\theta_{ij} \left(-\sin\left(\frac{\theta_{ij}}{2} + \psi_j(\rho_j) \right) - \sin\frac{\theta_{ij}}{2} \right) \right. & \text{if} \quad s_{ij} < 0 \\
\qquad \left. - \sin\theta_{ij} \left(-\cos\left(\frac{\theta_{ij}}{2} + \psi_j(\rho_j) \right) - \cos\frac{\theta_{ij}}{2} \right) \right] \times & \\
\qquad \left(B_{\rho_j}\big|_{z_i + \frac{h_m}{2}} - B_{\rho_j}\big|_{z_i - \frac{h_m}{2}} \right) \rho_j \, d\rho_j & \\
\displaystyle\int_{R+|s_{ij}|}^{|R-|s_{ij}||} M_0 \Bigg[\left(\cos\theta_{ij} \left(\sin\left(\frac{\theta_{ij}}{2} + \psi_j(\rho_j) \right) - \sin\frac{\theta_{ij}}{2} \right) \right. & \text{if} \quad s_{ij} > 0 \\
\qquad \left. - \sin\theta_{ij} \left(\cos\left(\frac{\theta_{ij}}{2} + \psi_j(\rho_j) \right) - \cos\frac{\theta_{ij}}{2} \right) \right] \times & \\
\qquad \left(B_{\rho_j}\big|_{z_i + \frac{h_m}{2}} - B_{\rho_j}\big|_{z_i - \frac{h_m}{2}} \right) \rho_j \, d\rho_j & \\
0 \qquad \text{if} \quad s_{ij} = 0 &
\end{cases}
\tag{3.56}
$$

Integration of F_{ij_z}

For completeness, we compute the Force over the $\hat{\mathrm{k}}$-direction. Since the $\hat{\mathrm{k}}$-direction doesn't require a transformation matrix from cylindrical to Cartesian coordinates, the integration over ψ is much simpler

$$\begin{aligned}\vec{F}_{ij_z} &= \iint M_0 B_{zj}\rho\, d\rho\, d\phi\Big|_{z_i+\frac{h_m}{2}} - \iint M_0 B_{zj}\rho\, d\rho\, d\phi\Big|_{z_i-\frac{h_m}{2}} \\ &= \int_{R+|s_{ij}|}^{|R-|s_{ij}||}\int M_0\left(B_{zj}\big|_{z_i+\frac{h_m}{2}} - B_{zj}\big|_{z_i-\frac{h_m}{2}}\right)\rho_j\, d\rho_j\, d\psi\end{aligned} \tag{3.57}$$

Integrating this when $s_{ij} > 0$

$$\begin{aligned}F_{ij_z} &= \int_{R+|s_{ij}|}^{|R-|s_{ij}||}\int_0^{\psi_j(\rho_j)} M_0\left(B_{zj}\big|_{z_i+\frac{h_m}{2}} - B_{zj}\big|_{z_i-\frac{h_m}{2}}\right)\rho_j\, d\rho_j\, d\psi \\ &= \int_{R+|s_{ij}|}^{|R-|s_{ij}||} M_0\left(B_{zj}\big|_{z_i+\frac{h_m}{2}} - B_{zj}\big|_{z_i-\frac{h_m}{2}}\right)\psi_j\left(\rho_j\right)\rho_j\, d\rho_j\end{aligned} \tag{3.58}$$

and in the case when $s_{ij} < 0$

$$\begin{aligned}F_{ij_z} &= \int_{R+|s_{ij}|}^{|R-|s_{ij}||}\int_{\psi_j(\rho_j)}^{0} M_0\left(B_{zj}\big|_{z_i+\frac{h_m}{2}} - B_{zj}\big|_{z_i-\frac{h_m}{2}}\right)\rho_j\, d\rho_j\, d\psi \\ &= \int_{R+|s_{ij}|}^{|R-|s_{ij}||} M_0\left(B_{zj}\big|_{z_i+\frac{h_m}{2}} - B_{zj}\big|_{z_i-\frac{h_m}{2}}\right)\left(\pi - \psi_j\left(\rho_j\right)\right)\rho_j\, d\rho_j\end{aligned} \tag{3.59}$$

As for when $s_{ij} = 0$, we get

$$\begin{aligned}F_{ij_z} &= \int_{R+|s_{ij}|}^{|R-|s_{ij}||}\int_0^{2\pi} M_0\left(B_{zj}\big|_{z_i+\frac{h_m}{2}} - B_{zj}\big|_{z_i-\frac{h_m}{2}}\right)\rho_j\, d\rho_j\, d\psi \\ &= 2\pi\int_{R+|s_{ij}|}^{|R-|s_{ij}||} M_0\left(B_{zj}\big|_{z_i+\frac{h_m}{2}} - B_{zj}\big|_{z_i-\frac{h_m}{2}}\right)\rho_j\, d\rho_j\end{aligned} \tag{3.60}$$

Therefore, we can summarize F_{ij_z} as

$$F_{ij_z} = \begin{cases} \displaystyle\int_{R+|s_{ij}|}^{|R-|s_{ij}||} M_0 \left(B_{zj}\big|_{z_i+\frac{h_m}{2}} - B_{zj}\big|_{z_i-\frac{h_m}{2}} \right) (\pi - \psi_j(\rho_j))\, \rho_j \, d\rho_j & \text{if} \quad s_{ij} < 0 \\ \displaystyle\int_{R+|s_{ij}|}^{|R-|s_{ij}||} M_0 \left(B_{zj}\big|_{z_i+\frac{h_m}{2}} - B_{zj}\big|_{z_i-\frac{h_m}{2}} \right) \psi_j(\rho_j)\, \rho_j \, d\rho_j & \text{if} \quad s_{ij} > 0 \\ \displaystyle 2\pi \int_{R+|s_{ij}|}^{|R-|s_{ij}||} M_0 \left(B_{zj}\big|_{z_i+\frac{h_m}{2}} - B_{zj}\big|_{z_i-\frac{h_m}{2}} \right) \rho_j \, d\rho_j & \text{if} \quad s_{ij} = 0 \end{cases} \tag{3.61}$$

We use equations (3.41), (3.44) and (3.47) for the magnetic field for each cases respectively, and where again

$$\psi_j(\rho_j) = \arccos\left(\frac{\rho_j^2 + s_{ij}^2 - R_m^2}{2 s_{ij} \rho_j} \right)$$

with

$$s_{ij} = 2\ell \sin\left(\frac{\theta_{ij}}{2} \right)$$

3.3 Equations of motion

3.3.1 Point-mass model

The equation of motion for pendulums i and j respectively are

$$\begin{aligned} m\ell^2 \ddot{\theta}_i + c_i \dot{\theta}_i + mg\ell \sin\theta_i &= \ell F_{ij_y} \\ m\ell^2 \ddot{\theta}_j + c_j \dot{\theta}_j + mg\ell \sin\theta_j &= -\ell F_{ij_y} \end{aligned} \tag{3.62}$$

Let $i = 1$ and $j = 2$, we introduce the state variables

$$\begin{aligned} x_1 &= \theta_1 \\ x_2 &= \ddot{\theta}_1 \\ x_3 &= \theta_2 \\ x_4 &= \ddot{\theta}_2 \end{aligned} \tag{3.63}$$

to rewrite the equations of motion as

$$
\begin{aligned}
\dot{x_1} &= x_2 \\
\dot{x_2} &= -\frac{c_1}{m\ell^2}x_2 - \frac{g}{\ell}\sin x_1 + \frac{1}{m\ell}F_{12_y} \\
\dot{x_3} &= x_4 \\
\dot{x_4} &= -\frac{c_2}{m\ell^2}x_4 - \frac{g}{\ell}\sin x_3 - \frac{1}{m\ell}F_{12_y}
\end{aligned}
\tag{3.64}
$$

where

$$
F_{12_y} = \begin{cases}
2\displaystyle\int_{R+|s_{12}|}^{|R-|s_{12}||} M_0 \Bigg[\Bigg(\cos\theta_{12}\left(-\sin\left(\frac{\theta_{12}}{2}+\psi_2(\rho_2)\right)-\sin\frac{\theta_{12}}{2}\right) \\
\qquad -\sin\theta_{12}\left(-\cos\left(\frac{\theta_{12}}{2}+\psi_2(\rho_2)\right)-\cos\frac{\theta_{12}}{2}\right)\Bigg]\times \\
\qquad \left(B_{\rho_2}\big|_{z_1+\frac{h_m}{2}} - B_{\rho_2}\big|_{z_1-\frac{h_m}{2}}\right)\rho_2\,d\rho_2 \quad \text{if} \quad s_{12}<0 \\
2\displaystyle\int_{R+|s_{12}|}^{|R-|s_{12}||} M_0 \Bigg[\Bigg(\cos\theta_{12}\left(\sin\left(\frac{\theta_{12}}{2}+\psi_2(\rho_2)\right)-\sin\frac{\theta_{12}}{2}\right) \\
\qquad -\sin\theta_{12}\left(\cos\left(\frac{\theta_{12}}{2}+\psi_2(\rho_2)\right)-\cos\frac{\theta_{12}}{2}\right)\Bigg]\times \\
\qquad \left(B_{\rho_2}\big|_{z_1+\frac{h_m}{2}} - B_{\rho_2}\big|_{z_1-\frac{h_m}{2}}\right)\rho_2\,d\rho_2 \quad \text{if} \quad s_{12}>0 \\
0 \qquad \text{if} \quad s_{12}=0
\end{cases}
\tag{3.65}
$$

with

$$
\psi_2(\rho_2) = \arccos\left(\frac{\rho_j^2+s_{12}^2-R_m^2}{2s_{12}\rho_j}\right)
$$

and

$$
s_{12} = 2l\sin\left(\frac{\theta_{12}}{2}\right)
$$

and (3.33) gives

$$
\begin{aligned}
B_{\rho j}\big|_{z_i+\frac{h_m}{2}} - B_{\rho j}\big|_{z_i-\frac{h_m}{2}} = \frac{\mu_0 M_0 R_m}{\pi\sqrt{R_m \rho_2}} \Bigg[& \frac{2}{\kappa_1}\left(\left(1-\frac{1}{2}\kappa_1^2\right)K\left(\kappa_1\right)-E\left(\kappa_1\right)\right) - \\
& \frac{1}{\kappa_2}\left(\left(1-\frac{1}{2}\kappa_2^2\right)K\left(\kappa_2\right)-E\left(\kappa_2\right)\right) - \\
& \frac{1}{\kappa_3}\left(\left(1-\frac{1}{2}\kappa_3^2\right)K\left(\kappa_3\right)-E\left(\kappa_3\right)\right)\Bigg]
\end{aligned}
\tag{3.66}
$$

and for $i = 1,\ j = 2$

$$
\begin{gathered}
a = R_m, \qquad\qquad b = \rho_2, \\
p_1 = ||-d||, \qquad\qquad p_2 = ||-d-h_m||, \qquad\qquad p_3 = ||-d+h_m||
\end{gathered}
$$

which gives for p_1, p_2 and p_3 respectively

$$
\kappa_1^2 = \frac{4R_m\rho_2}{d^2 + \left(R_m+\rho_2\right)^2}
$$

$$
\kappa_2^2 = \frac{4R\rho_2}{\left(-d-h_m\right)^2 + \left(R_m+\rho_2\right)^2}
$$

$$
\kappa_3^2 = \frac{4R_m\rho_2}{\left(-d+h_m\right)^2 + \left(R_m+\rho_2\right)^2}
$$

3.3.2 Distributed-mass model

For the distributed-mass model, the equations of motion for pendulums i and j respectively become

$$
\begin{aligned}
m r_g^2 \ddot{\theta}_i + c_i\dot{\theta}_i + m g \ell_g \sin\theta_i &= F_{ij_y}\ell \\
m r_g^2 \ddot{\theta}_j + c_j\dot{\theta}_j + m g \ell_g \sin\theta_j &= -F_{ij_y}\ell
\end{aligned}
\tag{3.67}
$$

Where r_g is the radius of gyration is found by dividing the mass moment of inertia by the mass of the pendulum and l_g is the distance from the point of rotation to the center of gravity of the pendulum.
Similarly to the point-mass model, we consider $i = 1$ and $j = 2$ and introduce the state

variables

$$
\begin{aligned}
x_1 &= \theta_1 \\
x_2 &= \ddot{\theta}_1 \\
x_3 &= \theta_2 \\
x_4 &= \ddot{\theta}_2
\end{aligned}
\tag{3.68}
$$

and rewrite the equation of motion

$$
\begin{aligned}
\dot{x_1} &= x_2 \\
\dot{x_2} &= -\frac{c_1}{mr_g^2}x_2 - \frac{g\ell_g}{r_g^2}\sin x_1 + \frac{\ell}{mr_g^2}F_{12_y} \\
\dot{x_3} &= x_4 \\
\dot{x_4} &= -\frac{c_2}{mr_g^2}x_4 - \frac{g\ell_g}{r_g^2}\sin x_3 - \frac{\ell}{mr_g^2}F_{12_y}
\end{aligned}
\tag{3.69}
$$

where the force and magnetic field are expressed similarly to the previous section.

Chapter 4

Results

In this chapter, we validate the results from our analytical system by solving the equation of motions numerically and comparing those results to the experimental results. Section 4.1 identifies the parameters needed to get numerical solutions of the rigid body model equations of motions experimentally. Section 4.2 shows a magnetic field simulation of the field lines in the $\hat{\imath}\hat{\jmath}$-plane.

In Section 4.4 and 4.5, we investigate the equilibrium points and the magnetic forces. Furthermore, to have a better understanding of the magnetic pendulums interactions, we create a diagram of the simulated magnetic forces acting on the first pendulum along with the response of the first and second pendulums over time as well as the basin of attraction of the system.

4.1 Parameter Identification

Using the parameters from our experimental design summarized in Table 4.1, we calculate the damping coefficients needed for our Mathematica simulation. These parameters include physical constants such as the acceleration due to gravity g and permeability of free space μ_0. For both the point-mass and distributed-mass models, to determine the response of our rigid body system, we use the equations of motions derived in Equation (3.64) and (3.69) where the damping coefficient of each pendulum is different $c_1 \neq c_2$.

In order to determine the damping coefficient c_1, we performed an experiment with two pendulums at separation distances of 35 mm and 40 mm respectively. We released the pendulum of interest from a 90° initial condition and allowed it to oscillate freely.

Table 4.1: Model parameter values

Description	Symbol	Value [SI]
Acceleration due to gravity	g	9.804 $\mathrm{m/s^2}$
Magnet mass	m	24.51×10^{-3} kg
Magnet radius	R	7.9 mm
Magnet thickness	h_m	3.17 mm
Magnet residual flux density	B_r	1.275 T
Permeability of free space	μ_0	12.56637×10^{-7} N/A
Magnet magnetization	$M_0 = B_r/\mu_0$	1.0146×10^6 A/m
Pendulum mass moment of inertia	I_{zz}	$248.467 \times 10^{-6}\ kg.m^2$
Pendulum length	ℓ	121 mm
Distance from center of gravity to origin	ℓ_g	83.78 mm
Pendulum separation	a	35 or 40 mm

Meanwhile, the second pendulum starts at an initial condition at the vertical axis. We measured the amplitude of oscillation over seven periods and used them to calculate the logarithmic decrement using the formula

$$\delta = \frac{1}{n-1} \ln \frac{X_1}{X_n} \tag{4.1}$$

where X_n is the displacement at the nth peak. Using the logarithmic decrement, we compute the damping ratio with the following equation

$$\zeta = \frac{1}{\sqrt{1 + (\frac{2\pi}{\delta})^2}} \tag{4.2}$$

Finally, the damping coefficient is found using

$$c = 2\zeta J_{zz}\omega_n \tag{4.3}$$

where J_{zz} is the mass moment of inertial found with

$$J_{zz} = \frac{mgd}{\omega_n^2} \tag{4.4}$$

where d is the distance from the center of gravity to origin and ω_n is the natural frequency of the system. ω_n is found using the first period of the damped oscillation τ_d to get the damped natural frequency

$$\omega_d = \frac{2\pi}{\tau_d} \tag{4.5}$$

The natural frequency is then found

$$\omega_n = \frac{\omega_d}{\sqrt{1-\zeta^2}} \tag{4.6}$$

Using the oscillation amplitude measured over seven period for a separation distance of35 mm and 40 mm respectively seen in Tables 4.2 and 4.3, we estimate the damping coefficient of each pendulum for both cases.

4.2 Magnetic Field

Using the input parameters in Table 4.1 in equation (3.33) found in the previous chapter, we create a simulation of the magnetic field in Mathematica. Figure 4.1 represents the magnetic field generated in the xy-plane viewed from the front of our system. The black and blue circles represent our magnets viewed from the front. The black magnet in the figure is stationery in the vertical plane and the blue magnet is at an angle θ with respect to the vertical axis.

The colour scheme of the field line goes from blue to yellow. The colder the colour, the weaker the magnetic field, hence blue represents the weakest part of the magnetic field and yellow the strongest. As can be seen, the strongest magnetic field lines are the ones coming out of the magnets and they get weaker as we move away from the magnet centers.

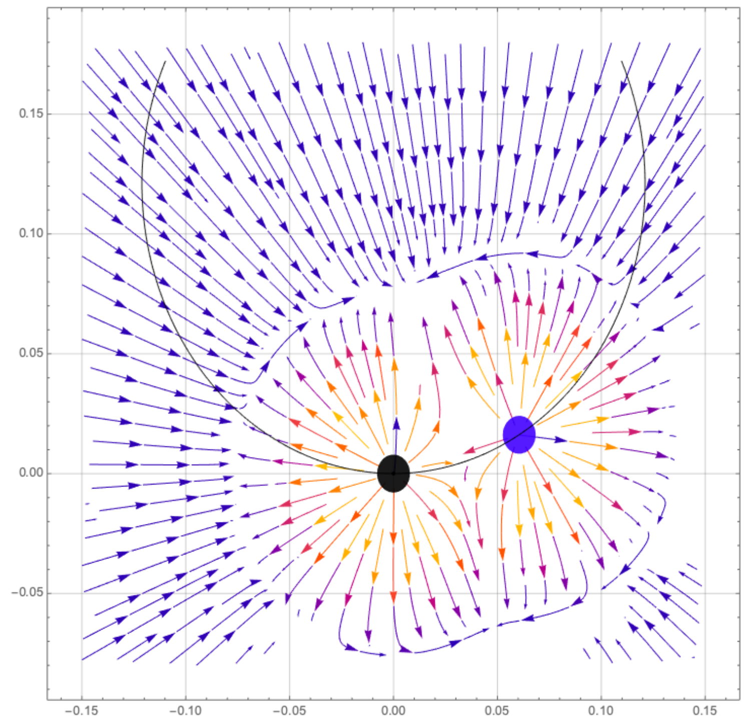

Figure 4.1: Magnetic field in the $\hat{\imath}\hat{\jmath}$-plane.

4.3 Pendulum Forces For Point-mass Model

After computing the damping coefficient and using the design dimensions and parameters mentioned in the previous section, we simulate the responses of our pendulums with the following initial conditions:

$$\theta_1(0) = 90^\circ \quad , \quad \dot{\theta}_1(0) = 0$$
$$\theta_2(0) = 0^\circ \quad , \quad \dot{\theta}_2(0) = 0$$

Figures 4.2 and 4.6 represent the simulated motion of our pendulums for a separation distance of 35 mm and 40 mm respectively using the point-mass model where we can see position in degrees with respect to the time in seconds. We give one of the pendulums presented by the blue line an initial condition of 90 degrees and we let it oscillate freely. The pendulum, represented by the yellow line, starting at 0 degrees start oscillating as the other pendulum continuously crosses it. We notice that as the first pendulums crossed the second, there is an energy exchange resulting in the pendulum initially being stationary to start moving. Then as both pendulum loose energy around the same time, they settle at different equilibrium points and opposite angles with respect to the vertical axis.

Overall, the first few oscillations following the first pendulum release resemble those of a simple single pendulum system due to the dominance of gravitational potential energy over the magnetic potential energy. Meanwhile, the second pendulum gains kinetic energy from the first pendulum and starts to oscillate due to the magnetic interaction. As a result, we notice that the first pendulum oscillations diminish while those of the second pendulum grow. The magnetic potential energy dominates gravitational potential energy and a second harmonic appears in the oscillations of the first and second pendulums. As the first pendulum looses most its energy, we notice the second pendulum reaching maximum motion before giving it back to the first pendulum.

- **When a=** 35 **mm:**

Table 4.2: Measured amplitudes of the first pendulum over seven periods for 35 mm separation distance.

X_1	X_2	X_3	X_4	X_5	X_6	X_7
90°	87°	85°	84°	82°	79°	75°

$$\theta_1(0) = 90^\circ \quad , \quad \dot{\theta}_1(0) = 0 \quad , \quad C_1 = 2.75 \times 10^{-5} kg.m^2.s^{-5}$$
$$\theta_2(0) = 0^\circ \quad , \quad \dot{\theta}_2(0) = 0 \quad , \quad C_2 = 5.25 \times 10^{-5} kg.m^2.s^{-5}$$

We also notice when comparing the figures of the two separation distance that when the distance is 40 mm the oscillations take longer to stop than with the separation being 35 mm. That can be explained with the magnetic force between the magnets being weaker, therefore not hindering the motion as much. There is also a difference in the equilibrium points that the pendulums settle at between the two cases. While a separation distance of 35 mm lets the pendulums settle at around ±6.7°, a distance of 40 mm results in ±5.8° equilibrium angles. This can also be explained by the weakening of the magnetic force due to distance increase and is discussed more in the next section.

To validate that the simulation and experiment responses are in good agreement, we consider figures 4.3, 4.4, 4.7 and 4.8. As we can see, with the right input damping coefficients, the simulation and experiment follow a very similar path.

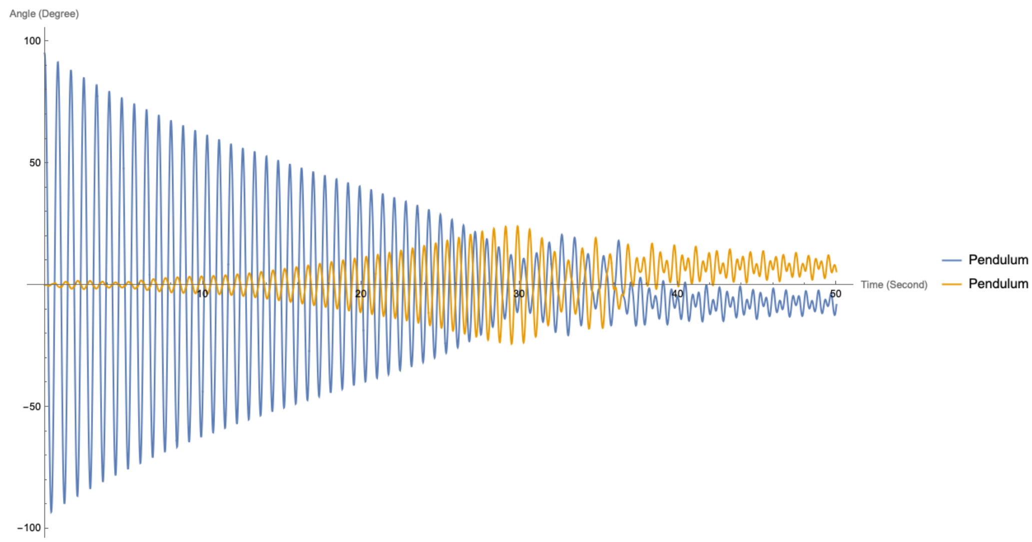

Figure 4.2: The blue line and the yellow line represent a simulation using the point-mass model of the angular displacement θ_1 and θ_2 with respect to time with 35 mm separation distance.

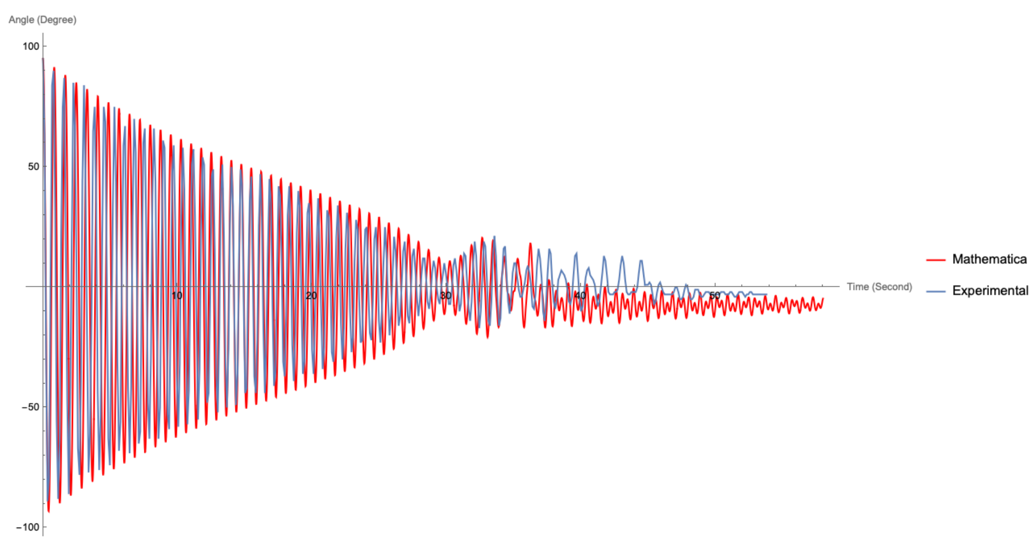

Figure 4.3: The simulated red line for the point-mass model and the measured blue line represent the angular displacement θ_1 of the first pendulum with respect to time with 35 mm separation distance.

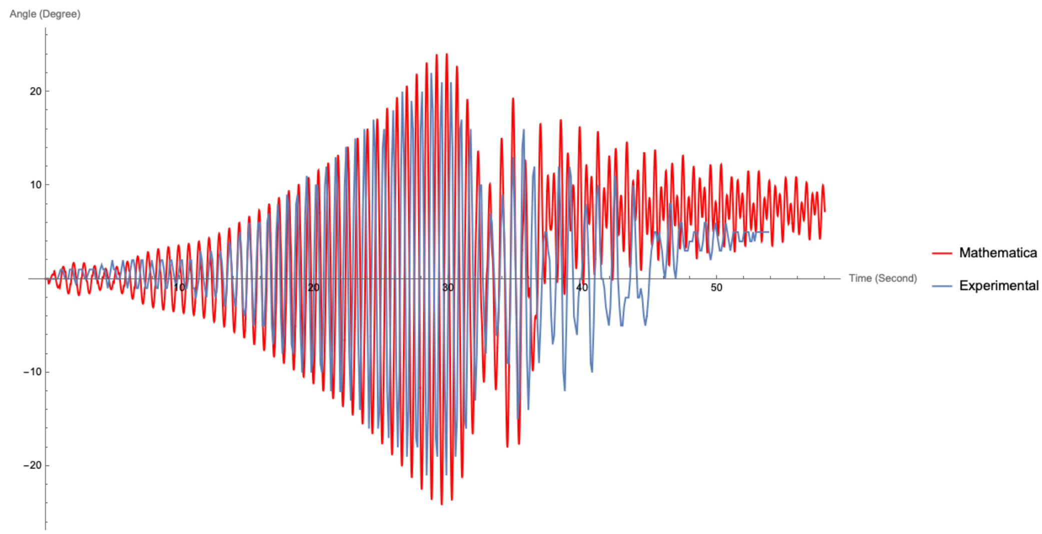

Figure 4.4: The simulated red line for the point-mass model and the measured blue line represent the angular displacement θ_2 of the second pendulum with respect to time with 35 mm separation distance.

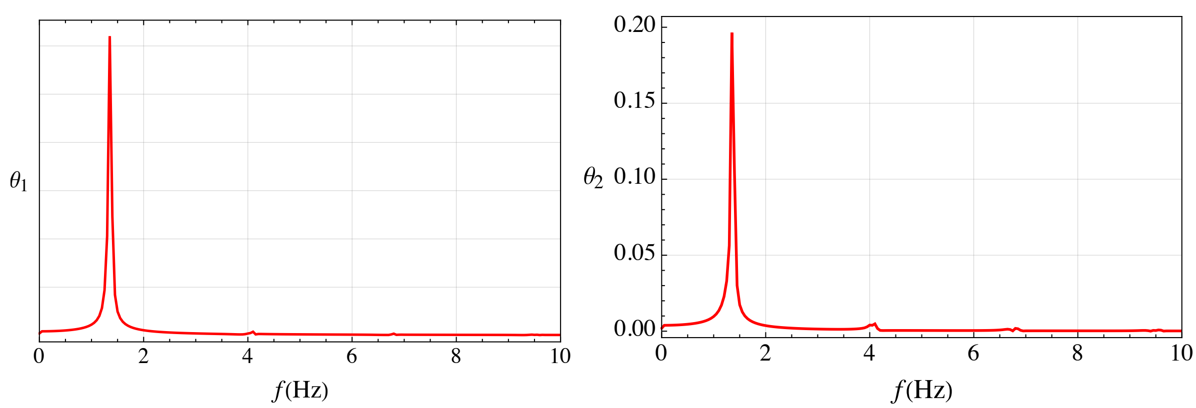

Figure 4.5: Simulated Fast Fourier Transform of the angular displacement θ_1 and θ_2 of the first and second pendulum respectively.

Finally, taking the Fast Fourier Transform (FFT) of the first and second pendulum's simulated responses for both separation distances 35 mm and 40 mm are shown in Figures 4.5 and 4.9.

For the 35 mm separation distance, the experimental natural frequency of the first pendulum is 1.264 Hz. Meanwhile, as seen in Figure 4.5, the simulated natural frequency is relatively close at 1.3 Hz making a difference of 2.8 percent. The experimental natural frequency of the second pendulum is 1.352 Hz and the simulated natural frequency is 1.34 Hz with a difference of 0.9 percent. This frequency corresponds to the dominant harmonic in the first stage of the pendulums' oscillations.

- **When a=** 40 **mm:**

Table 4.3: Measured amplitudes of the first pendulum over seven periods for 40 mm separation distance.

X_1	X_2	X_3	X_4	X_5	X_6	X_7
90°	85°	79°	76°	74°	73°	70°

Table 4.3 represents the measured first amplitudes of the first pendulum that starts at an initial condition of 90 Degree. With a separation distance of 40 mm, we kept the damping coefficients identical to the ones used when the separation distance is 35 mm. As seen in Figures 4.7 and 4.8, with those damping coefficients, the pendulums in the point-mass simulation gives a very similar output to the experimental results.

$$\begin{aligned} \theta_1(0) = 90^\circ \quad &, \quad \dot{\theta}_1(0) = 0 \quad , \quad C_1 = 2.75 \times 10^{-5} kg.m^2.s^{-5} \\ \theta_2(0) = 0^\circ \quad &, \quad \dot{\theta}_2(0) = 0 \quad , \quad C_2 = 5.25 \times 10^{-5} kg.m^2.s^{-5} \end{aligned}$$

For the 40 mm separation distance, the experimental natural frequency of the first pendulum is 1.25 Hz. Meanwhile, as seen in Figure 4.5, the simulated natural frequency is relatively close at 1.31 Hz making it a difference of 4.6 percent. The experimental natural frequency of the second pendulum is 1.263 Hz and the simulated natural frequency is 1.32 Hz with a difference of 4.4 percent.

4.4 Pendulum Forces For Distributed-mass Model

Similarly to the point-mass model, after finding the damping coefficient, we simulate the responses of our pendulums with the same initial conditions. Figures 4.10 and 4.15 represent the simulated motion of our pendulums for a separation distance of 35 mm and 40 mm

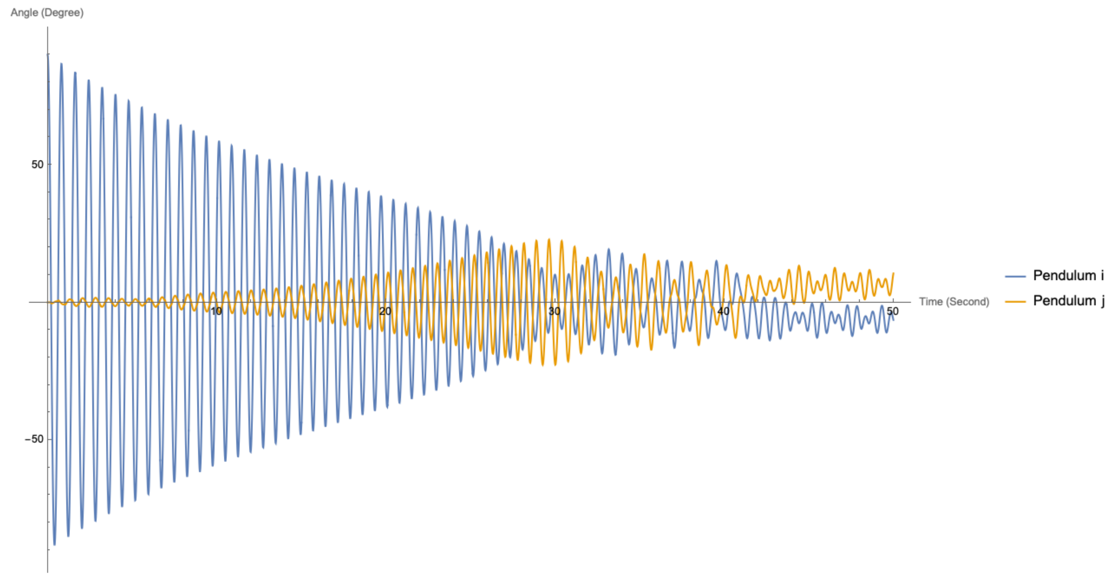

Figure 4.6: The blue line and the yellow line represent the angular displacement θ_1 and θ_2 with respect to time with 40 mm separation distance.

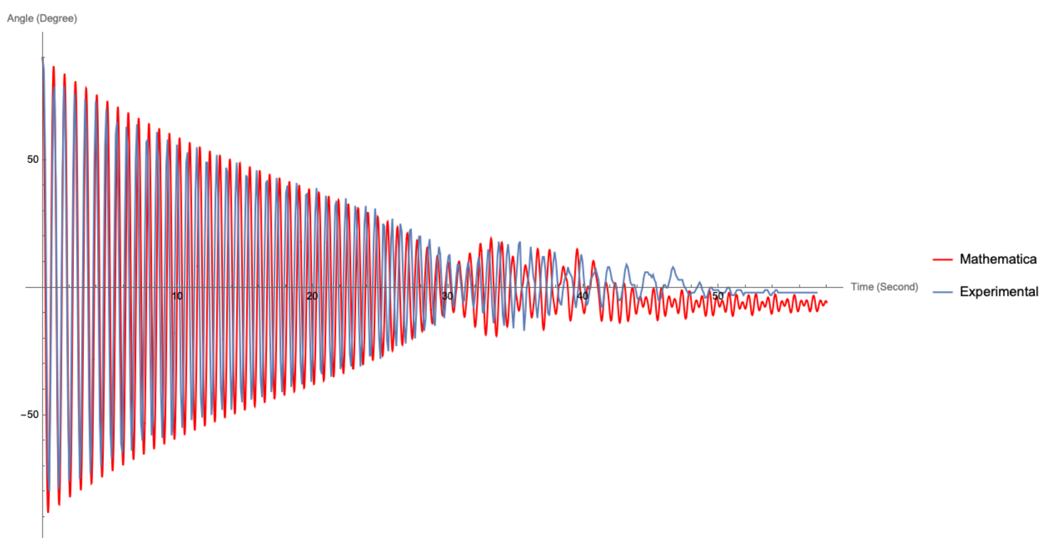

Figure 4.7: The simulated red line and the measured blue line represent the angular displacement θ_1 of the first pendulum with respect to time with 40 mm separation distance.

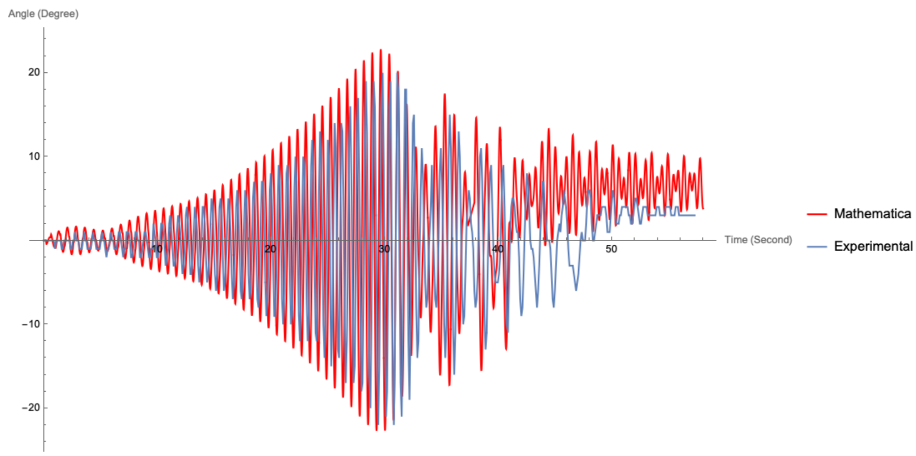

Figure 4.8: The simulated red line and the measured blue line represent the angular displacement θ_2 of the second pendulum with respect to time with 40 mm separation distance.

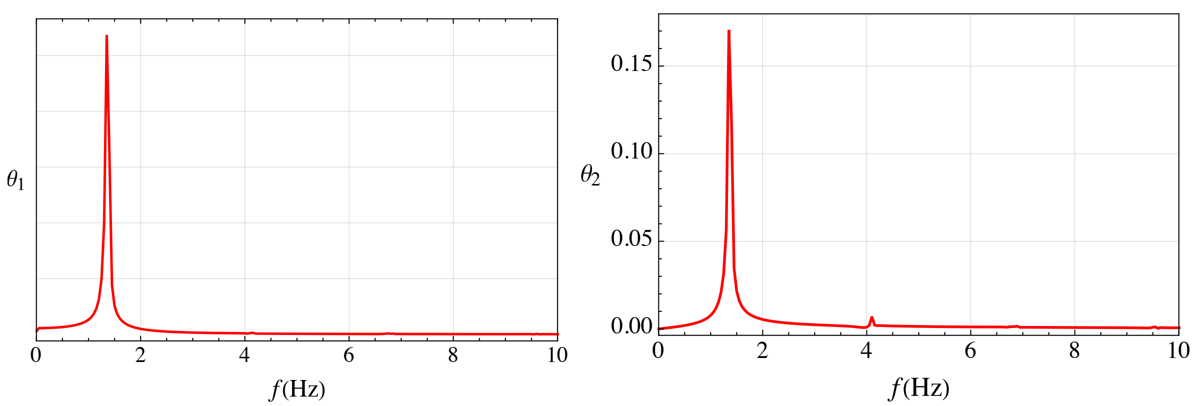

Figure 4.9: Simulated Fast Fourier Transform of the angular displacement θ_1 and θ_2 of the first and second pendulum respectively.

respectively using the distributed-mass model where we can see position in degrees with respect to the time in seconds. The pendulum follows a very similar path as described in the previous section. In this section, we also compare the distributed-mass model's output with that of our previous model outlined in Razieh's work [9]. For this model, the damping coefficients for both separation distance cases have been changed to get a better fit. The change in those damping coefficient values is due to the differences in the equations of motion.

- **When a=** 35 **mm:**

$$\theta_1(0) = 90^\circ \quad , \quad \dot{\theta}_1(0) = 0 \quad , \quad C_1 = 1.90 \times 10^{-5} kg.m^2.s^{-5}$$
$$\theta_2(0) = 0^\circ \quad , \quad \dot{\theta}_2(0) = 0 \quad , \quad C_2 = 3.63 \times 10^{-5} kg.m^2.s^{-5}$$

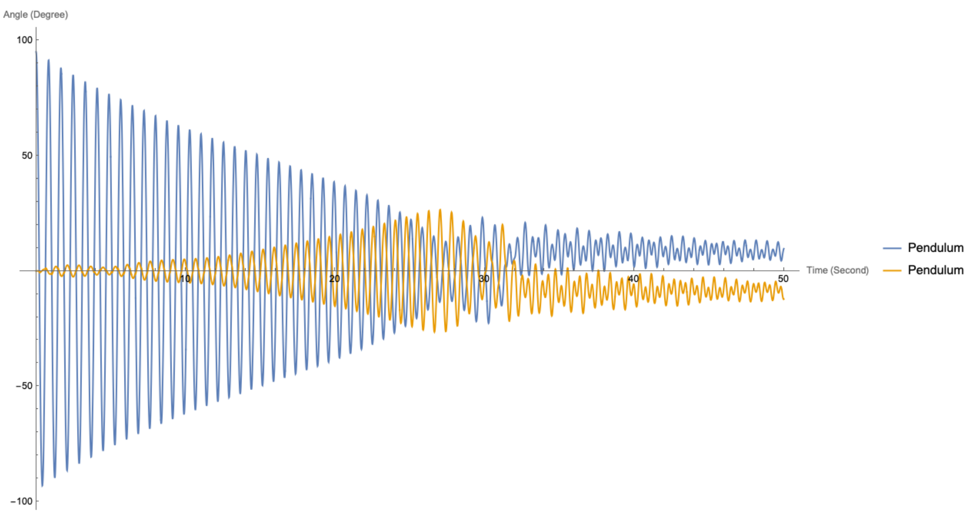

Figure 4.10: The blue line and the yellow line represent the angular displacement θ_1 and θ_2 with respect to time with 35 mm separation distance.

Overall, we notice that although the motion of the pendulums follow a similar path with the same frequency as the point-mass model, we see that the energy exchange between the pendulums and settling at the equilibrium points comes much sooner than the experimental results. The main differences therefore lies in the damping coefficient and the accuracy of the outputs in comparison to the point-mass model and experimental results. Another difference is in the equilibrium points where, in this case, a separation distance of 35 mm lets the pendulums settle at around $\pm 8.1^\circ$, while a distance of 40 mm results in $\pm 7.5^\circ$ equilibrium angles. This can also be explained by the weakening of the magnetic force due to distance increase and is discussed more in the next section.

To compare the the distributed-mass simulation and experiment responses, we consider figures 4.11, 4.12, 4.16 and 4.17. It is important to note that the disagreement seen is due the parameters inputs such as that of the damping coefficient and mass moment of inertia. We can obtain better agreement with better parameter identification. Another

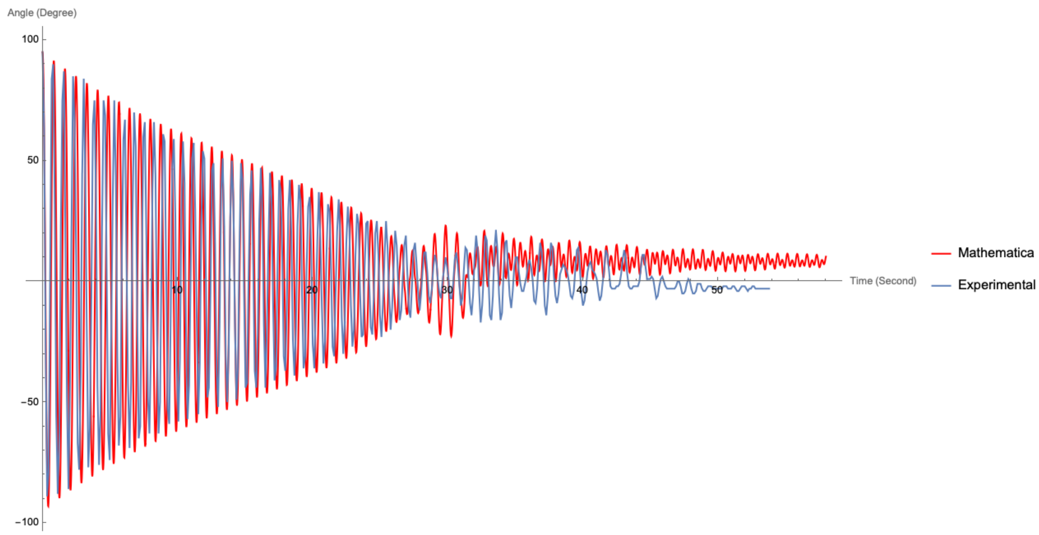

Figure 4.11: The simulated red line and the measured blue line represent the angular displacement θ_1 of the first pendulum with respect to time with 35 mm separation distance.

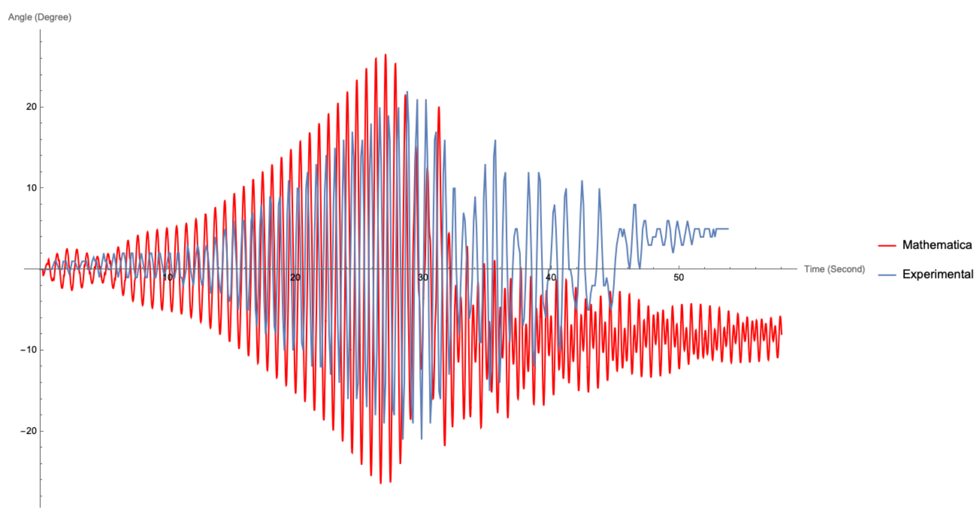

Figure 4.12: The simulated red line and the measured blue line represent the angular displacement θ_2 of the second pendulum with respect to time with 35 mm separation distance.

reason behind the disagreement is, as with the point-mass model, our damping model is too simple to capture all the complex friction and damping mechanisms that affect our system.

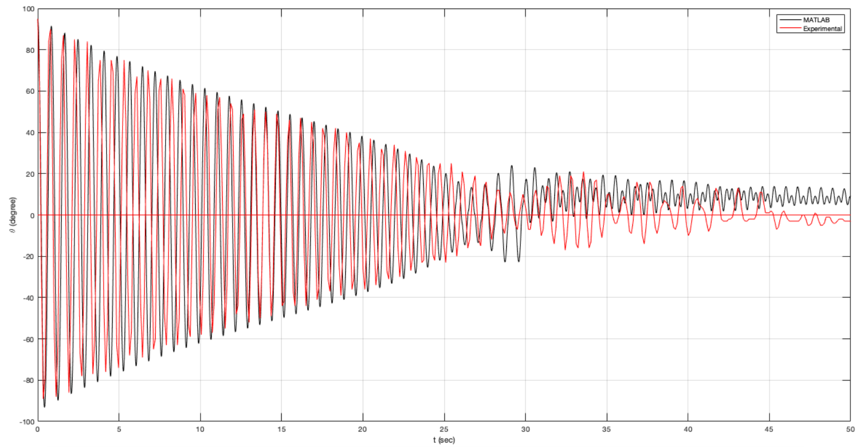

Figure 4.13: The simulated black line line and the measured red line represent the angular displacement θ_1 of the second pendulum with respect to time with 35 mm separation distance.

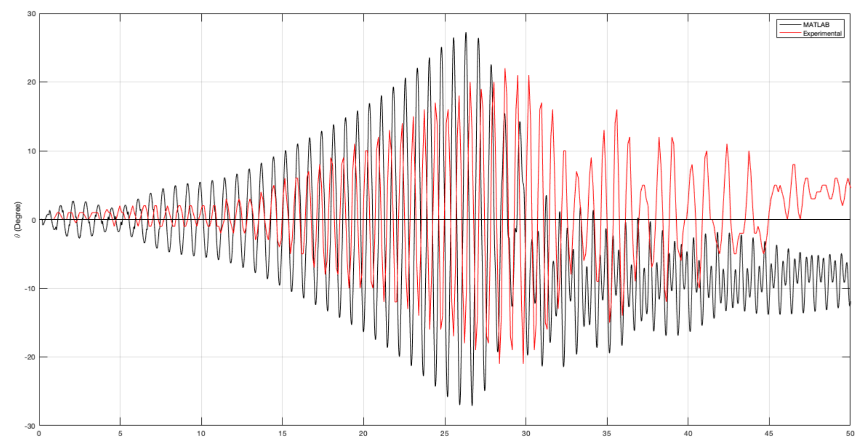

Figure 4.14: The simulated black line line and the measured red line represent the angular displacement θ_2 of the second pendulum with respect to time with 35 mm separation distance.

Finally, we take the Fast Fourier Transform (FFT) of the first and second pendulum's simulated responses for the distributed-mass model for both separation distances 35 mm and 40 mm. We notice a very similar output as with the point-mass model and experimental results for both separation distances. For the 35 mm separation distance, the experimental natural frequency of the first pendulum is 1.264 Hz. Meanwhile, the simulated natural frequency is relatively close at 1.31 Hz making a difference of 3.5 percent. The experimental natural frequency of the second pendulum is 1.352 Hz and the simulated natural frequency is 1.34 Hz with a difference of 0.89 percent. This frequency corresponds to the dominant harmonic in the first stage of the pendulums' oscillations.

- **When a=** 40 **mm:**

Table 4.4: Measured amplitudes of the first pendulum over seven periods for 40 mm separation distance.

X_1	X_2	X_3	X_4	X_5	X_6	X_7
90°	85°	79°	76°	74°	73°	70°

$$\theta_1(0) = 90^\circ \quad , \quad \dot{\theta}_1(0) = 0 \quad , \quad C_1 = 3.70 \times 10^{-5} kg.m^2.s^{-5}$$
$$\theta_2(0) = 0^\circ \quad , \quad \dot{\theta}_2(0) = 0 \quad , \quad C_2 = 5.15 \times 10^{-5} kg.m^2.s^{-5}$$

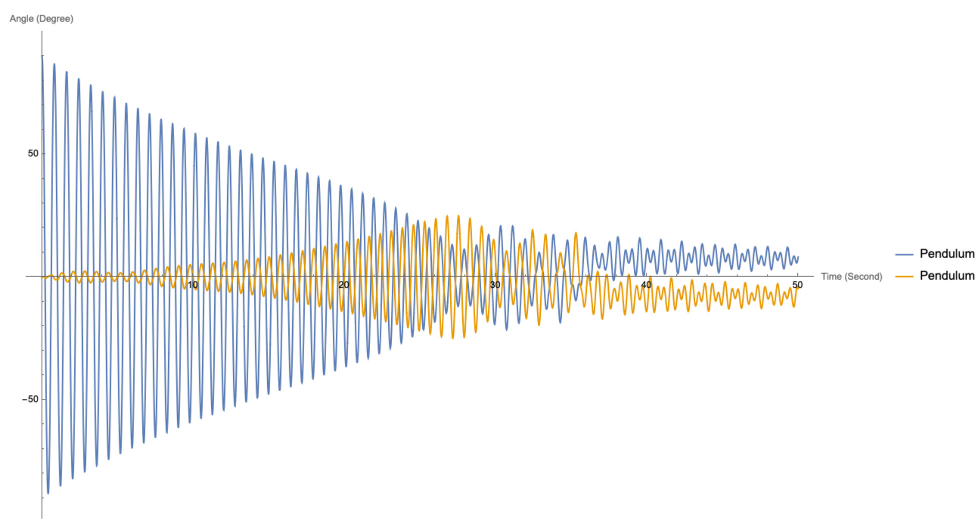

Figure 4.15: The blue line and the yellow line represent the angular displacement θ_1 and θ_2 with respect to time with 40 mm separation distance.

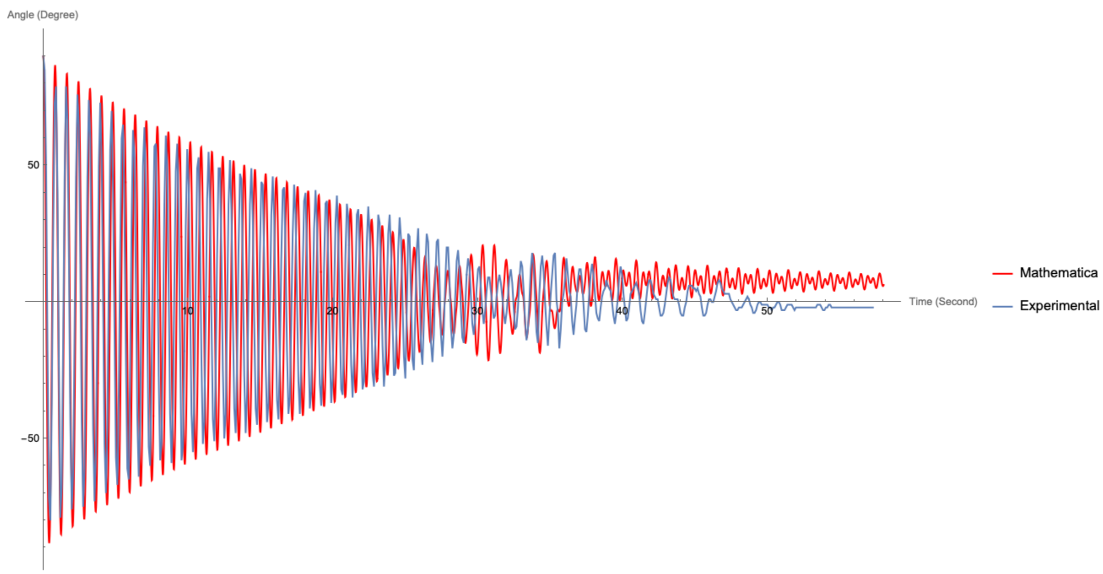

Figure 4.16: The simulated red line and the measured blue line represent the angular displacement θ_1 of the first pendulum with respect to time with 40 mm separation distance.

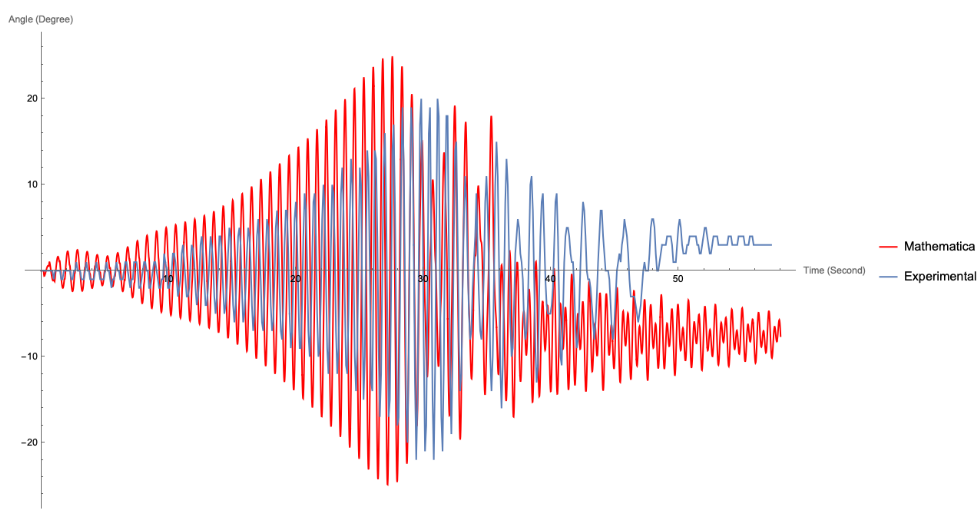

Figure 4.17: The simulated red line and the measured blue line represent the angular displacement θ_2 of the second pendulum with respect to time with 40 mm separation distance.

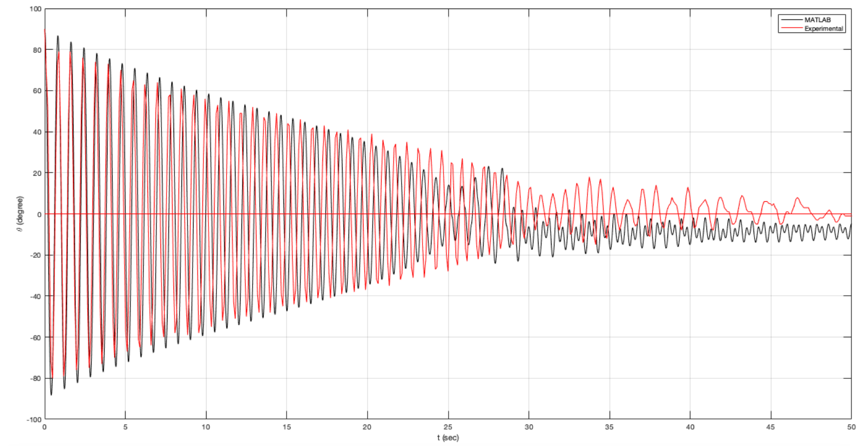

Figure 4.18: The simulated black line line and the measured red line represent the angular displacement θ_1 of the second pendulum with respect to time with 40 mm separation distance.

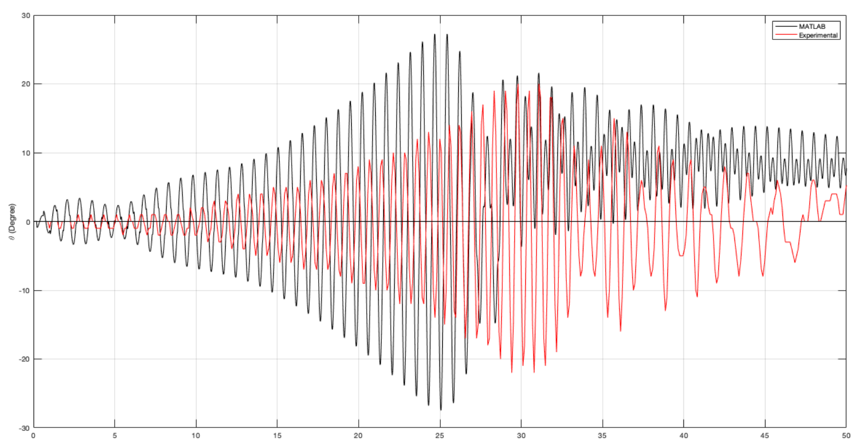

Figure 4.19: The simulated black line and the measured red line represent the angular displacement θ_2 of the second pendulum with respect to time with 40 mm separation distance.

For the 40 mm separation distance, the experimental natural frequency of the first pendulum is 1.25 Hz. Meanwhile, the simulated natural frequency is relatively close at 1.32 Hz making it a difference of 5.4 percent. The experimental natural frequency of the second pendulum is 1.263 Hz and the simulated natural frequency is 1.33 Hz with a difference of 5.4 percent as well.

With the same inputs and damping coefficient, we compare the quality of the distributed-mass simulation to our previous model [9]. As seen in Figures 4.13 and 4.14 for 35 mm separation distance, and 4.18 and 4.19 for 40 mm, we see that our new model gives closer simulation to the experimental results. With same input parameters, we notice an even lager difference between the old model's simulation with respect to the experimental results. Our new model takes in consideration the cylindrical shape and dimensions of the magnets, while in the previous work, a magnetic point source magnet model was used.

4.5 Equilibria

Another aspect of our system was the equilibrium points for its stability. To determine the equilibrium points of the two-pendulum system, we set the time derivatives $\dot{\theta}_1$, $\ddot{\theta}_1$, $\dot{\theta}_2$ and $\ddot{\theta}_1$ in Equation (3.64) equal to zero. Solving these algebraic equations, we find the equilibrium points for different separation distances from the minimum distance being 4 mm (the height of our cylindrical magnet) to 55 mm where the magnetic force becomes insignificant. By doing this, we checked how the separation distance between the magnets affects the pendulum equilibrium points.

As seen in Figure 4.20, we get a parabolic shape where the maximum equilibrium angles occur when the separation distance is around 22 mm. There results are governed by the conservation property of magnetism and are due to the magnetic field getting stronger but narrower with the separation distance decreasing. To check the validity of these results, we looked into similar research with cylindrical uniformly magnetized magnets.

The system presented by Mahmud et al. [33] consists of two permanent magnet groups arranged in a triangular array fashion with groups of three cylindrical magnets in each corner of the triangle. With their system, they checked how both the lateral and axial force changes with axial and lateral distance respectively [1]. The measured and calculated results showed that as the axial separation distance decreases the axial force (F_z) increases. However, the lateral forces (F_x and F_y) change following a parabolic shape which is in line with our results.

[1]Lateral force/displacement represent those in the $\hat{\imath}\hat{\jmath}$-plane while the axial force/displacement refer to the one in the $\hat{k}$-direction

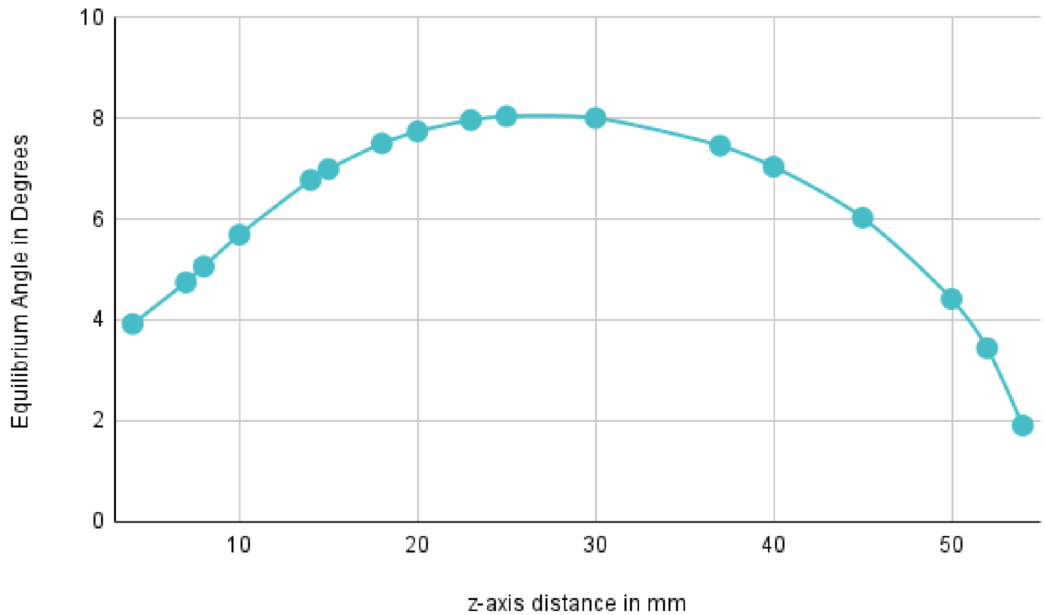

Figure 4.20: Change in equilibrium angle in degrees with respect to the separation distance in mm.

4.6 Basins of Attraction

After checking the equilibrium points both experimentally and analytically, we checked the basin of attraction of the two equilibrium points of our system based on those values. After running a simulation for initial conditions of the first pendulum going from -90° to 90° and for initial conditions of its angular velocity going from -800°/s to 800°/s. Figure 4.21 shows the basin of attraction of the system where the blue colour indicates that it's landing on the negative equilibrium and the yellow on the positive equilibrium.

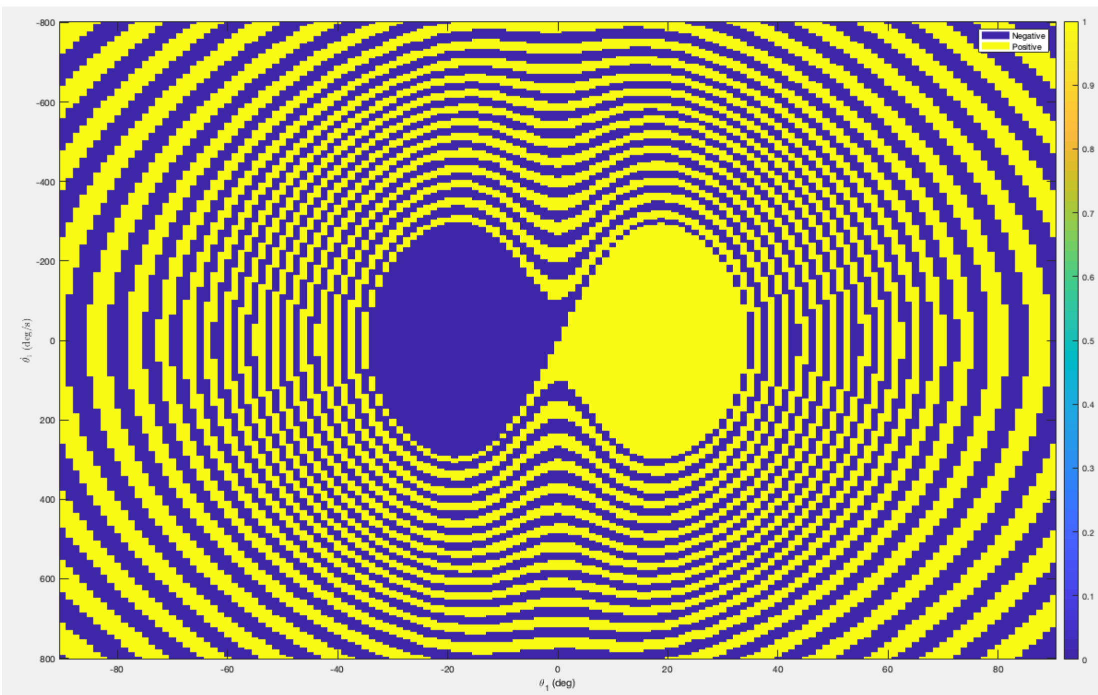

Figure 4.21: Basin of Attraction of the system.

Chapter 5

Conclusions and Future Work

In conclusion, a system consisting of a chain of magnetic pendulum is interesting to study due to their equation of motion and its similarity to the Josephson junction governing equation. In our case, our designed system will be used to better understand the behaviour of memory cells of quantum computing as they are developed by tunneling Josephson Junction.

This research built on previous work to develop an improved system model and investigate the nonlinear motion and magnetic forces of a chain of magnetic pendulums with cylindrical magnets. We analytically derived the equations of motion for a system of two pendulums with the aim of simulating its dynamics. We considered two models: a point-mass model and a distributed-mass model. The distributed-mass model provides an overall better simulation tool as it provides higher fidelity. The models were deployed to study the interaction forces between the magnets and the nonlinear motions of the system. To obtain the natural frequencies of the constituent pendulums, we used the Fast Fourier Transform.

Finally, we were able to validate the accuracy of our system of equations using a Mathematica simulation response and comparing its behaviour to that of an experimental setup consisting of two coupled magnetic pendulums. The project resulted in a fully adjustable, portable magnetic oscillator that could be switched between injection locking and injection pulling without disassembly of the entire system. Ultimately, the results we obtained through comparing the simulated system response and the designed experiment response indicated that our analytical model can accurately predict the behaviour of such a system.

In future work, it would be interesting to investigate systems with minimal distance between the magnets and shorter pendulums to explore the system dynamics under stronger magnetic coupling and at higher response frequencies, respectively. It would also be useful to reduce energy losses in the system to explore more interesting dynamics. Eventually, the pendulum system will be deployed as an analog of individual (point) or arrays of JJs by adding stationary magnets to represent DC current (constant moment) and / or a motor that moves an external magnet at a fixed rate to represent AC current (moment).

Letters of Copyright Permission

Re: Request to reuse figure from IOP Publishing

Permissions <permissions@ioppublishing.org>
Mon 7/18/2022 9:20 AM
To: Mariam Lahlou <mlahlou@uwaterloo.ca>

Dear Mariam,

Thank you for your request to reproduce material published by IOP Publishing *in your thesis,* ***"Interaction Forces of Coupled Magnetic Pendulums"***

Regarding:

Title of ebook: *Quantum Computing: A pathway to quantum logic design*
Chapter title: *Basic definitions of quantum logic*
DOI: *https://doi.org/10.1088/978-0-7503-2747-3ch2*
Copyright owner: *IOP Publishing*
Figure number: *2.1*

We are happy to grant permission for the use you request on the terms set out below.

License to publish material published by IOP Publishing

Conditions

Non-exclusive, non-transferrable, revocable, worldwide, permission to use the material in print and electronic form will be granted **subject to the following conditions:**

- Permission will be cancelled without notice if you fail to fulfil any of the conditions of this letter.
- You will make reasonable efforts to contact the author(s) to seek consent for your intended use. Contacting one author acting expressly as authorised agent for their co-authors is acceptable.
- You will reproduce the following prominently alongside the material:
  - the source of the material, including author, chapter title, title of ebook, chapter number, page range (or first page if this is the only information available) and date of first publication. This information can be contained in a footnote or reference note; or
  - a link back to the ebook abstract (via DOI); and
  - if practical and IN ALL CASES for works published under any of the Creative Commons licences the words "© IOP Publishing. Reproduced with permission. All rights reserved""
- The material will not, without the express permission of the author(s), be used in any way which, in the opinion of IOP Publishing, could distort or alter the author(s)' original intention(s) and meaning, be prejudicial to the honour or reputation of the author(s) and/or imply endorsement by the author(s) and/or IOP Publishing.
- Payment of £0 is received in full by IOP Publishing prior to use.

This permission does not apply to any material/figure which is credited to another source in our publication or has been obtained from a third party. Express permission for such materials/figures must be obtained from the copyright owner.

Kind regards,

Sophie
Copyright & Permissions Team
Sophie Brittain - Rights & Permissions Assistant
Cameron Wood - Legal & Rights Adviser
Contact Details
E-mail: permissions@ioppublishing.org

For further information about copyright and how to request permission:
https://publishingsupport.iopscience.iop.org/copyright-journals/
See also: https://publishingsupport.iopscience.iop.org/
Please see our Author Rights Policy https://publishingsupport.iopscience.iop.org/author-rights-policies/
Please note: We do not provide signed permission forms as a separate attachment. Please print this email and provide it to your publisher as proof of permission. **Please note**: Any statements made by IOP Publishing to the effect that authors do not need to get permission to use any content where IOP Publishing is not the publisher is not intended to constitute any sort of legal advice. Authors must make their own decisions as to the suitability of the content they are using and whether they require permission for it to be published within their article.

From: Mariam Lahlou <mlahlou@uwaterloo.ca>
Sent: 15 July 2022 19:17
To: Permissions <permissions@ioppublishing.org>
Subject: Request to reuse figure from IOP Publishing

Hello,

My name is Mariam Lahlou and I am currently completing my thesis as a Master student in the University of Waterloo. I want to request reusing a figure from Hafiz Md Hasan Babu's Quantum Computing: A Pathway to quantum logic design. I was hoping to reuse Figure 2.1 for my thesis titled Interaction Forces of Coupled Magnetic Pendulums.

Please let me know what the process is to reuse the figures or if you need any additional information from me

Sincerely,
Mariam

RE: Request to reuse figure

AIPRights Permissions <Rights@aip.org>
Tue 7/26/2022 3:56 PM
To: Mariam Lahlou <mlahlou@uwaterloo.ca>

Dear Mariam Lahlou,

Thank you for requesting permission to reproduce material from AIP Publishing publications.

Material for which permission is requested:
D. B. Sullivan and J. E. Zimmerman, "Medical analogs of time dependent Josephson phenomena," Am. J. Phys. **39**(12), 1504-1517 (1971), doi:10.1119/1.1976705, Figure 5.
P. K. Hansma and G. I. Rochlin, "Josephson weal links: shunted-junction and mechanical-model results," J. Appl. Phys. **43**(11), 4721-4727 (1972), doi:10.1063/1.1660994, Figure 3.
Koji Nakajima, Tsutomu Yamashita, and Yutaka Onodera, "Mechanical analogue of active Josephson transmission line," J. Appl. Phys. **45**(7), 3141-3145 (1974), doi:10.1063/1.1663738, Figure 2.
Ernesto Altshuler and R. Garcia, "Josephson junctions in a magnetic field: Insights from coupled pendula," Am. J. Phys. 71(4), 405-408 (2003), doi:10.1119/1.1533052, Figure 5.

To be reproduced in the following new work: Alexander Horn, forthcoming article, to be published.

Permission is granted subject to these conditions:

1. AIP Publishing grants you non-exclusive world rights in all languages and media. This permission extends to all subsequent and future editions of the new work.

2. The following notice must appear with the material (please fill in the information indicated by capital letters):

"Reproduced from [FULL CITATION], with the permission of AIP Publishing." (for the articles from J. Appl. Phys.)

"Reprodiced from [FULL CITATION], with permission of Anerican Association of Physics Teachers." (for articles from Am. J. Phys.)

When reusing figures, photographs, covers, or tables, the notice may appear in the caption, in a footnote, or in the reference list.

In cases where the new publication is licensed under a Creative Commons license, the full notice as stated above must appear with the reproduced material.

3. If the material is published in electronic format, we ask that a link be created pointing back to the abstract of the article on the journal website. This can be accomplished using the article's DOI.

4. This permission does not apply to any materials credited to another source.

For content reuse requests that qualify for permission under the STM Permissions Guidelines, which may be updated from time to time, the STM Permissions Guidelines supersede the terms and conditions contained in this license.

For future permission requests, we encourage you to use RightsLink, which is a tool that allows you to obtain permission quickly and easily online. To launch the RightsLink application, simply access the appropriate article on the journal site, click on the "Tools" link in the abstract, and select "Reprints & Permissions."

Please let us know if you have any questions.
Sincerely,
Brian McKenna

CCC Marketplace™

Order Date	20-Jul-2022	**Type of Use**	Republish in a thesis/dissertation
Order License ID	1249582-1	**Publisher**	Springer International Publishing
ISBN-13	9783030832735	**Portion**	Image/photo/illustration

LICENSED CONTENT

Publication Title	Quantum Computing: An Applied Approach	**Country**	Switzerland
Author/Editor	Hidary, Jack D.	**Rightsholder**	Springer
Date	11/03/2021	**Publication Type**	Book
Language	English		

REQUEST DETAILS

Portion Type	Image/photo/illustration	**Distribution**	Canada
Number of images / photos / illustrations	1	**Translation**	Original language of publication
Format (select all that apply)	Electronic	**Copies for the disabled?**	No
Who will republish the content?	Academic institution	**Minor editing privileges?**	No
Duration of Use	Current edition and up to 5 years	**Incidental promotional use?**	No
Lifetime Unit Quantity	Up to 499	**Currency**	CAD
Rights Requested	Main product		

NEW WORK DETAILS

Title	Interaction Forces of coupled magnetic pendulums	**Institution name**	University of Waterloo
Instructor name	Glenn Heppler and Eihab Abdel-Rahman	**Expected presentation date**	2022-08-10

ADDITIONAL DETAILS

Order reference number	N/A	**The requesting person / organization to appear on the license**	Mariam Lahlou- University of Waterloo

REUSE CONTENT DETAILS

Title, description or numeric reference of the portion(s)	Figure 2.1. Basic Quantum Gates	**Title of the article/chapter the portion is from**	Chapter 2 Basic definitions of quantum logic
Editor of portion(s)	N/A	**Author of portion(s)**	Hidary, Jack D.
Volume of serial or monograph	N/A	**Issue, if republishing an article from a serial**	N/A
Page or page range of portion	Page 2-2	**Publication date of portion**	2021-11-03

RIGHTSHOLDER TERMS AND CONDITIONS

A maximum of 10% of the content may be licensed for republication. The user is responsible for identifying and seeking separate licenses for any third party materials that are identified anywhere in the work. Without a separate license, such third party materials may not be reused.
If you are placing a request on behalf of/for a corporate organization, please use RightsLink. For further information visit http://www.nature.com/reprints/permission-requests.html and https://www.springer.com/gp/rights-permissions/obtaining-permissions/882. If the content you are requesting to reuse is under a CC-BY 4.0 licence (or previous version), you do not need to seek permission from Springer Nature for this reuse as long as you provide appropriate credit to the original publication. https://creativecommons.org/licenses/by/4.0/
STM Permissions Guidelines STM Permissions Guidelines (2022) - STM (stm-assoc.org) will complement the Terms & Conditions on this page CCC Payment T&Cs (copyright.com)

Marketplace Order General Terms and Conditions

The following terms and conditions ("General Terms"), together with any applicable Publisher Terms and Conditions, govern User's use of Works pursuant to the Licenses granted by Copyright Clearance Center, Inc. ("CCC") on behalf of the applicable Rightsholders of such Works through CCC's applicable Marketplace transactional licensing services (each, a "Service").

1) **Definitions.** For purposes of these General Terms, the following definitions apply:

"License" is the licensed use the User obtains via the Marketplace platform in a particular licensing transaction, as set forth in the Order Confirmation.

"Order Confirmation" is the confirmation CCC provides to the User at the conclusion of each Marketplace transaction. "Order Confirmation Terms" are additional terms set forth on specific Order Confirmations not set forth in the General Terms that can include terms applicable to a particular CCC transactional licensing service and/or any Rightsholder-specific terms.

"Rightsholder(s)" are the holders of copyright rights in the Works for which a User obtains licenses via the Marketplace platform, which are displayed on specific Order Confirmations.

"Terms" means the terms and conditions set forth in these General Terms and any additional Order Confirmation Terms collectively.

"User" or "you" is the person or entity making the use granted under the relevant License. Where the person accepting the Terms on behalf of a User is a freelancer or other third party who the User authorized to accept the General Terms on the User's behalf, such person shall be deemed jointly a User for purposes of such Terms.

"Work(s)" are the copyright protected works described in relevant Order Confirmations.

2) **Description of Service.** CCC's Marketplace enables Users to obtain Licenses to use one or more Works in accordance with all relevant Terms. CCC grants Licenses as an agent on behalf of the copyright rightsholder identified in the relevant Order Confirmation.

3) **Applicability of Terms.** The Terms govern User's use of Works in connection with the relevant License. In the event of any conflict between General Terms and Order Confirmation Terms, the latter shall govern. User acknowledges that Rightsholders have complete discretion whether to grant any permission, and whether to place any limitations on any grant, and that CCC has no right to supersede or to modify any such discretionary act by a Rightsholder.

4) **Representations; Acceptance.** By using the Service, User represents and warrants that User has been duly authorized by the User to accept, and hereby does accept, all Terms.

5) **Scope of License; Limitations and Obligations.** All Works and all rights therein, including copyright rights, remain the sole and exclusive property of the Rightsholder. The License provides only those rights expressly set forth in the terms

and conveys no other rights in any Works

6) **General Payment Terms.** User may pay at time of checkout by credit card or choose to be invoiced. If the User chooses to be invoiced, the User shall: (i) remit payments in the manner identified on specific invoices, (ii) unless otherwise specifically stated in an Order Confirmation or separate written agreement, Users shall remit payments upon receipt of the relevant invoice from CCC, either by delivery or notification of availability of the invoice via the Marketplace platform, and (iii) if the User does not pay the invoice within 30 days of receipt, the User may incur a service charge of 1.5% per month or the maximum rate allowed by applicable law, whichever is less. While User may exercise the rights in the License immediately upon receiving the Order Confirmation, the License is automatically revoked and is null and void, as if it had never been issued, if CCC does not receive complete payment on a timely basis.

7) **General Limits on Use.** Unless otherwise provided in the Order Confirmation, any grant of rights to User (i) involves only the rights set forth in the Terms and does not include subsequent or additional uses, (ii) is non-exclusive and non-transferable, and (iii) is subject to any and all limitations and restrictions (such as, but not limited to, limitations on duration of use or circulation) included in the Terms. Upon completion of the licensed use as set forth in the Order Confirmation, User shall either secure a new permission for further use of the Work(s) or immediately cease any new use of the Work(s) and shall render inaccessible (such as by deleting or by removing or severing links or other locators) any further copies of the Work. User may only make alterations to the Work if and as expressly set forth in the Order Confirmation. No Work may be used in any way that is defamatory, violates the rights of third parties (including such third parties' rights of copyright, privacy, publicity, or other tangible or intangible property), or is otherwise illegal, sexually explicit, or obscene. In addition, User may not conjoin a Work with any other material that may result in damage to the reputation of the Rightsholder. User agrees to inform CCC if it becomes aware of any infringement of any rights in a Work and to cooperate with any reasonable request of CCC or the Rightsholder in connection therewith.

8) **Third Party Materials.** In the event that the material for which a License is sought includes third party materials (such as photographs, illustrations, graphs, inserts and similar materials) that are identified in such material as having been used by permission (or a similar indicator), User is responsible for identifying, and seeking separate licenses (under this Service, if available, or otherwise) for any of such third party materials; without a separate license, User may not use such third party materials via the License.

9) **Copyright Notice.** Use of proper copyright notice for a Work is required as a condition of any License granted under the Service. Unless otherwise provided in the Order Confirmation, a proper copyright notice will read substantially as follows: "Used with permission of [Rightsholder's name], from [Work's title, author, volume, edition number and year of copyright]; permission conveyed through Copyright Clearance Center, Inc." Such notice must be provided in a reasonably legible font size and must be placed either on a cover page or in another location that any person, upon gaining access to the material which is the subject of a permission, shall see, or in the case of republication Licenses, immediately adjacent to the Work as used (for example, as part of a by-line or footnote) or in the place where substantially all other credits or notices for the new work containing the republished Work are located. Failure to include the required notice results in loss to the Rightsholder and CCC, and the User shall be liable to pay liquidated damages for each such failure equal to twice the use fee specified in the Order Confirmation, in addition to the use fee itself and any other fees and charges specified.

10) **Indemnity.** User hereby indemnifies and agrees to defend the Rightsholder and CCC, and their respective employees and directors, against all claims, liability, damages, costs, and expenses, including legal fees and expenses, arising out of any use of a Work beyond the scope of the rights granted herein and in the Order Confirmation, or any use of a Work which has been altered in any unauthorized way by User, including claims of defamation or infringement of rights of copyright, publicity, privacy, or other tangible or intangible property.

11) **Limitation of Liability.** UNDER NO CIRCUMSTANCES WILL CCC OR THE RIGHTSHOLDER BE LIABLE FOR ANY DIRECT, INDIRECT, CONSEQUENTIAL, OR INCIDENTAL DAMAGES (INCLUDING WITHOUT LIMITATION DAMAGES FOR LOSS OF BUSINESS PROFITS OR INFORMATION, OR FOR BUSINESS INTERRUPTION) ARISING OUT OF THE USE OR INABILITY TO USE A WORK, EVEN IF ONE OR BOTH OF THEM HAS BEEN ADVISED OF THE POSSIBILITY OF SUCH DAMAGES. In any event, the total liability of the Rightsholder and CCC (including their respective employees and directors) shall not exceed the total amount actually paid by User for the relevant License. User assumes full liability for the actions and omissions of its principals, employees, agents, affiliates, successors, and assigns.

12) **Limited Warranties.** THE WORK(S) AND RIGHT(S) ARE PROVIDED "AS IS." CCC HAS THE RIGHT TO GRANT TO USER THE RIGHTS GRANTED IN THE ORDER CONFIRMATION DOCUMENT. CCC AND THE RIGHTSHOLDER DISCLAIM ALL OTHER WARRANTIES RELATING TO THE WORK(S) AND RIGHT(S), EITHER EXPRESS OR IMPLIED, INCLUDING WITHOUT LIMITATION IMPLIED WARRANTIES OF MERCHANTABILITY OR FITNESS FOR A PARTICULAR PURPOSE. ADDITIONAL RIGHTS MAY BE REQUIRED TO USE ILLUSTRATIONS, GRAPHS, PHOTOGRAPHS, ABSTRACTS, INSERTS, OR OTHER PORTIONS OF THE WORK (AS OPPOSED TO THE ENTIRE WORK) IN A MANNER CONTEMPLATED BY USER; USER UNDERSTANDS AND AGREES THAT NEITHER CCC NOR THE RIGHTSHOLDER MAY HAVE SUCH ADDITIONAL RIGHTS TO GRANT.

13) **Effect of Breach.** Any failure by User to pay any amount when due, or any use by User of a Work beyond the scope of the License set forth in the Order Confirmation and/or the Terms, shall be a material breach of such License. Any breach

not cured within 10 days of written notice thereof shall result in immediate termination of such License without further notice. Any unauthorized (but licensable) use of a Work that is terminated immediately upon notice thereof may be liquidated by payment of the Rightsholder's ordinary license price therefor; any unauthorized (and unlicensable) use that is not terminated immediately for any reason (including, for example, because materials containing the Work cannot reasonably be recalled) will be subject to all remedies available at law or in equity, but in no event to a payment of less than three times the Rightsholder's ordinary license price for the most closely analogous licensable use plus Rightsholder's and/or CCC's costs and expenses incurred in collecting such payment.

14) **Additional Terms for Specific Products and Services.** If a User is making one of the uses described in this Section 14, the additional terms and conditions apply:

a) ***Print Uses of Academic Course Content and Materials (photocopies for academic coursepacks or classroom handouts).*** For photocopies for academic coursepacks or classroom handouts the following additional terms apply:

i) The copies and anthologies created under this License may be made and assembled by faculty members individually or at their request by on-campus bookstores or copy centers, or by off-campus copy shops and other similar entities.

ii) No License granted shall in any way: (i) include any right by User to create a substantively non-identical copy of the Work or to edit or in any other way modify the Work (except by means of deleting material immediately preceding or following the entire portion of the Work copied) (ii) permit "publishing ventures" where any particular anthology would be systematically marketed at multiple institutions.

iii) Subject to any Publisher Terms (and notwithstanding any apparent contradiction in the Order Confirmation arising from data provided by User), any use authorized under the academic pay-per-use service is limited as follows:

A) any License granted shall apply to only one class (bearing a unique identifier as assigned by the institution, and thereby including all sections or other subparts of the class) at one institution;

B) use is limited to not more than 25% of the text of a book or of the items in a published collection of essays, poems or articles;

C) use is limited to no more than the greater of (a) 25% of the text of an issue of a journal or other periodical or (b) two articles from such an issue;

D) no User may sell or distribute any particular anthology, whether photocopied or electronic, at more than one institution of learning;

E) in the case of a photocopy permission, no materials may be entered into electronic memory by User except in order to produce an identical copy of a Work before or during the academic term (or analogous period) as to which any particular permission is granted. In the event that User shall choose to retain materials that are the subject of a photocopy permission in electronic memory for purposes of producing identical copies more than one day after such retention (but still within the scope of any permission granted), User must notify CCC of such fact in the applicable permission request and such retention shall constitute one copy actually sold for purposes of calculating permission fees due; and

F) any permission granted shall expire at the end of the class. No permission granted shall in any way include any right by User to create a substantively non-identical copy of the Work or to edit or in any other way modify the Work (except by means of deleting material immediately preceding or following the entire portion of the Work copied).

iv) Books and Records; Right to Audit. As to each permission granted under the academic pay-per-use Service, User shall maintain for at least four full calendar years books and records sufficient for CCC to determine the numbers of copies made by User under such permission. CCC and any representatives it may designate shall have the right to audit such books and records at any time during User's ordinary business hours, upon two days' prior notice. If any such audit shall determine that User shall have underpaid for, or underreported, any photocopies sold or by three percent (3%) or more, then User shall bear all the costs of any such audit; otherwise, CCC shall bear the costs of any such audit. Any amount determined by such audit to have been underpaid by User shall immediately be paid to CCC by User, together with interest thereon at the rate of 10% per annum from the date such amount was originally due. The provisions of this paragraph shall survive the termination of this License for any reason.

b) ***Digital Pay-Per-Uses of Academic Course Content and Materials (e-coursepacks, electronic reserves, learning management systems, academic institution intranets).*** For uses in e-coursepacks, posts in electronic reserves, posts in learning management systems, or posts on academic institution intranets, the following additional terms apply:

i) The pay-per-uses subject to this Section 14(b) include:

A) **Posting e-reserves, course management systems, e-coursepacks for text-based content,** which grants authorizations to import requested material in electronic format, and allows electronic access to this material to members of a designated college or university class, under the direction of an instructor designated by the college or university, accessible only under appropriate electronic controls (e.g., password);

B) **Posting e-reserves, course management systems, e-coursepacks for material consisting of photographs or other still images not embedded in text,** which grants not only the authorizations described in Section 14(b)(i)(A) above, but also the following authorization: to include the requested material in course materials for use consistent with Section 14(b)(i)(A) above, including any necessary resizing, reformatting or modification of the resolution of such requested material (provided that such modification does not alter the underlying editorial content or meaning of the requested material, and provided that the resulting modified content is used solely within the scope of, and in a manner consistent with, the particular authorization described in the Order Confirmation and the Terms), but not including any other form of manipulation, alteration or editing of the requested material;

C) **Posting e-reserves, course management systems, e-coursepacks or other academic distribution for audiovisual content,** which grants not only the authorizations described in Section 14(b)(i)(A) above, but also the following authorizations: (i) to include the requested material in course materials for use consistent with Section 14(b)(i)(A) above; (ii) to display and perform the requested material to such members of such class in the physical classroom or remotely by means of streaming media or other video formats; and (iii) to "clip" or reformat the requested material for purposes of time or content management or ease of delivery, provided that such "clipping" or reformatting does not alter the underlying editorial content or meaning of the requested material and that the resulting material is used solely within the scope of, and in a manner consistent with, the particular authorization described in the Order Confirmation and the Terms. Unless expressly set forth in the relevant Order Conformation, the License does not authorize any other form of manipulation, alteration or editing of the requested material.

ii) Unless expressly set forth in the relevant Order Confirmation, no License granted shall in any way: (i) include any right by User to create a substantively non-identical copy of the Work or to edit or in any other way modify the Work (except by means of deleting material immediately preceding or following the entire portion of the Work copied or, in the case of Works subject to Sections 14(b)(1)(B) or (C) above, as described in such Sections) (ii) permit "publishing ventures" where any particular course materials would be systematically marketed at multiple institutions.

iii) Subject to any further limitations determined in the Rightsholder Terms (and notwithstanding any apparent contradiction in the Order Confirmation arising from data provided by User), any use authorized under the electronic course content pay-per-use service is limited as follows:

A) any License granted shall apply to only one class (bearing a unique identifier as assigned by the institution, and thereby including all sections or other subparts of the class) at one institution;

B) use is limited to not more than 25% of the text of a book or of the items in a published collection of essays, poems or articles;

C) use is limited to not more than the greater of (a) 25% of the text of an issue of a journal or other periodical or (b) two articles from such an issue;

D) no User may sell or distribute any particular materials, whether photocopied or electronic, at more than one institution of learning;

E) electronic access to material which is the subject of an electronic-use permission must be limited by means of electronic password, student identification or other control permitting access solely to students and instructors in the class;

F) User must ensure (through use of an electronic cover page or other appropriate means) that any person, upon gaining electronic access to the material, which is the subject of a permission, shall see:

- a proper copyright notice, identifying the Rightsholder in whose name CCC has granted permission,
- a statement to the effect that such copy was made pursuant to permission,
- a statement identifying the class to which the material applies and notifying the reader that the material has been made available electronically solely for use in the class, and
- a statement to the effect that the material may not be further distributed to any person outside the class, whether by copying or by transmission and whether electronically or in paper form, and User must also

ensure that such cover page or other means will print out in the event that the person accessing the material chooses to print out the material or any part thereof.

G) any permission granted shall expire at the end of the class and, absent some other form of authorization, User is thereupon required to delete the applicable material from any electronic storage or to block electronic access to the applicable material.

iv) Uses of separate portions of a Work, even if they are to be included in the same course material or the same university or college class, require separate permissions under the electronic course content pay-per-use Service. Unless otherwise provided in the Order Confirmation, any grant of rights to User is limited to use completed no later than the end of the academic term (or analogous period) as to which any particular permission is granted.

v) Books and Records; Right to Audit. As to each permission granted under the electronic course content Service, User shall maintain for at least four full calendar years books and records sufficient for CCC to determine the numbers of copies made by User under such permission. CCC and any representatives it may designate shall have the right to audit such books and records at any time during User's ordinary business hours, upon two days' prior notice. If any such audit shall determine that User shall have underpaid for, or underreported, any electronic copies used by three percent (3%) or more, then User shall bear all the costs of any such audit; otherwise, CCC shall bear the costs of any such audit. Any amount determined by such audit to have been underpaid by User shall immediately be paid to CCC by User, together with interest thereon at the rate of 10% per annum from the date such amount was originally due. The provisions of this paragraph shall survive the termination of this license for any reason.

c) ***Pay-Per-Use Permissions for Certain Reproductions (Academic photocopies for library reserves and interlibrary loan reporting) (Non-academic internal/external business uses and commercial document delivery).*** The License expressly excludes the uses listed in Section (c)(i)-(v) below (which must be subject to separate license from the applicable Rightsholder) for: academic photocopies for library reserves and interlibrary loan reporting; and non-academic internal/external business uses and commercial document delivery.

i) electronic storage of any reproduction (whether in plain-text, PDF, or any other format) other than on a transitory basis;

ii) the input of Works or reproductions thereof into any computerized database;

iii) reproduction of an entire Work (cover-to-cover copying) except where the Work is a single article;

iv) reproduction for resale to anyone other than a specific customer of User;

v) republication in any different form. Please obtain authorizations for these uses through other CCC services or directly from the rightsholder.

Any license granted is further limited as set forth in any restrictions included in the Order Confirmation and/or in these Terms.

d) ***Electronic Reproductions in Online Environments (Non-Academic-email, intranet, internet and extranet).*** For "electronic reproductions", which generally includes e-mail use (including instant messaging or other electronic transmission to a defined group of recipients) or posting on an intranet, extranet or Intranet site (including any display or performance incidental thereto), the following additional terms apply:

i) Unless otherwise set forth in the Order Confirmation, the License is limited to use completed within 30 days for any use on the Internet, 60 days for any use on an intranet or extranet and one year for any other use, all as measured from the "republication date" as identified in the Order Confirmation, if any, and otherwise from the date of the Order Confirmation.

ii) User may not make or permit any alterations to the Work, unless expressly set forth in the Order Confirmation (after request by User and approval by Rightsholder); provided, however, that a Work consisting of photographs or other still images not embedded in text may, if necessary, be resized, reformatted or have its resolution modified without additional express permission, and a Work consisting of audiovisual content may, if necessary, be "clipped" or reformatted for purposes of time or content management or ease of delivery (provided that any such resizing, reformatting, resolution modification or “clipping” does not alter the underlying editorial content or meaning of the Work used, and that the resulting material is used solely within the scope of, and in a manner consistent with, the particular License described in the Order Confirmation and the Terms.

15) **Miscellaneous.**

a) User acknowledges that CCC may, from time to time, make changes or additions to the Service or to the Terms, and that Rightsholder may make changes or additions to the Rightsholder Terms. Such updated Terms will replace the prior terms and conditions in the order workflow and shall be effective as to any subsequent Licenses but shall not apply to Licenses already granted and paid for under a prior set of terms.

b) Use of User-related information collected through the Service is governed by CCC's privacy policy, available online at www.copyright.com/about/privacy-policy/.

c) The License is personal to User. Therefore, User may not assign or transfer to any other person (whether a natural person or an organization of any kind) the License or any rights granted thereunder; provided, however, that, where applicable, User may assign such License in its entirety on written notice to CCC in the event of a transfer of all or substantially all of User's rights in any new material which includes the Work(s) licensed under this Service.

d) No amendment or waiver of any Terms is binding unless set forth in writing and signed by the appropriate parties, including, where applicable, the Rightsholder. The Rightsholder and CCC hereby object to any terms contained in any writing prepared by or on behalf of the User or its principals, employees, agents or affiliates and purporting to govern or otherwise relate to the License described in the Order Confirmation, which terms are in any way inconsistent with any Terms set forth in the Order Confirmation, and/or in CCC's standard operating procedures, whether such writing is prepared prior to, simultaneously with or subsequent to the Order Confirmation, and whether such writing appears on a copy of the Order Confirmation or in a separate instrument.

e) The License described in the Order Confirmation shall be governed by and construed under the law of the State of New York, USA, without regard to the principles thereof of conflicts of law. Any case, controversy, suit, action, or proceeding arising out of, in connection with, or related to such License shall be brought, at CCC's sole discretion, in any federal or state court located in the County of New York, State of New York, USA, or in any federal or state court whose geographical jurisdiction covers the location of the Rightsholder set forth in the Order Confirmation. The parties expressly submit to the personal jurisdiction and venue of each such federal or state court.

ELSEVIER LICENSE
TERMS AND CONDITIONS

Sep 19, 2022

This Agreement between University of Waterloo -- Mariam Lahlou ("You") and Elsevier ("Elsevier") consists of your license details and the terms and conditions provided by Elsevier and Copyright Clearance Center.

License Number	5350310499313
License date	Jul 15, 2022
Licensed Content Publisher	Elsevier
Licensed Content Publication	Journal of Systems Architecture
Licensed Content Title	Quantum ternary parallel adder/subtractor with partially-look-ahead carry
Licensed Content Author	Mozammel H.A. Khan,Marek A. Perkowski
Licensed Content Date	Jul 1, 2007
Licensed Content Volume	53
Licensed Content Issue	7
Licensed Content Pages	12
Start Page	453
End Page	464
Type of Use	reuse in a thesis/dissertation
Portion	figures/tables/illustrations

Number of figures/tables/illustrations	1
Format	electronic
Are you the author of this Elsevier article?	No
Will you be translating?	No
Title	Interaction Forces of Coupled Magnetic Pendulums
Institution name	University of Waterloo
Expected presentation date	Aug 2022
Portions	Figure 9 from Quantum ternary parallel adder/subtractor with partially-look-ahead carry
Requestor Location	University of Waterloo 200 University Ave W Waterloo, ON N2L 3G5 Canada Attn: University of Waterloo
Publisher Tax ID	GB 494 6272 12
Total	0.00 CAD

Terms and Conditions

INTRODUCTION

1. The publisher for this copyrighted material is Elsevier. By clicking "accept" in connection with completing this licensing transaction, you agree that the following terms and conditions apply to this transaction (along with the Billing and Payment terms and conditions established by Copyright Clearance Center, Inc. ("CCC"), at the time that you opened your Rightslink account and that are available at any time at http://myaccount.copyright.com).

GENERAL TERMS

2. Elsevier hereby grants you permission to reproduce the aforementioned material subject to the terms and conditions indicated.

3. Acknowledgement: If any part of the material to be used (for example, figures) has appeared in our publication with credit or acknowledgement to another source, permission must also be sought from that source. If such permission is not obtained then that material may not be included in your publication/copies. Suitable acknowledgement to the source must be made, either as a footnote or in a reference list at the end of your publication, as follows:

"Reprinted from Publication title, Vol /edition number, Author(s), Title of article / title of chapter, Pages No., Copyright (Year), with permission from Elsevier [OR APPLICABLE SOCIETY COPYRIGHT OWNER]." Also Lancet special credit - "Reprinted from The Lancet, Vol. number, Author(s), Title of article, Pages No., Copyright (Year), with permission from Elsevier."

4. Reproduction of this material is confined to the purpose and/or media for which permission is hereby given.

5. Altering/Modifying Material: Not Permitted. However figures and illustrations may be altered/adapted minimally to serve your work. Any other abbreviations, additions, deletions and/or any other alterations shall be made only with prior written authorization of Elsevier Ltd. (Please contact Elsevier's permissions helpdesk here). No modifications can be made to any Lancet figures/tables and they must be reproduced in full.

6. If the permission fee for the requested use of our material is waived in this instance, please be advised that your future requests for Elsevier materials may attract a fee.

7. Reservation of Rights: Publisher reserves all rights not specifically granted in the combination of (i) the license details provided by you and accepted in the course of this licensing transaction, (ii) these terms and conditions and (iii) CCC's Billing and Payment terms and conditions.

8. License Contingent Upon Payment: While you may exercise the rights licensed immediately upon issuance of the license at the end of the licensing process for the transaction, provided that you have disclosed complete and accurate details of your proposed use, no license is finally effective unless and until full payment is received from you (either by publisher or by CCC) as provided in CCC's Billing and Payment terms and conditions. If full payment is not received on a timely basis, then any license preliminarily granted shall be deemed automatically revoked and shall be void as if never granted. Further, in the event that you breach any of these terms and conditions or any of CCC's Billing and Payment terms and conditions, the license is automatically revoked and shall be void as if never granted. Use of materials as described in a revoked license, as well as any use of the materials beyond the scope of an unrevoked license, may constitute copyright infringement and publisher reserves the right to take any and all action to protect its copyright in the materials.

9. Warranties: Publisher makes no representations or warranties with respect to the licensed material.

10. Indemnity: You hereby indemnify and agree to hold harmless publisher and CCC, and their respective officers, directors, employees and agents, from and against any and all claims arising out of your use of the licensed material other than as specifically authorized pursuant to this license.

11. No Transfer of License: This license is personal to you and may not be sublicensed, assigned, or transferred by you to any other person without publisher's written permission.

12. No Amendment Except in Writing: This license may not be amended except in a writing signed by both parties (or, in the case of publisher, by CCC on publisher's behalf).

13. Objection to Contrary Terms: Publisher hereby objects to any terms contained in any purchase order, acknowledgment, check endorsement or other writing prepared by you, which terms are inconsistent with these terms and conditions or CCC's Billing and Payment terms and conditions. These terms and conditions, together with CCC's Billing and Payment terms and conditions (which are incorporated herein), comprise the entire agreement between you and publisher (and CCC) concerning this licensing transaction. In the event of any conflict between your obligations established by these terms and conditions and those established by CCC's Billing and Payment terms and conditions, these terms and conditions shall control.

14. Revocation: Elsevier or Copyright Clearance Center may deny the permissions described in this License at their sole discretion, for any reason or no reason, with a full refund payable to you. Notice of such denial will be made using the contact information provided by you. Failure to receive such notice will not alter or invalidate the denial. In no event will Elsevier or Copyright Clearance Center be responsible or liable for any costs, expenses or damage incurred by you as a result of a denial of your permission request, other than a refund of the amount(s) paid by you to Elsevier and/or Copyright Clearance Center for denied permissions.

LIMITED LICENSE

The following terms and conditions apply only to specific license types:

15. **Translation**: This permission is granted for non-exclusive world **English** rights only unless your license was granted for translation rights. If you licensed translation rights you may only translate this content into the languages you requested. A professional translator must perform all translations and reproduce the content word for word preserving the integrity of the article.

16. **Posting licensed content on any Website**: The following terms and conditions apply as follows: Licensing material from an Elsevier journal: All content posted to the web site must maintain the copyright information line on the bottom of each image; A hyper-text must be included to the Homepage of the journal from which you are licensing at http://www.sciencedirect.com/science/journal/xxxxx or the Elsevier homepage for books at http://www.elsevier.com; Central Storage: This license does not include permission for a scanned version of the material to be stored in a central repository such as that provided by Heron/XanEdu.

Licensing material from an Elsevier book: A hyper-text link must be included to the Elsevier homepage at http://www.elsevier.com . All content posted to the web site must maintain the copyright information line on the bottom of each image.

Posting licensed content on Electronic reserve: In addition to the above the following clauses are applicable: The web site must be password-protected and made available only to bona fide students registered on a relevant course. This permission is granted for 1 year only. You may obtain a new license for future website posting.

17. **For journal authors:** the following clauses are applicable in addition to the above:

Preprints:

A preprint is an author's own write-up of research results and analysis, it has not been peer-reviewed, nor has it had any other value added to it by a publisher (such as formatting, copyright, technical enhancement etc.).

Authors can share their preprints anywhere at any time. Preprints should not be added to or enhanced in any way in order to appear more like, or to substitute for, the final versions of articles however authors can update their preprints on arXiv or RePEc with their Accepted Author Manuscript (see below).

If accepted for publication, we encourage authors to link from the preprint to their formal publication via its DOI. Millions of researchers have access to the formal publications on ScienceDirect, and so links will help users to find, access, cite and use the best available version. Please note that Cell Press, The Lancet and some society-owned have different preprint policies. Information on these policies is available on the journal homepage.

Accepted Author Manuscripts: An accepted author manuscript is the manuscript of an article that has been accepted for publication and which typically includes author-incorporated changes suggested during submission, peer review and editor-author communications.

Authors can share their accepted author manuscript:

- immediately
    - via their non-commercial person homepage or blog
    - by updating a preprint in arXiv or RePEc with the accepted manuscript
    - via their research institute or institutional repository for internal institutional uses or as part of an invitation-only research collaboration work-group
    - directly by providing copies to their students or to research collaborators for their personal use
    - for private scholarly sharing as part of an invitation-only work group on commercial sites with which Elsevier has an agreement
- After the embargo period
    - via non-commercial hosting platforms such as their institutional repository
    - via commercial sites with which Elsevier has an agreement

In all cases accepted manuscripts should:

- link to the formal publication via its DOI
- bear a CC-BY-NC-ND license - this is easy to do
- if aggregated with other manuscripts, for example in a repository or other site, be shared in alignment with our hosting policy not be added to or enhanced in any way to appear more like, or to substitute for, the published journal article.

Published journal article (JPA): A published journal article (PJA) is the definitive final record of published research that appears or will appear in the journal and embodies all value-adding publishing activities including peer review co-ordination, copy-editing, formatting, (if relevant) pagination and online enrichment.

Policies for sharing publishing journal articles differ for subscription and gold open access articles:

Subscription Articles: If you are an author, please share a link to your article rather than the full-text. Millions of researchers have access to the formal publications on ScienceDirect, and so links will help your users to find, access, cite, and use the best available version.

Theses and dissertations which contain embedded PJAs as part of the formal submission can be posted publicly by the awarding institution with DOI links back to the formal publications on ScienceDirect.

If you are affiliated with a library that subscribes to ScienceDirect you have additional private sharing rights for others' research accessed under that agreement. This includes use for classroom teaching and internal training at the institution (including use in course packs and courseware programs), and inclusion of the article for grant funding purposes.

Gold Open Access Articles: May be shared according to the author-selected end-user license and should contain a CrossMark logo, the end user license, and a DOI link to the formal publication on ScienceDirect.

Please refer to Elsevier's posting policy for further information.

18. **For book authors** the following clauses are applicable in addition to the above: Authors are permitted to place a brief summary of their work online only. You are not allowed to download and post the published electronic version of your chapter, nor may you scan the printed edition to create an electronic version. **Posting to a repository:** Authors are permitted to post a summary of their chapter only in their institution's repository.

19. **Thesis/Dissertation**: If your license is for use in a thesis/dissertation your thesis may be submitted to your institution in either print or electronic form. Should your thesis be published commercially, please reapply for permission. These requirements include permission for the Library and Archives of Canada to supply single copies, on demand, of the complete thesis and include permission for Proquest/UMI to supply single copies, on demand, of the complete thesis. Should your thesis be published commercially, please reapply for permission. Theses and dissertations which contain embedded PJAs as part of the formal submission can be posted publicly by the awarding institution with DOI links back to the formal publications on ScienceDirect.

Elsevier Open Access Terms and Conditions

You can publish open access with Elsevier in hundreds of open access journals or in nearly 2000 established subscription journals that support open access publishing. Permitted third party re-use of these open access articles is defined by the author's choice of Creative Commons user license. See our open access license policy for more information.

Terms & Conditions applicable to all Open Access articles published with Elsevier:

Any reuse of the article must not represent the author as endorsing the adaptation of the article nor should the article be modified in such a way as to damage the author's honour or reputation. If any changes have been made, such changes must be clearly indicated.

The author(s) must be appropriately credited and we ask that you include the end user license and a DOI link to the formal publication on ScienceDirect.

If any part of the material to be used (for example, figures) has appeared in our publication with credit or acknowledgement to another source it is the responsibility of the user to ensure their reuse complies with the terms and conditions determined by the rights holder.

Additional Terms & Conditions applicable to each Creative Commons user license:

CC BY: The CC-BY license allows users to copy, to create extracts, abstracts and new works from the Article, to alter and revise the Article and to make commercial use of the Article (including reuse and/or resale of the Article by commercial entities), provided the user gives appropriate credit (with a link to the formal publication through the relevant DOI), provides a link to the license, indicates if changes were made and the licensor is not represented as endorsing the use made of the work. The full details of the license are available at http://creativecommons.org/licenses/by/4.0.

CC BY NC SA: The CC BY-NC-SA license allows users to copy, to create extracts, abstracts and new works from the Article, to alter and revise the Article, provided this is not done for commercial purposes, and that the user gives appropriate credit (with a link to the formal publication through the relevant DOI), provides a link to the license, indicates if changes were made and the licensor is not represented as endorsing the use made of the work. Further, any new works must be made available on the same conditions. The full details of the license are available at http://creativecommons.org/licenses/by-nc-sa/4.0.

CC BY NC ND: The CC BY-NC-ND license allows users to copy and distribute the Article, provided this is not done for commercial purposes and further does not permit distribution of the Article if it is changed or edited in any way, and provided the user gives appropriate credit (with a link to the formal publication through the relevant DOI), provides a link to the license, and that the licensor is not represented as endorsing the use made of the work. The full details of the license are available at http://creativecommons.org/licenses/by-nc-nd/4.0. Any commercial reuse of Open Access articles published with a CC BY NC SA or CC BY NC ND license requires permission from Elsevier and will be subject to a fee.

Commercial reuse includes:

- Associating advertising with the full text of the Article
- Charging fees for document delivery or access
- Article aggregation
- Systematic distribution via e-mail lists or share buttons

Posting or linking by commercial companies for use by customers of those companies.

20. **Other Conditions**:

v1.10

Questions? customercare@copyright.com or +1-855-239-3415 (toll free in the US) or +1-978-646-2777.

References

[1] T. Bassan. A brief introduction to quantum computing., January 2018. [Online; posted 23-January-2018].

[2] H. Md. Hasan Babu. *Quantum Computing: A Pathway to quantum logic design*. IOP Publishing, wholly owned by The Institute of Physics, London, 2020.

[3] D.B. Sullivan and J.E. Zimmerman. Mechanical analogs of time dependent josephson phenomena. *American Journal of Physics*, 39(12):1504–1517, 1971.

[4] P.K. Hansma and G.I. Rochlin. Josephson weak links: shunted-junction and mechanical-model results. *Journal of Applied Physics*, 43(11):4721–4727, 1972.

[5] K. Nakajima, T. Yamashita, and Y. Onodera. Mechanical analogue of active josephson transmission line. *Journal of Applied Physics*, 45(7):3141–3145, 1974.

[6] E. Altshuler and R. Garcıa. Josephson junctions in a magnetic field: Insights from coupled pendula. *American Journal of Physics*, 71(4):405–408, 2003.

[7] KJ Magnetics Ltd. Kj magnetics: Da2-n52. Accessed: 10 July 2022.

[8] J. Frankenfield. Quantum computing. [Online; posted 16-April-2019].

[9] R. S. Saeidi Hosseini. *Interactions of Magnetic Pendulums*. UWSpace, 2019.

[10] P. Benioff. The computer as a physical system: A microscopic quantum mechanical hamiltonian model of computers as represented by turing machines. *Journal of statistical physics*, 22(5):563–591, 1980.

[11] S. Akama. *Elements of quantum computing*. Springer, 2015.

[12] Y.I. Manin. Computable and noncomputable (in russian). *Sov. Radio.*, pages 13–15, 1980.

[13] R.P. Feynman. A computer-algebraic approach to the simulation of multi-qubit systems. *International Journal of Theoretical Physics*, 21:467, 1982.

[14] D. J. Hidary and Hidary. *Quantum computing: an applied approach*, volume 1. Springer, 2019.

[15] D. Deutsch. Quantum theory, the church–turing principle and the universal quantum computer. *Proceedings of the Royal Society of London. A. Mathematical and Physical Sciences*, 400(1818):97–117, 1985.

[16] E. Bernstein and U. Vazirani. Quantum complexity theory. *SIAM Journal on computing*, 26(5):1411–1473, 1997.

[17] L. K. Grover. A fast quantum mechanical algorithm for database search. In *Proceedings of the twenty-eighth annual ACM symposium on Theory of computing*, pages 212–219, 1996.

[18] A. Neil Gershenfeld and L. Isaac Chuang. Bulk spin-resonance quantum computation. *science*, 275(5298):350–356, 1997.

[19] M.K. Lieven Vandersypen, M. Steffen, Gregory Breyta, Costantino S Yannoni, H. Mark Sherwood, and L. Isaac Chuang. Experimental realization of shor's quantum factoring algorithm using nuclear magnetic resonance. *Nature*, 414(6866):883–887, 2001.

[20] H.A. M. Khan and M. A. Perkowski. Quantum ternary parallel adder/subtractor with partially-look-ahead carry. *Journal of Systems Architecture*, 53(7):453–464, 2007.

[21] N. Jia, L. Banchi, A. Bayat, Guangjiong Dong, and Sougato Bose. Integrated information storage and transfer with a coherent magnetic device. *Scientific reports*, 5(1):1–12, 2015.

[22] E. Goldobin, H. Sickinger, M. Weides, N. Ruppelt, H. Kohlstedt, R. Kleiner, and D. Koelle. Memory cell based on a φ josephson junction. *Applied Physics Letters*, 102(24):242602, 2013.

[23] H. Steven Strogatz. *Nonlinear dynamics and chaos: with applications to physics, biology, chemistry, and engineering.* CRC press, 2018.

[24] P. W. Anderson and J. M. Rowell. Probable observation of the josephson superconducting tunneling effect. *Physical Review Letters*, 10(6):230, 1963.

[25] A. James Blackburn, Yang Zhou-Jing, S Vik, HJT Smith, and MAH Nerenberg. Experimental study of chaos in a driven pendulum. *Physica D: Nonlinear Phenomena*, 26(1-3):385–395, 1987.

[26] A. Giordano R. De Luca and I. D'Acunto. Mechanical analog of an over-damped josephson junction. *European Journal of Physics*, 36(5):055042, 2015.

[27] S. Watanabe, S.J. van der Zant, Herre, S. H. Strogatz, and T. P. Orlando. Dynamics of circular arrays of josephson junctions and the discrete sine-gordon equation. *Physica D: Nonlinear Phenomena*, 97(4):429–470, 1996.

[28] C. Azzi. Design and analysis of magnetic pendulums internship report. unpublished.

[29] M. del Rosso. Design and construction of a portable, expandable, coupled magnetic oscillator. unpublished.

[30] A.G. Avila Bernal and L.E. Linares García. The modelling of an electromagnetic energy harvesting architecture. *Applied Mathematical Modelling*, 36(10):4728–4741, 2012.

[31] L. L. Yudell. *Integrals of Bessel functions*. Courier Corporation, 2014.

[32] C. Heuman. Tables of complete elliptic integrals. *Journal of Mathematics and Physics*, 20(1-4):127–206, 1941.

[33] A. Mahmud, J.R.R. Mayer, and L. Baron. Magnetic attraction forces between permanent magnet group arrays in a mobile magnetic clamp for pocket machining. *CIRP Journal of Manufacturing Science and Technology*, 11:82–88, 2015.

[34] P. Richard Feynman. Quantum mechanical computers. *Foundations of physics*, 16(6):507–531, 1986.

APPENDICES

Appendix A

Magnetic Force integration between the faces of the magnets

A.1 Integrations over the surface of the magnet

Now that we have the force general equation, it is necessary to determine the limits of integration. The task is to integrate over the surface of one the cylindrical pendulum i with respect to the origin of the other pendulum j. With reference to Figure A.1, we find

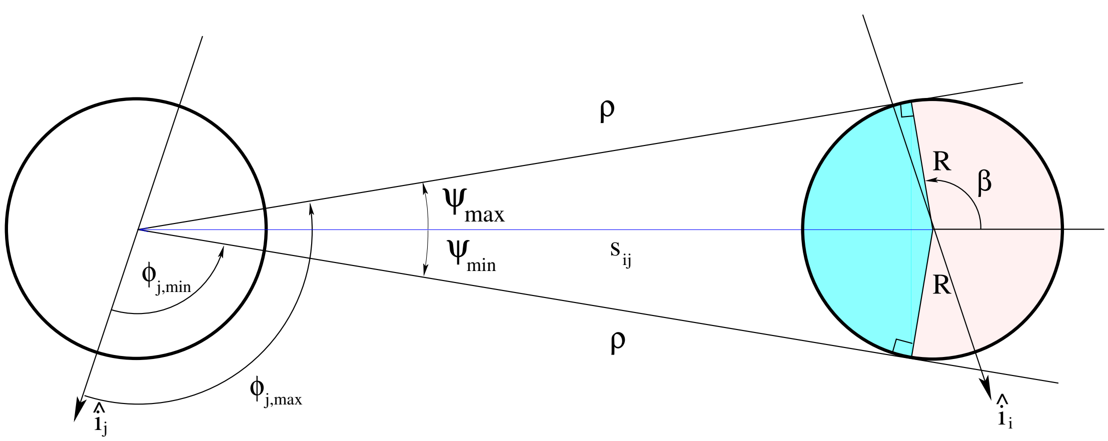

Figure A.1: View of the upper and lower limit of ρ.

the upper and lower limit for ρ as follow

$$\rho = s_{ij}\cos(\psi) \pm \sqrt{R^2 - s_{ij}^2\sin^2(\psi)} \tag{A.1}$$

where

$$s_{ij} = 2l\sin\left(\frac{\theta_{ij}}{2}\right)$$

and the angle ϕ_j ranges from 0 to ϕ_{max} such that

$$\phi_{max} = \arcsin\left(\frac{R}{s_{ij}}\right)$$

However, for simplicity reasons, we choose to integrate over ψ first. Since executing the area integral is for a fixed point in time, we can consider θ_{ij} fixed and consequently $d\psi_{ij} = d\phi_{ij}$. Therefore, we need to write ψ in term of ρ Using Equation A.1, we rearrange it and square both sides

$$\begin{aligned}
\rho - s_{ij}\cos(\psi) &= \pm\sqrt{R^2 - r_{ij}^2\sin(\psi)^2} \\
(\rho - s_{ij}\cos(\psi))^2 &= R^2 - s_{ij}^2\sin(\psi)^2 \\
\rho^2 + s_{ij}^2\cos^2(\psi) - 2s_{ij}\rho\cos(\psi) &= R^2 - s_{ij}^2\sin(\psi)^2
\end{aligned}$$

Using the identity $\sin^2(\phi) + \cos^2(\phi) = 1$, we get

$$\begin{aligned}
\rho^2 + s_{ij}^2 - 2s_{ij}\rho\cos(\psi) &= R^2 \\
\cos(\psi) &= \frac{R^2 - \rho^2 - s_{ij}^2}{-2s_{ij}\rho}
\end{aligned}$$

Then ψ is given by

$$\psi = \arccos\left(\frac{\rho^2 + s_{ij}^2 - R^2}{2s_{ij}\rho}\right) \tag{A.2}$$

A.2 Different cases

Now that the formulation of ψ is found, the limits of integration will be determined on case by case basis according to the positions of the magnets with respect to one another. Consequently, we note five main cases as follow

- **Case 1:** $\theta_{ij} > 0, s_{ij} \geq R$

  The first case illustrated in the figure bellow. When we integrate over ψ_j first from 0 to ψ_j, the limit of integration over ρ is from $s_{ij} - R$ to $s_{ij} + R$. However, to avoid

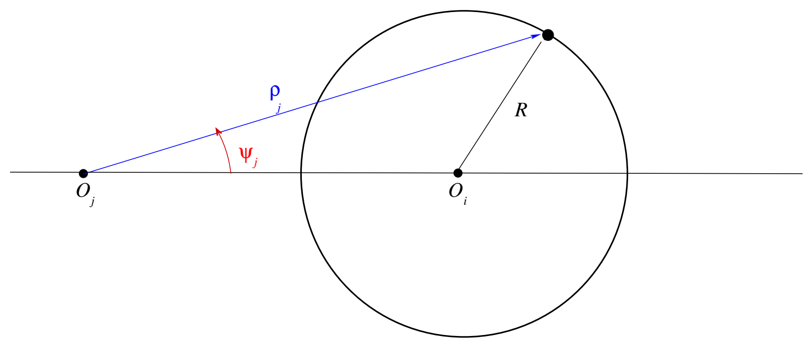

Figure A.2: Case 1: $\theta_{ij} > 0$ and $s_{ij} \geq R$

  getting imaginary numbers for ψ_j, we need the Arccos argument to be on the interval $[-1, 1]$. Therefore, solving the two equations

$$\frac{\rho^2 + s_{ij}^2 - R^2}{2s_{ij}\rho} = -1, \quad \text{and} \quad \frac{\rho^2 + s_{ij}^2 - R^2}{2s_{ij}\rho} = 1$$

  we find

$$\rho_j = \{-R - s_{ij}, R - s_{ij}\} \quad \text{and} \quad \rho_j = \{-R + s_{ij}, R + s_{ij}\}$$

  Due to the Elliptic integrals present in the magnetic fields, we need $\rho_j > 0$. We choose the two positive pairs.

- **Case 2:** $\theta_{ij} > 0, s_{ij} < R$

  In this case the centre of magnet j is inside the perimeter of magnet i as illustrated in Figure A.3. For this, we integrate ψ_j from 0 to ψ_j and ρ from $R - s_{ij}$ to $s_{ij} + R$.

- **Case 3:** $\theta_{ij} = 0, s_{ij} = R$

  Here, with θ_{ij} being 0, ϕ_j is independent of ρ_j. So when integrating over ϕ_j, we simply get 2π.

- **Case 4:** $\theta_{ij} < 0, -R < s_{ij} < 0$

  Similarly to case 2, here the center of magnet j is inside the perimeter of magnet i. But here $s_{ij} < 0$ so we integrate ψ_j from ψ_j to π and ρ from $R + s_{ij}$ to $-s_{ij} + R$.

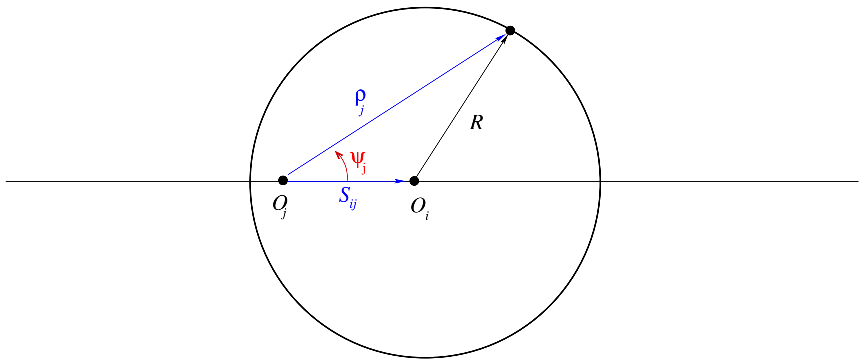

Figure A.3: Case 2: $\theta_{ij} > 0$ and $s_{ij} < R$

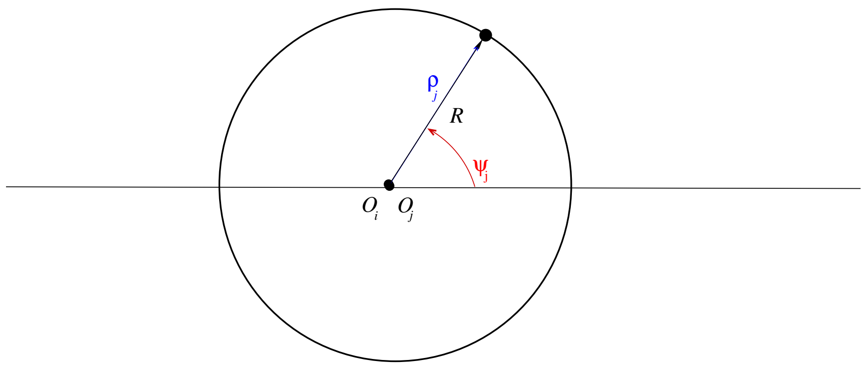

Figure A.4: Case 3: $\theta_{ij} = 0$ and $s_{ij} = R$

- **Case 5:** $\theta_{ij} < 0, s_{ij} \leq -R$

  Finally, the last case illustrated in Figure A.6 is when $\theta_i < \theta_j$. So that ψ_j is integrated from ψ_j to π and ρ from $-R - s_{ij}$ to $-s_{ij} + R$.

A.3 Integrations over ϕ_j

As mentioned earlier, we can consider θ_{ij} fixed so that $d\psi_{ij} = d\phi_{ij}$. In the cases mentioned above, ψ only covers the upper half of the circle. To cover the full surface of the magnet, we will need to integrate from 0 to $\phi(\rho)$ twice such as

$$2 \int_0^{\psi_j(\rho_j)} \vec{F_{ij}}\, d\psi_j \tag{A.3}$$

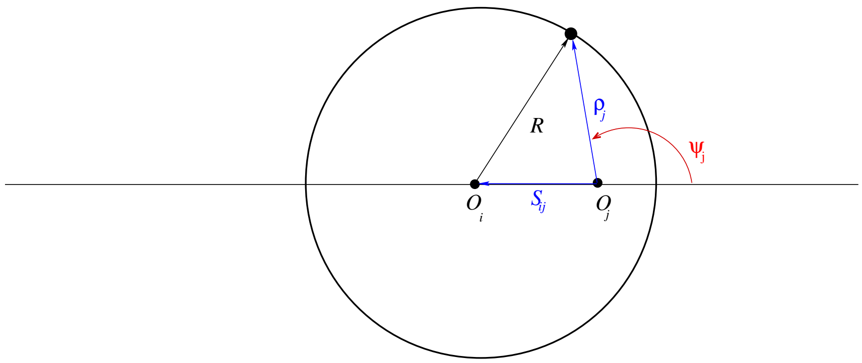

Figure A.5: Case 4: $\theta_{ij} < 0$ and $-R < s_{ij} < 0$

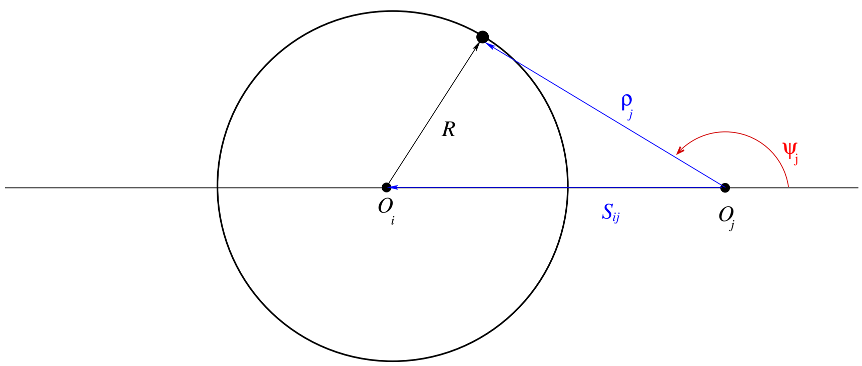

Figure A.6: Case 5: $\theta_{ij} < 0$ and $s_{ij} \leq -R$

One important difference to note between F_{ij_x}, F_{ij_y} and F_{ij_z} is that the latter is not a function of ϕ_j. This means the the integration of F_{ij_z} over ϕ_j can easily be done separately. However, the integration of F_{ij_x} and F_{ij_y} will require evaluating trigonometric functions over ϕ_j of the form

$$\int \cos(\phi_j)\, d\phi_j \qquad \text{and} \qquad \int \sin(\phi_j)\, d\phi_j$$

Considering Figure A.7, we have $\phi_j = \frac{\pi}{2} + \frac{\theta_{ij}}{2} + \psi_j$. In cases 1 and 2, when $\theta_{ij} > 0$, we get

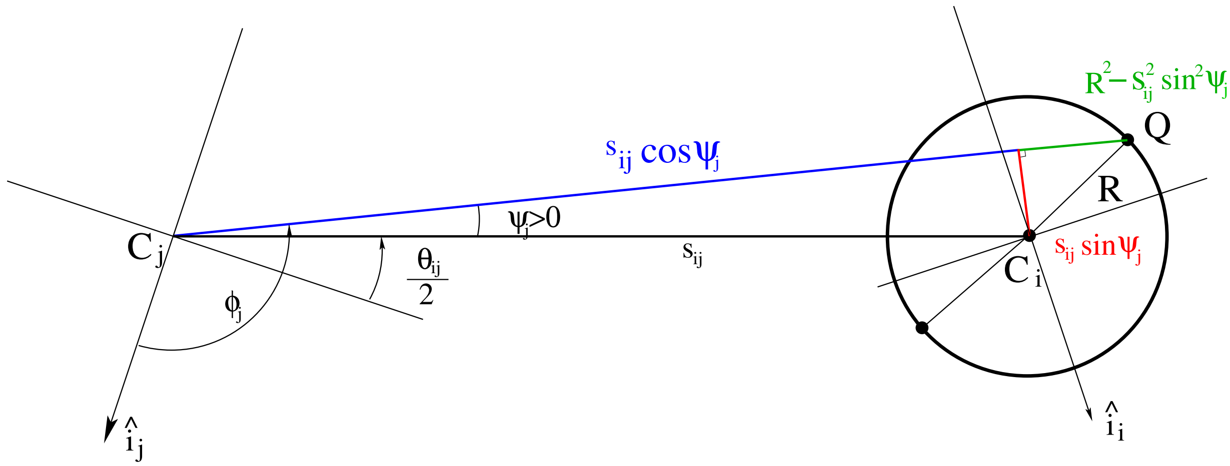

Figure A.7: View of the two pendulums.

the following integration limits

$$\begin{aligned}\int_0^{\psi_j(\rho_j)} \cos(\phi_j) d\phi_j &= \int_0^{\psi_j(\rho_j)} \cos\left(\frac{\pi}{2} + \frac{\theta_{ij}}{2} + \psi_j\right) d\psi_j \\ &= -\sin\left(\frac{\pi}{2} + \frac{\theta_{ij}}{2}\right) + \sin\left(\frac{\pi}{2} + \frac{\theta_{ij}}{2} + \psi_j(\rho_j)\right) \\ &= -\cos\left(\frac{\theta_{ij}}{2}\right) + \cos\left(\frac{\theta_{ij}}{2} + \psi_j(\rho_j)\right) \\ &= \cos\left(\frac{\theta_{ij}}{2} + \psi_j(\rho_j)\right) - \cos\left(\frac{\theta_{ij}}{2}\right)\end{aligned} \tag{A.4}$$

and

$$\begin{aligned}\int_0^{\psi_j(\rho_j)} \sin(\phi_j) d\phi_j &= \int_0^{\psi_j(\rho_j)} \sin\left(\frac{\pi}{2} + \frac{\theta_{ij}}{2} + \psi_j\right) d\psi_j \\ &= \cos\left(\frac{\pi}{2} + \frac{\theta_{ij}}{2}\right) - \cos\left(\frac{\pi}{2} + \frac{\theta_{ij}}{2} + \psi_j(\rho_j)\right) \\ &= -\sin\left(\frac{\theta_{ij}}{2}\right) + \sin\left(\frac{\theta_{ij}}{2} + \psi_j(\rho_j)\right) \\ &= \sin\left(\frac{\theta_{ij}}{2} + \psi_j(\rho_j)\right) - \sin\left(\frac{\theta_{ij}}{2}\right)\end{aligned} \tag{A.5}$$

In case 3, where $\theta_{ij} = 0$

$$\int_0^{2\pi} \sin(\psi_j)\, d\psi_j = \int_0^{2\pi} \cos(\psi_j)\, d\psi_j = 0 \tag{A.6}$$

And when $\theta_{ij} < 0$, the integrals range as follow

$$\begin{aligned}
\int_{\psi_j(\rho_j)}^{\pi} \cos(\phi_j) d\phi_j &= \int_{\psi_j(\rho_j)}^{\pi} \cos\left(\frac{\pi}{2} + \frac{\theta_{ij}}{2} + \psi_j\right) d\psi_j \\
&= \sin\left(\frac{\pi}{2} + \frac{\theta_{ij}}{2} + \pi\right) - \sin\left(\frac{\pi}{2} + \frac{\theta_{ij}}{2} + \psi_j(\rho_j)\right) \\
&= \cos\left(\frac{\theta_{ij}}{2} + \pi\right) - \cos\left(\frac{\theta_{ij}}{2} + \psi_j(\rho_j)\right) \\
&= -\cos\left(\frac{\theta_{ij}}{2}\right) - \cos\left(\frac{\theta_{ij}}{2} + \psi_j(\rho_j)\right)
\end{aligned} \tag{A.7}$$

and

$$\begin{aligned}
\int_{\psi_j(\rho_j)}^{\pi} \sin(\phi_j) d\phi_j &= \int_{\psi_j(\rho_j)}^{\pi} \sin\left(\frac{\pi}{2} + \frac{\theta_{ij}}{2} + \psi_j\right) d\psi_j \\
&= -\cos\left(\frac{\pi}{2} + \frac{\theta_{ij}}{2} + \pi\right) + \cos\left(\frac{\pi}{2} + \frac{\theta_{ij}}{2} + \psi_j(\rho_j)\right) \\
&= \sin\left(\frac{\theta_{ij}}{2} + \pi\right) - \sin\left(\frac{\theta_{ij}}{2} + \psi_j(\rho_j)\right) \\
&= -\sin\left(\frac{\theta_{ij}}{2}\right) - \sin\left(\frac{\theta_{ij}}{2} + \psi_j(\rho_j)\right)
\end{aligned} \tag{A.8}$$